Universitat Autònoma de Barcelona

Molecular mechanisms regulated by the transcriptional coactivator CRTC1 in synaptic plasticity

Anna del Ser Badia

Institut de Neurociències

Departament de Bioquímica i Biologia Molecular

Unitat de Bioquímica i Biologia Molecular, Facultat de Medicina

Universitat Autònoma de Barcelona

Molecular mechanisms regulated by the transcriptional coactivator CRTC1 in synaptic plasticity

Anna del Ser Badia

Doctoral Thesis

Bellaterra, September 2022

Institut de Neurociències

Departament de Bioquímica i Biologia Molecular

Unitat de Bioquímica i Biologia Molecular, Facultat de Medicina

Universitat Autònoma de Barcelona

Molecular mechanisms regulated by the transcriptional coactivator CRTC1 in synaptic plasticity

Mecanismos moleculares regulados por el coactivador transcripcional CRTC1 en plasticidad sináptica

Memoria de tesis doctoral presentada por Anna del Ser Badia para optar al grado de Doctora en Neurociencias por la Universitat Autònoma de Barcelona.

Trabajo realizado en la Unidad de Bioquímica y Biología Molecular de la Facultad de Medicina del Departamento de Bioquímica y Biología Molecular, y en el Institut de Neurociències de la Universitat Autònoma de Barcelona, bajo la dirección del Doctor Carlos A. Saura Antolín.

El trabajo realizado en esta tesis doctoral ha estado financiado por los proyectos de investigación del Programa Estatal de Investigación, Desarrollo e Innovación Orientada a los Retos de la Sociedad de la Agencia Estatal de Investigación/Ministerio de Ciencia e Innovación SAF2016-80027-R y PID2019-106615RB-I00, y por la Generalitat de Catalunya 2017 SGR749 y una beca de formación de doctores FI-AGAUR 2018FI_B00858.

A mis padres y hermano

Optare meliora.

Cogitare difficillima.

Ferre quaecumque euenerint.

(CICERÓN)

Table of contents

List of abbreviations

4-AP 4-aminopyridine
AAV Adeno-associated viral particle
ABD Agonist binding domain
Abi1 Abelson interacting protein
AC Adenylate cyclase
ActD Actinomycin D
AD Alzheimer's disease
AIDA1 Amyloid beta protein precursor intracellular domain associated protein 1
AKAPs A-kinase anchoring proteins
AMPA α-amino-3-hydroxy-5-methyl-4-isoxazole
AMPAR AMPA receptor
AMPK AMP-activated kinase
ANOVA Analysis of variance
APP Amyloid precursor protein
Aβ Amyloid beta
BDNF Brain-derived neurotrophic factor
Bic 1(S),9(R)-(-)-Bicuculline methiodide
BRET Bioluminescence resonance energy transfer
BSA Bovine serum albumin
bZIP Basic leucine zipper
Cald Caldendrin
Caln Calneuron
CaM Calmodulin
CaMK Ca^{2+}/Calmodulin-dependent protein kinase
cAMP Cyclic adenosine monophosphate
CaN Calcineurin
CBD Corticobasal degeneration
CBD CREB-binding domain
CBP CREB-binding protein
cDKO Conditional double knock-out
CFC Contextual fear conditioning
cKO Conditional knockout
CMV Cytomegalovirus
CNS Central nervous system
CQ Chloroquine
CRE cAMP response element
CREB cAMP response element binding protein
CRTC CREB-regulated transcriptional coactivator
CTD C-terminal domain
CTZ Coelenterazine H
DG Dentate gyrus
DIV Days *in vitro*
DNA Deoxyribonucleic acid
DNAse Deoxyribonuclease
dNTPs Deoxynucleotide triphosphates
E-LTP Early long-term potentiation
ER Endoplasmic reticulum
ERK Extracellular signal-regulated kinase
FAD Familial Alzheimer's disease

FBS	Fetal bovine serum
FISH	Fluorescence *in situ* hybridization
FSK	Forskolin
FTLD	Frontotemporal lobar degeneration
GABA	γ-aminobutyric acid
GAPDH	Glyceraldehyde-3-phosphate dehydrogenase
GF	GF-109203X hydrochloride
GFP	Green fluorescent protein
Glut	L-Glutamic acid
GPCRs	G protein-coupled receptors
H1	Histone 1
HA	Hemagglutinin
HBS	HEPES-buffered saline
HD	Huntington's disease
HEK	Human embryonic kidney
HMW	High molecular weight
HRP	Horseradish peroxidase
iGluR	Ionotropic glutamate receptor
IP	Infective particle
iPSC	Induced pluripotent stem cell
IRES	Internal ribosome entry site
ITR	Inverted terminal repeat
KCl	Potassium chloride
kDa	Kilodalton
KID	Kinase-inducible domain
LC3	Microtubule-associated protein light chain 3
L-LTP	Late long-term potentiation
LMW	Low molecular weight
LTD	Long-term depression
LTP	Long-term potentiation
LV	Lentiviral particles
MAP2	Microtubule-associated protein 2
MAPK	Mitogen-activated protein kinase
mBU	Mili BRET units
mGluR	Metabotropic glutamate receptor
MKL	Megakaryoblastic leukaemia
MRI	Magnetic resonance imaging
mRNA	Messenger RNA
mTOR	Mammalian target of rapamycin
NES	Nuclear export sequence
NF-κB	Nuclear factor kappa-light-chain-enhancer of active B cells
NGS	Normal goat serum
NLS	Nuclear localization sequence
NMDA	N-methyl-D-aspartate
NMDAR	NMDA receptor
NTD	N-terminal domain
O/N	Overnight
PAK4	p21-activated kinase 4
PBS	Phosphate buffered saline

PD	Parkinson's disease
PEI	Polyethylenimine
PET	Positron emission tomography
PFA	Paraformaldehyde
PiD	Pick's disease
PKA	Protein kinase A
PKC	Protein kinase C
PLC	Phospholipase C
PMA	Phorbol-12-myristate 13-acetate
PP1	Protein phosphatase type 1
PP2A	Protein phosphatase type 2A
PS/PSEN	Presenilin
PSD	Postsynaptic density
PVDF	Polyvinylidene fluoride
RBP	RNA binding protein
RLuc	Renilla luciferase
RNA	Ribonucleic acid
RNF10	RING finger protein 10
RSV	Rous sarcoma virus
RT	Room temperature
SCN	Suprachiasmatic nucleus
Scr	Scramble
SD	Splicing domain
SEM	Standard error of the mean
Shank3	SH3 and multiple ankyrin repeat domains 3
SIKs	Salt-inducible kinases
SNARE	Soluble N-ethylmaleimide-sensitive factor attachment protein receptor
SNP	Single nucleotide polymorphisms
SQSTM1	Sequestome 1
STD	Short-term depression
STF	Short-term facilitation
STP	Short-term synaptic plasticity
TAD	Transactivation domain
TARPs	Transmembrane AMPAR regulatory proteins
TBS	Tris-buffered saline
TMD	Transmembrane domain
TTX	Tetrodotoxin citrate
ULK1	Unc-51-like kinase 1
UTR	Untranslated regions
Veh	Vehicle
VGCC	Voltage-gated calcium channels
YFP	Yellow fluorescent protein
γCaMKII	Ca^{2+}/calmodulin-dependent protein kinase II gamma

Abstract

Activity-dependent remodeling of synapses or synaptic plasticity is considered the cellular basis of several brain physiological processes, including learning and memory. A balanced proteome is essential for efficient synaptic transmission and its deregulation is a hallmark of neurodegenerative diseases such as Alzheimer's disease (AD). The synaptonuclear factor CREB-regulated transcription coactivator-1 (CRTC1) links glutamate receptor activation to CREB-dependent gene programs at the nucleus, contributing to neuronal development, survival, and plasticity. However, the CRTC1-dependent molecular mechanisms regulating synaptic proteome in physiological and pathological conditions remain poorly understood. The hypotheses of this doctoral thesis are: (1) that CRTC1 mediates synaptic plasticity locally at synapses by regulating its proteome, and distally at the nucleus by modulating the expression of neuroplasticity genes; and (2) that CRTC1 deregulation is associated with neuropathological changes in tauopathy dementias. The objectives of this doctoral thesis are to investigate the synaptic CRTC1-dependent molecular mechanisms involved in synaptic plasticity, and to study the link of CRTC1 and presenilin (PS) in pathological tau at synapses. Our results show that CRTC1 is essential for long-term associative memory and modulates N-methyl-D-aspartate receptors (NMDARs; GluN)-mediated neurotransmission. CRTC1 regulates NMDARs subunit composition, protein kinase C (PKC)-dependent GluN1 phosphorylation and synaptic localization. Remarkably, by using a constitutively cytosolic CRTC1 mutant harboring triple S64/151/245A mutation, I demonstrate that GluN1 phosphorylation and synaptic localization are independent of CRTC1 nuclear activity. In addition, CRTC1 contributes to maintain neuronal proteome by promoting mRNA transport and protein synthesis at dendritic compartments. Biochemical analyses of purified synaptosomes from PS1 conditional knockout (PS1 cKO);Tau mouse model reveal increased pathological tau and reduced CRTC1 at synapses. Analysis of autophagy in PS1 cKO;Tau mouse model and human samples show that PS1 negatively regulates autophagy induction and maintains autolysosomes clearance, and its loss likely contributes to accumulation and aggregation of pathological tau. In conclusion, our findings indicate that synaptic CRTC1 locally modulates NMDAR-mediated neurotransmission and that increased pathological tau accumulation due to PS1 loss of function leads to CRTC1 deregulation and synapse pathology.

Introduction

1. Brain plasticity

The brain perceives, adapts and responds to environmental and internal body changes throughout the complex interaction of neurons and non-neuronal cells in neural circuits. The Nobel laureate Santiago Ramón y Cajal postulated a century ago that the strengthening and modification of neural circuits could contribute to the storage of new information (Ramón y Cajal, 1894). This theory was further developed by Donald O. Hebb, who proposed that memories are formed by the strengthening of synaptic connections between a presynaptic terminal and a postsynaptic neuron (Hebb, 1949). But it was not until the 1970s that the first experimental evidence of changes in synaptic strength was revealed (Bliss and Gardner-Medwin, 1973). Since then, activity-dependent remodeling of synapses, known as synaptic plasticity, has been extensively studied as it is considered the basis of several brain physiological processes, including learning and memory. Despite the ~71,000 scientific articles that include the words 'synaptic plasticity' in the U.S. National Library of Medicine (PubMed), the molecular mechanisms linking synapse activation and synapse remodeling that underlie memory are still largely unclear.

1.1. Hippocampal-dependent learning and memory

Several brain regions play a role in the consolidation of different forms of learning and memory, whereas the hippocampus is considered essential for storing and retrieving memories related to declarative memory of life experiences (Lynch, 2004, Neves et al., 2008). It was in 1957 when Scoville and Milner observed that the removal of part of the medial temporal lobe, including the hippocampus, to treat epilepsy induced anterograde amnesia in Henry Molaison (Scoville and Milner, 1957). Defective hippocampal-dependent memory is observed in animal studies in which controlled lesions were induced in the hippocampus (Martin et al., 2005) or when hippocampal synaptic plasticity was altered by pharmacological treatments (Morris et al., 1986). Therefore, it is widely accepted that the hippocampus is key in the consolidation of declarative memories and context-dependent spatial learning, as well as the regulation of emotional behaviors (El-Falougy and Benuska, 2006).

The hippocampus receives most inputs through the perforant pathway that are axons projecting from the entorhinal cortex. Medial and lateral layer II from the entorhinal cortex receive spatial and visual object information, respectively, and innervate granule cells of the dentate gyrus (DG). Granule cells axons, known as mossy fibers, project to the proximal apical dendrites of CA3 pyramidal cells, which innervate ipsilateral CA1 pyramidal cells, through Schaffer collaterals, and contralateral CA3 and CA1 pyramidal cells, through commissural fibers. There are also other

pathways in addition to this trisynaptic circuit. Layer II also innervates CA3 through the perforant pathway; CA1 pyramidal cells also receive inputs from layer III; and some excitatory and inhibitory interneurons contribute to the modulation of this circuit [(Neves et al., 2008, Lazarov and Hollands, 2016), **Figure 1**]. The subiculum and the CA1 subregions contribute to the outflow of the hippocampal circuit. These two regions innervate the entorhinal cortex, which in turn, re-connects with the neocortical regions that provide the original input. Additionally, the subiculum and CA1 monosynaptically contact with other brain areas, including the amygdala, the medial prefrontal and orbitofrontal cortices, the nucleus acumbens, and the anterior and posterior cingulate cortex (Small et al., 2011). Consequently, the complexity of the hippocampal circuitry extends beyond its internal circuit organization.

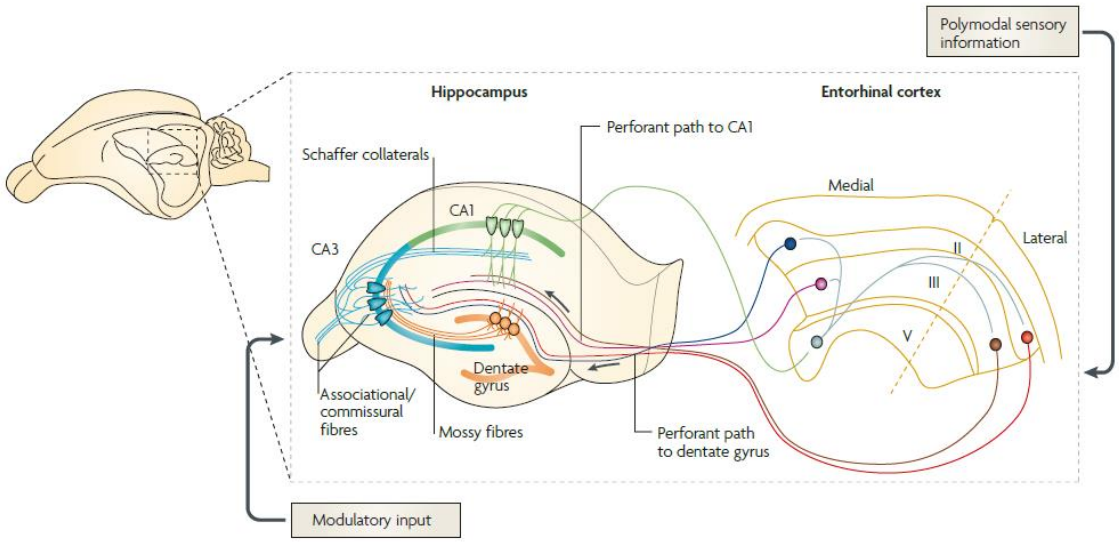

Figure 1. Mouse hippocampal circuitry. The hippocampus located in the temporal lobe is critical for learning and memory storage. The three regions of the hippocampus (CA1, green; CA3, blue; and dentate gyrus, orange) receive excitatory inputs from the entorhinal cortex, which is the brain region responsible of processing sensory stimuli. This excitatory synaptic network is also modulated by excitatory and inhibitory interneurons and it receives modulatory inputs from other brain areas. Image from (Neves et al., 2008).

1.2. Neuropathology and hippocampal dysfunction in tauopathies

Altered activity of the hippocampus is associated with memory deficits in aging and neurodegenerative diseases. Tauopathies are age-dependent heterogeneous dementias that are neuropathologically characterized by intracellular accumulation of the microtubule-associated protein tau (**Figure 2A**). The neuropathological hallmarks of tauopathies are neuronal loss, gliosis and spongiosis, which contribute to motor, sensory, behavioral and cognitive alterations (Lee et al., 2001). Primary tauopathies, a subgroup of frontotemporal lobar degeneration (FTLD), are mainly characterized by tau depositions. Among others, Pick's disease (PiD) and corticobasal degeneration (CBD) are primary tauopathies that differ in the affected cell types and brain regions, as well as the

accumulated tau isoforms (3R or 4R isoforms) [for a review (Götz et al., 2019, Chung et al., 2021)]. Thus, PiD is characterized by intracellular deposits of 3R tau, aslo known as Pick bodies, predominantly in neurons and with less extent to glial cells of the hippocampus and frontal and temporal cortices (Murayama et al., 1990, Probst et al., 1996, Ferrer et al., 2014, Falcon et al., 2018). In CBD, cerebral atrophy due to 4R tau inclusions occurs in the frontoparietal cortex and some subcortical areas affecting prominently the substantia nigra (Kouri et al., 2011, Zhang et al., 2020).

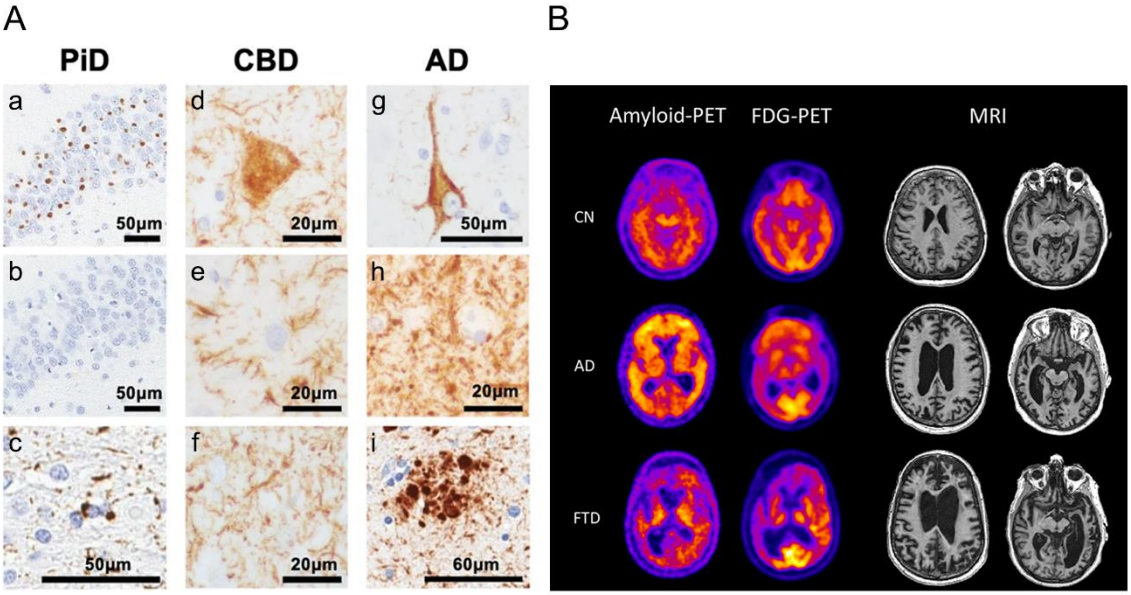

Figure 2. Neuropathological tau deposits and *in vivo* imaging of tauopathies. (A) Tau pathology in PiD (a-c), CBD (d-f) and AD (g-i). PiD is characterized by neuronal Pick bodies positive for 3R tau (a) but not for 4R tau (b), as well as for tau inclusion in oligodendrocytes (c). In CBD, tau-positive ballooned neurons (d), astrocytic (e) and neuropil tau threads (f) are observed. AD is characterized by neurofibrillary tangles (g), neuropil tau threads (t) and dystrophic neurites associated with a neurotic plaque (i). Image modified from (Chung et al., 2021) **(B)** Amyloid positron emission tomography (amyloid-PET), fluorodeoxyglucose PET (FDG-PET) and magnetic resonance imaging (MRI) in a cognitively normal (CN), AD and FTD individual. AD and FTD patients show significant hypometabolisms and brain atrophy compared to CN, whereas only AD patient shows β-amyloid pathology. Image from (Murray et al., 2014).

On the other hand, Alzheimer's disease (AD) which is the most prevalent form of dementia, is considered a secondary tauopathy as the extracellular accumulation of insoluble β-amyloid (Aβ) peptides also plays a central role in the pathogenesis (Hyman et al., 2012, Götz et al., 2019). In AD, neuropathology initially develops in the transentorhinal cortex and spreads to the entorhinal cortex, the hippocampus, and finally to the neocortex (Braak and Braak, 1991). The hippocampal regions most affected by AD are the subiculum and CA1 area, where the deposits of amyloid plaques and neurofibrillary tangles are particularly abundant (Frisoni et al., 2006). Loss of afferent inputs from the entorhinal cortex leads to a decline in the DG volume and in the total number of synaptic contacts (Scheff et al., 2006). This hippocampal damage disrupts the communication

between the hippocampus and the limbic and neocortical areas, which are required for the correct cognitive function (Hyman et al., 1984). Indeed, positron emission tomography (PET) and magnetic resonance imaging (MRI) have revealed metabolic and morphometric brain patterns underlying these diseases [(Pennanen et al., 2004, Li et al., 2011b, Murray et al., 2014), **Figure 2B**].

1.3. Short-term and long-term synaptic plasticity

Synaptic plasticity is an important event during developing and adult brain since mediates, among others, sensory inputs processing, and learning and memory. Excitatory neurotransmission mediated by the neurotransmitter glutamate and the ionotropic (iGluRs) and metabotropic glutamate receptors (mGluRs) contribute to different forms of synaptic plasticity (Traynelis et al., 2010, Reiner and Levitz, 2018, Mukherjee and Manahan-Vaughan, 2013). Synaptic activity can be enhanced or depressed, and last from milliseconds to hours leading to different forms of synaptic plasticity (Citri and Malenka, 2008).

Short-term synaptic plasticity (STP) refers to transient changes in synaptic strength that lasts from milliseconds to several minutes and that do not require persistent changes in the signaling machinery (Zucker and Regehr, 2002). During short-term facilitation (STF) there is an enhancement of the synaptic strength, whereas during short-term depression (STD), the synaptic efficacy of presynaptic terminals decreases in time due to less neurotransmitter release or less activation of postsynaptic receptors (Barroso-Flores et al., 2015). STP has an important role in sensory adaptation and habituation since it allows strong responses to novel stimuli and diminishes the responses to repeated inputs (Chung et al., 2002).

Long-term potentiation (LTP) is the most studied form of synaptic plasticity, particularly in the hippocampus, and is considered the cellular mechanism underlying learning and memory. LTP is divided into an early phase (E-LTP) and a late phase (L-LTP). E-LTP is caused by a single train of stimuli and lasts maximum a couple of hours. E-LTP does not require protein synthesis to induce a change in potentiation of synaptic transmission (Kandel, 2001). The activation of glutamate receptors in the postsynaptic neurons raises intracellular calcium levels leading to the activation of different cellular effectors such as kinases and phosphatases. These effectors induce covalent modifications of already synthesized proteins at synapses, potentiating preexisting synaptic connections (Malenka and Nicoll, 1999). On the contrary, L-LTP is caused by repeated trains of stimuli, lasts for about 24 hours, and requires gene transcription and protein synthesis (Kandel, 2001). LTP displays three physiological properties that makes it a plausible cellular mechanism underlying learning and memory: cooperativity, associativity and input specificity (Nicoll et al.,

1988). Cooperativity means that LTP can be produced by the coordinate activation of a certain number of synapses. Associativity refers to the ability to potentiate a weak stimulus when is associated with a strong stimulus. Input specificity implies that LTP is evoked only at activated synapses and not at inactive synapses from the same postsynaptic neuron. Importantly, this last feature increases the capacity of neurons to selectively store information (Citri and Malenka, 2008).

Long-term depression (LTD) is the complementary process of LTP and selectively weakens synaptic transmission when synaptic connectivity reaches the maximum level of efficacy. Therefore, LTP as well as LTD mediate learning and memory along with other forms of experience-dependent plasticity (Malenka and Bear, 2004).

1.4. Neuronal proteostasis and synaptic activity and plasticity

A balanced functional proteome is necessary for synapse maintenance and remodeling, and its deregulation is a hallmark of several age-related diseases (Cohen et al., 2013, Hipp et al., 2019). Protein homeostasis, or proteostasis, is the process by which cells adjust their protein content in response to intracellular or extracellular stimuli. This dynamic process relies on the accurate control of protein synthesis, conformation, post-translational modifications, localization, and degradation (Giandomenico et al., 2022).

1.4.1. Local protein synthesis in neurons

Long-lasting forms of synaptic plasticity require mRNAs and protein synthesis (Kandel, 2001). Increasing evidence demonstrate that mRNAs localize in axons and dendrites, where are locally translated into proteins [for recent reviews, (Holt et al., 2019, Biever et al., 2019)]. Local protein synthesis provides a strategy to rapidly fulfill local protein demand upon a certain stimuli, contributing to neuronal development, synaptogenesis, survival and synaptic plasticity (Holt et al., 2019). Transcripts are delivered to distal compartments in a microtubule-dependent manner through the interaction with RNA binding proteins (RBPs) (Bassell et al., 1998, Eom et al., 2003). Although no canonical sequence that drives mRNA trafficking has been found, the 3’ and 5’ untranslated (UTR) regions play a key role in the transport and localization of the mRNAs (Meer et al., 2012, Tushev et al., 2018, Ciolli Mattioli et al., 2019). Most hippocampal transcripts contain more than one 3’ UTR isoform, and the regulation of these particular isoforms upon synaptic plasticity may change transcript localization and translation (Tushev et al., 2018). Experiments in Aplysia have shown that while the 3’ UTR drives translocation of mRNAs to dendrites, the 5’ UTR is specifically required for synaptic localization (Meer et al., 2012). Epitranscriptomic modifications of mRNAs may also be involved in regulating the transport and local translation of transcripts

(Merkurjev et al., 2018). Additionally, the presence of the transcriptional machinery is indispensable for local protein synthesis. Electron microscopy experiments have visualized pools of ribosomes in dendritic shafts as well as in the base of dendritic spines (Steward and Levy, 1982).

More than 2,500 transcripts localized at axons and/or dendrites in hippocampal neurons have been identified, most encoding for synaptic receptors, scaffolds and signaling proteins (Cajigas et al., 2012). Several proteins have been detected to be locally synthesized in dendritic compartments, such as CaMKIIα, β-actin and Arc (tom Dieck et al., 2015, Yoon et al., 2016, Na et al., 2016). LTP induction is associated with enhanced polyribosome detection in dendritic spines to potentiate local protein synthesis (Ostroff et al., 2002, Ostroff et al., 2018). Under basal conditions, some transcripts, such as *Bdnf*, localize mainly at the soma but, upon synaptic activity, mRNA levels are upregulated and migrate to distal dendrites (Baj et al., 2011). Consequently, disruption of local protein synthesis leads to impairments in stabilization of synaptic plasticity and memory consolidation (Miller et al., 2002, Bradshaw et al., 2003, Younts et al., 2016). These observations suggest that local protein synthesis is crucial for synaptic plasticity and learning/memory processes (Huber et al., 2000, Miller et al., 2002, Bradshaw et al., 2003).

1.4.2. Local protein degradation in neurons

Besides local protein synthesis, regulation of synaptic protein degradation is necessary for adjusting the levels of functional proteins and controlling cellular accumulation of misfolded and/or damaged proteins. Two main proteolytic pathways regulate protein degradation in the cell: the ubiquitin-proteasome system and the autophagosomal-lysosomal pathway. Small, short-lived, and misfolded proteins are degraded by the proteasome, whereas large, long-lived molecules, protein aggregates and organelles are degraded through the autophagy pathway (Dikic, 2017).

Autophagy is a catabolic cellular process in which proteins and organelles are delivered to lysosomes for degradation. Depending on how cargoes are delivered to the lysosome, autophagy pathways are classified as: chaperone-mediated autophagy, microautophagy and macroautophagy (Mizushima et al., 2010, Hansen et al., 2018). In chaperone-mediated autophagy, proteins are unfolded and transported into the lysosome by a chaperone complex (Kanno et al., 2022); in microautophagy, lysosomes directly engulf cytosolic components through invaginations in their membrane (Schuck, 2020); and in macroautophagy, hereafter simply referred as autophagy, cargoes are delivered to the lysosomes inside a double-membraned organelle called autophagosome (Levine and Kroemer, 2008, Mizushima et al., 2010). Autophagy is a conserved cellular mechanism that follows into five steps: (1) initiation triggered by Unc-51-like kinase 1 (ULK1) phosphorylation; (2) formation and expansion of an isolation membrane (phagophore); (3)

phagophore elongation and enclosure of the cytosolic cargo that results in the formation of the autophagosome; (4) fusion of the autophagosome with the lysosome to form an autolysosome; and (5) degradation of the captured materials together with the inner autophagosomal membrane [(Levine and Kroemer, 2008, Mizushima et al., 2010, Egan et al., 2011, Hansen et al., 2018), **Figure 3**].

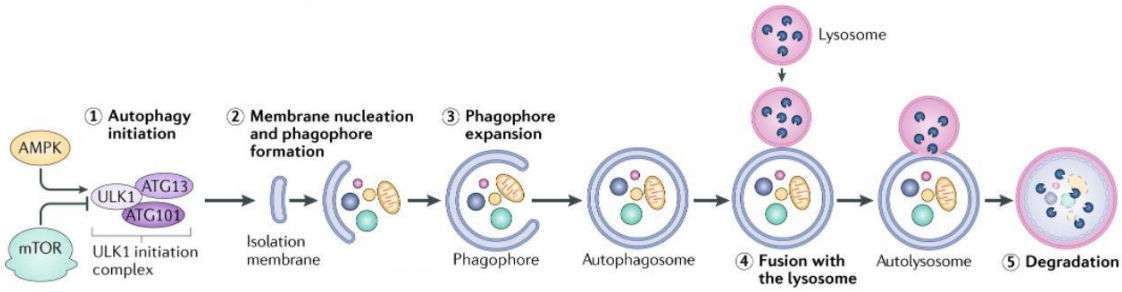

Figure 3. Diagram of autophagy flux. Autophagy is initiated by ULK1 phosphorylation, which is regulated by the sensors mTOR and AMPK. Then, the phagophore elongates to engulf the cargoes, including a portion of cytoplasm. When the edges of the phagophore fuse, the autophagosome is formed. Finally, the autophagosome fuses with the lysosome to form an autolysosome, leading to the degradation of the autophagic cargoes by lysosomal hydrolases. Degradation products, such as amino acids and other small molecules, are delivered back to the cytoplasm for new biosynthetic reactions. mTOR: mammalian target of rapamycin; AMPK: AMP-activated kinase; ULK1: Unc-51-like kinase 1. Image modified from (Hansen et al., 2018).

Synapses are plastic structures whose proteome change constantly in response to neuronal activity. Interestingly, autophagosomes are localized in pre- and postsynaptic compartments, and along the axon (Maday and Holzbaur, 2016, Kallergi et al., 2022). Although postsynaptic scaffolding proteins PSD95, PICK1 and Shank3 are found inside autophagosomes (Nikoletopoulou et al., 2017), it is still controversial whether degradation of synaptic proteins via autophagy occurs locally at synaptic compartments or exclusively in the soma (Hollenbeck, 1993, Goo et al., 2017, Kulkarni et al., 2021, Yap et al., 2022). Axonal and dendritic autophagosomes can be retrogradely transported to the soma for degradation (Hollenbeck, 1993, Yap et al., 2022). But the recruitment of lysosomes and formation of autolysosomes in synapses has also been reported, suggesting that synaptic cargoes can be locally degraded (Goo et al., 2017, Ji et al., 2019, Kulkarni et al., 2021). Moreover, autophagy can be activated or inhibited in an activity-dependent manner, indicating its important role in synaptic strength regulation (Ehlers, 2000, Shehata et al., 2012, Nikoletopoulou et al., 2017). While chemical-LTD induces autophagy and contributes to AMPARs degradation (Ehlers, 2000, Shehata et al., 2012, Pan et al., 2021), BDNF-mediated LTP inhibits autophagy (Nikoletopoulou et al., 2017).

Perturbances in autophagy are associated with pathological protein accumulation and aggregation in age-related neurodegenerative diseases (Wong and Cuervo, 2010). Failure in different steps of

autophagy flux can lead to the accumulation of intracellular hyperphosphorylated tau, which is the common hallmark of tauopathies (Boland et al., 2018). Accumulation of autophagosomes in dystrophic neurites in AD samples and mouse models of neurodegeneration suggests that accumulation of pathological tau originates from alterations in autophagosomes clearance rather than in a deficient autophagy induction (Nixon et al., 2005, Lee et al., 2007, Boland et al., 2008). This accumulation of autophagosomes indicates decreased degradative activity of lysosomes. In fact, PS1 mutations associated with early-onset familial Alzheimer's disease (FAD) disrupt lysosomes acidification and function (Lee et al., 2010, Neely et al., 2011, Hung and Livesey, 2018). Different pharmacological approaches to enhance autophagy initiation, autophagosomes transport and lysosomal degradative activity reduce aggregated hyperphosphorylated tau [for a detailed review see (Boland et al., 2018). However, for the success of the autophagy-based therapy in neurodegenerative diseases it is still necessary the identification of the specific altered autophagy steps.

2. Glutamatergic neurotransmission

Hippocampal activity is dependent on glutamatergic neurotransmission, which modulates synaptic plasticity and, therefore, learning and memory. Glutamatergic neurotransmission is mediated by glutamate, an aminoacidic neurotransmitter that acts as the major excitatory neurotransmitter in the mammalian central nervous system (CNS).

Glutamate is released in a calcium and soluble N-ethylmaleimide-sensitive factor attachment protein receptor (SNARE)-dependent manner from the presynaptic neuron (Pang and Südhof, 2010). The postsynaptic effect of glutamate can be mediated by two types of glutamate receptors: metabotropic glutamate receptors (mGluRs) and ionotropic glutamate receptors (iGluRs) (Scheefhals and MacGillavry, 2018). mGluRs are G protein-coupled receptors that are divided into three subfamilies depending on their sequence homology, second messenger coupling and pharmacological properties. Group I (mGluR1 and mGluR5) are mainly localized at postsynaptic sites and are coupled to $G_{\alpha,q}$, which stimulates phospholipase C (PLC) leading to an increase of intracellular Ca^{2+} and protein kinase C (PKC) activation. Group II (mGluR2 and mGluR3) and group III (mGluR4, mGluR6, mGluR7 and mGluR8) localized in axonal terminals and are coupled to G_i/G_0 proteins that inhibit adenylate cyclase (AC), reducing the levels of cAMP and inhibiting protein kinase A (PKA) [for a review, (Suh et al., 2018)]. iGluRs are tetrameric channels that allow sodium and calcium influx upon glutamate binding to the extracellular ligand-binding domain. Depending on their pharmacological properties, iGluRs can be subdivided into: α-amino-3-hydroxy-5-methyl-

4-isoxazole (AMPA), N-methyl-D-aspartate (NMDA) and kainite receptors (Traynelis et al., 2010). iGluRs are enriched in the PSD core near glutamate release sites, whereas mGluRs are localized further from the presynaptic release site at perisynaptic domains. The spatial distribution of mGluRs and iGluRs varies among the postsynaptic density (PSD) and has functional implications on the activation of these receptors (Scheefhals and MacGillavry, 2018).

2.1. AMPA receptors

AMPA receptors (AMPARs) are the principal transducers of fast excitatory neurotransmission in the CNS. Developmental and activity-dependent changes in the number and composition of AMPARs are fundamental for neural circuit formation and maturation, excitatory synapse formation and stabilization, and synaptic plasticity. On the contrary, disruption of AMPAR function, expression and/or trafficking at PSD are linked to neurological disorders (Henley and Wilkinson, 2013, Diering and Huganir, 2018).

2.1.1. AMPA receptor subunit composition

AMPARs are heterotetrameric complexes composed by different combination of four subunits (GluA1-GluA4) that are encoded by four closely related genes (*Gria1-4*) (Traynelis et al., 2010). Each subunit has a highly conserved ligand binding domain and transmembrane domain that allow glutamate binding and channel pore assembly, and a variable extracellular amino-terminal and intracellular carboxy-terminal (Diering and Huganir, 2018). GluA1, GluA2 and GluA3 are extensively expressed in the CNS; whereas GluA4 is expressed during brain development and it is barely expressed in the adult brain, where it is mainly found in the cerebellum (Schwenk et al., 2014, Zhu et al., 2000). In the hippocampus, AMPARs are GluA1/GluA2 or GluA2/GluA3 heteromers, but also a small amount of GluA1/GluA3 heteromers have been found (Wenthold et al., 1996, Lu et al., 2009).

2.1.2. AMPA receptor trafficking

Several molecular and cellular mechanisms controlling AMPARs delivery to synapses are critical for induction and maintenance of LTP. At early development, GluA4-containing AMPARs are delivered to synapses by spontaneous activity (Zhu et al., 2000). But, in the adult brain, there are two types of synaptic delivery depending on the subunit composition of AMPARs. On the one hand, GluA1/GluA2 heteromers are transported to synapses in an activity-dependent manner, and once in the PSD they enhance synaptic transmission. On the other hand, GluA2/GluA3 heteromers are continuously being delivered to the synapse in an activity-independent manner. This process might

be involved in the preservation of stable transmission for longer periods of time or in the absence of neuronal activity (Hayashi et al., 2000, Shi et al., 2001).

Other hypothetical models postulate that AMPARs trafficking is independent of subunit composition and that ultrastructural rearrangements are required to recruit, anchor and remove glutamate receptors at PSD. Thus, in the absence of neuronal activity, AMPARs are constitutively recycled between the cell surface and cytosolic endosomes. But during LTP induction, AMPAR exocytosis is enhanced and they laterally diffuse from extrasynaptic to synaptic sites to potentiate synaptic plasticity. In this activity-dependent recruitment of AMPARs, different structural proteins such as A-kinase anchoring proteins (AKAPs), or transmembrane AMPAR regulatory proteins (TARPs) are key players [(Cheng et al., 2020, Chen et al., 2000), **Figure 4**].

Phosphorylation of the carboxy-terminal region also regulates the subcellular localization and trafficking of AMPARs. PKA-dependent phosphorylation of GluA1 at Ser845 promotes GluA1-containing receptors retention at the cell surface, hence priming the synapse for future potentiation (Roche et al., 1996, Diering et al., 2016). Additional phosphorylation of GluA1 at Ser831 by PKC and Ca^{2+}/calmodulin-dependent protein kinase II (CaMKII) promotes GluA1 targeting to PSD as well as channel conductance to potentiate synaptic transmission [(Barria et al., 1997, Mammen et al., 1997, Diering et al., 2016), **Figure 4**].

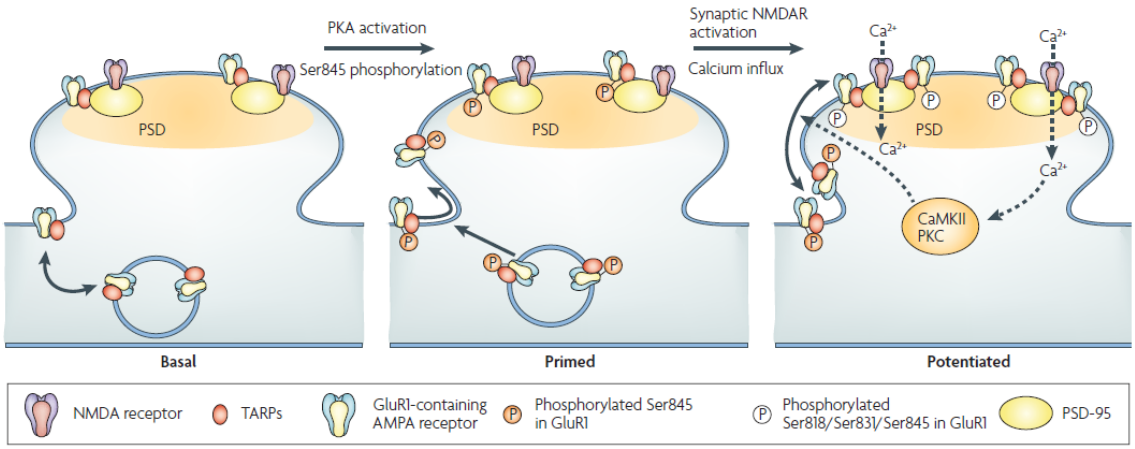

Figure 4. AMPA receptors delivery to synapses. In basal conditions, AMPARs constitutively recycle between endosomes and the cell surface. GluA1 subunit phosphorylation by PKA at Ser 845 facilitates the incorporation of AMPARs to extrasynaptic sites, priming the synapse for future potentiation. Ca^{2+} influx through NMDAR activates PKC and CaMKII, triggering AMPARs stabilization at the PSD through GluA1 phosphorylation at Ser 831. This process is also regulated by TARPs, scaffolding proteins such as PSD95 and the actin cytoskeleton reorganization. Image from (Derkach et al., 2007).

By contrast, GluA2 subunit is important in AMPARs removal from the PSD during LTD. PKC-dependent phosphorylation of GluA2 at Ser880 destabilizes GluA2 interaction with PSD scaffolding

proteins, promoting receptor endocytosis (Steinberg et al., 2006). Interestingly, when GluA2 C-terminal is replaced with GluA1 C-terminal, NMDAR-LTD is suppressed in the hippocampus, indicating that GluA2 is essential for AMPARs endocytosis (Zhou et al., 2018b).

2.1.3. AMPA receptor dysregulation in Alzheimer's disease

Deregulation of synaptic transmission and plasticity is present at early stages of AD, and eventually leads to cognitive decline and memory loss (Selkoe, 2002). Alterations in AMPARs synaptic localization and/or turnover are, to a certain extent, responsible of these neuropathological symptoms. Synaptic degeneration induced by Aβ has been associated with the synaptic removal and endocytosis of AMPARs (Hsieh et al., 2006, Zhao et al., 2010, Miñano-Molina et al., 2011, Zhang et al., 2018). Aβ-treated neuronal cultures as well as APP transgenic mouse model showed a decrease in GluA1 subunit levels at the cell surface and impaired AMPAR-mediated currents (Almeida et al., 2005, Hsieh et al., 2006, Gu et al., 2009, Miñano-Molina et al., 2011). Increased calcineurin-dependent dephosphorylation of GluA1 Ser 845 along with a reduction in CaMKII synaptic pools contribute to the Aβ-dependent downregulation of AMPARs cell surface localization (Miñano-Molina et al., 2011, Gu et al., 2009). Additionally, Aβ interaction with GluA2-containing AMPARs induce receptor internalization and degradation, which is mediated by ubiquitination (Zhao et al., 2010, Guntupalli et al., 2017, Zhang et al., 2018). Neuronal cultures incubated with Aβ and brain tissue from AD patients showed an increase in AMPARs ubiquitination and, consequently, a reduction in total AMPARs levels (Guntupalli et al., 2017, Zhang et al., 2018). Consequently, the removal of AMPARs from PSD sites leads to LTD and changes in the number and morphology of dendritic spines (Baglietto-Vargas et al., 2018). Moreover, pathological hyperphosphorylated tau accumulation at dendritic spines suppressed AMPAR-mediated synaptic responses prior to synapse loss through the disruption of AMPARs trafficking or anchoring at postsynaptic sites (Hoover et al., 2010). In contrast, Whitcomb and collaborators reported that Aβ oligomers can facilitate synaptic transmission by the insertion of GluA1 homomeric AMPARs, which are highly permeable to calcium, via the PKA-dependent phosphorylation of Ser 845. This potentiation in AMPAR-mediated synaptic currents occurs as a first response to the presence of Aβ and could prime the subsequent dysfunction in synaptic transmission (Whitcomb et al., 2015).

2.2. NMDA receptors

NMDA receptors (NMDARs) are high Ca^{2+}-permeable ion channels that mediate slow glutamatergic neurotransmission since they are blocked by extracellular Mg^{2+} in basal conditions, and they need a previous depolarization of the membrane to become active (Nowak et al., 1984). Additionally, the

co-agonist glycine or D-serine are required together with glutamate for their activation (Paoletti et al., 2013). Like AMPARs, NMDARs can transform neuronal activity patterns into long-term changes and, therefore, their dysregulation is related to neurological and psychiatric disorders.

2.2.1. NMDA receptor subunit composition

NMDARs subunits are classified into three subfamilies depending on their sequence homology (GluN1, GluN2 and GluN3). GluN1 subunit is encoded by a single gene (*Grin1*) but has eight different splice variants with variable length of the C-terminal domain that confer to these subunits different pharmacological and trafficking properties (Winkler et al., 1999, Horak and Wenthold, 2009). GluN2 subunits are encoded by four different genes (*Grin2a, Grin2b, Grin2c* and *Grin2d*), whereas two genes encode two different GluN3 subunits (*Grin3a* and *Grin3b*) [(Monyer et al., 1994, Pachernegg et al., 2012), **Figure 5A**]. This subunit heterogeneity generates a wide array of receptors that show a different spatiotemporal expression pattern (**Figure 5C**). Although there are some differences in GluN1 isoforms expression profile, GluN1 is ubiquitously expressed in the brain from embryonic stages to adulthood (Laurie and Seeburg, 1994). In early development, GluN2B, GluN2D and GluN3A are the subunits mainly expressed but, then, their expression progressively declines and is restricted to certain brain areas (Monyer et al., 1994). This suggests that these subunits are important for synaptogenesis and synaptic maturation (Pachernegg et al., 2012). GluN2A and GluN2C are also expressed early after birth, but while GluN2A becomes widely expressed in every area of the adult brain, GluN2C expression is restricted to the cerebellum and the olfactory bulb (Monyer et al., 1994). In the adult brain, especially in the cortex and hippocampus, GluN2A and GluN2B are the most abundant subunits suggesting that they have a relevant role in synaptic plasticity (Monyer et al., 1994).

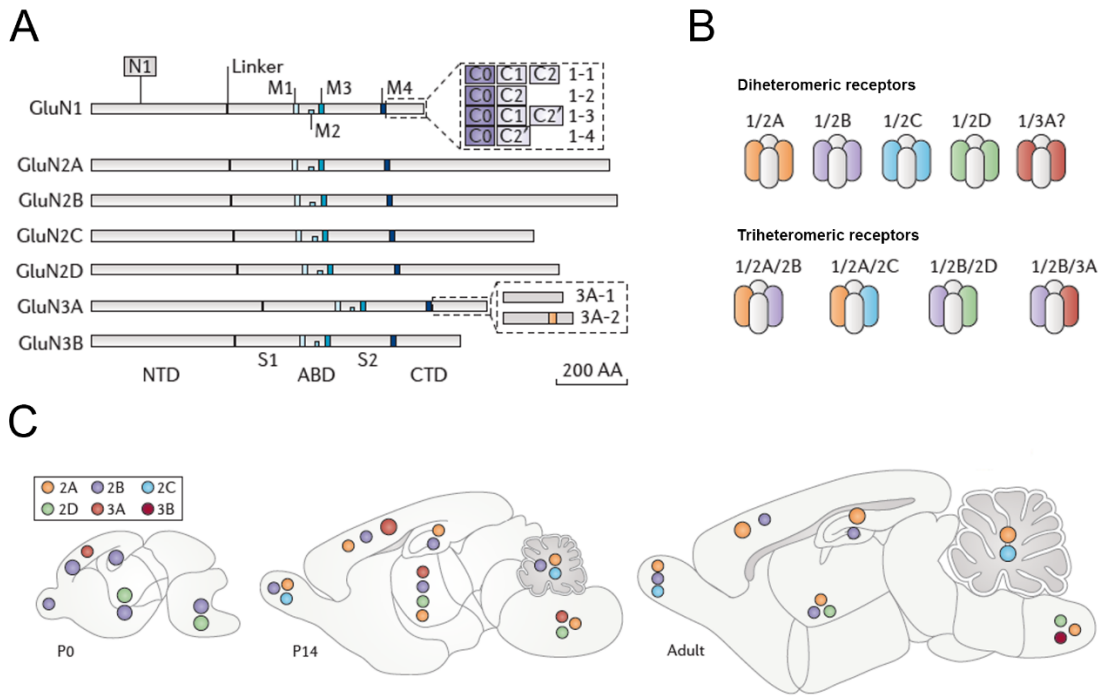

Figure 5. NMDARs subunits heterogeneity and expression in the CNS. (**A**) Seven independent genes (*Grin1, Grin2a, Grin2b, Grin2c, Grin2d, Grin3a* and *Grin3b*) encode the NMDAR subunits (GluN1, GluN2A-GluN2D and GluN3A-GluN3B), and alternative splicing leads to a higher diversity of subunits. NTD: N-terminal domain; ABD: agonist binding domain; CTD: C-terminal domain; M1-M4: transmembrane domains. (**B**) These subunits are assembled into heterotetramers constituted always by two GluN1 subunits plus two GluN2 and/or GluN3 subunits that can be identical (diheteromeric receptors) or different (triheteromeric receptors). (**C**) NMDAR subunit distribution and expression in the mouse brain at postnatal day 0 (P0) and 14 (P14), and in the adult stage. Image modified from (Paoletti et al., 2013).

NMDARs subunits share a similar structure with AMPARs consisting on four domains: (1) a N-terminal domain (NTD); (2) an agonist binding domain (ABD) that binds glycine or D-serine in GluN1 and GluN3 or glutamate in GluN2; (3) a transmembrane domain (TMD) that forms the channel pore; and (4) an intracellular C-terminal domain (CTD). The NTD and CTD are the most variable regions and, consequently, confer specific properties to the subunits (Paoletti et al., 2013). NMDARs usually combine two copies of the obligatory subunit GluN1 and two copies of GluN2 and/or GluN3 subunits forming di- or triheteromeric receptors [(Sheng et al., 1994), **Figure5B**].

Channel conductance and Ca^{2+} permeability are potentiated by GluN1/GluN2A and GluN1/GluN2B heteromers, whereas these properties are decreased in GluN2C- and GluN2D-containing NMDARs. These observations suggest that GluN2 subunit is critical for determining channel conductance, including maximal channel open probability, agonist sensitivity, Ca^{2+} permeability and deactivation kinetics (Paoletti, 2011).

2.2.2. NMDA receptor trafficking

NMDARs localize at the PSD as part of a macromolecular complex composed by scaffolding and adaptor proteins, which links NMDAR activation to downstream signaling proteins (Scannevin and Huganir, 2000). However, NMDARs composition and number at synapses is not static and varies during development and in response to synaptic activity. GluN1 subunit drives NMDARs trafficking from the endoplasmic reticulum (ER) to the postsynaptic membrane. GluN1 subunit C-terminal has an ER retention motif (ER) as well as phosphorylation sites that drive NMDARs delivery. Unassembled GluN1 subunits are retained in the ER, but, once they are assembled with GluN2 subunits, the retention motif is masked and the heteromeric receptor is inserted in the cell surface through SNARE-dependent exocytosis (McIlhinney et al., 1998, Lan et al., 2001). Furthermore, phosphorylation of GluN1 subunit near its ER retention motif by PKA (Ser897) and PKC (Ser890 and Ser896) potentiates NMDARs delivery to the cell surface [(Scott et al., 2003), **Figure 6**]. The interaction between GluN2 subunits PDZ-binding motif with scaffolding proteins such as PSD95 ensures synaptic localization of NMDARs and, also, contributes to channel gating and conductance (Roche et al., 2001, Lin et al., 2004, Prybylowski et al., 2005, Lin et al., 2006, Kim et al., 2007). Indeed, tyrosine dephosphorylation within the internalization domain of GluN2A and GluN2B subunits leads to receptor destabilization at the PSD and the consequent internalization and degradation of NMDARs (Roche et al., 2001, Vissel et al., 2001, Groc et al., 2006).

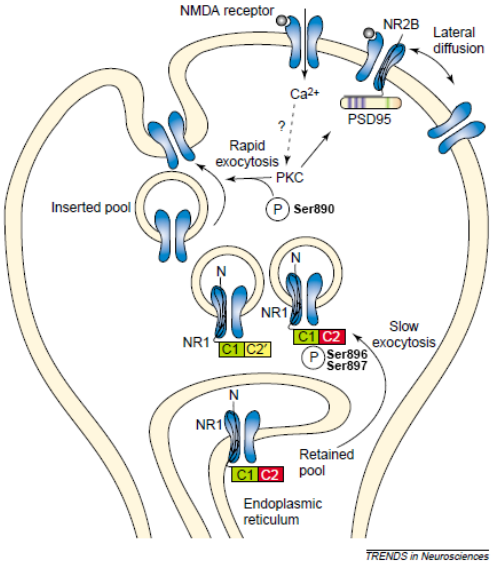

Figure 6. Activity-dependent synaptic delivery of NMDA receptors. In the endoplasmic reticulum (ER) there is a pool of NMDARs that are ready to be delivered to the postsynaptic membrane upon synaptic activity. Activity-dependent activation of PKA and PKC regulate NMDAR trafficking by different mechanisms. First, phosphorylation of GluN1 at Ser 896 and Ser 897 by PKC and PKA, respectively, induce a slow exocytosis from the ER through the secretory pathway. Second, PKC-mediated GluN1 phosphorylation at Ser 890 induces a rapid exocytosis that ends with the docking of the receptor at the cell surface. Imaged modified from (Carroll and Zukin, 2002).

2.2.3. NMDA receptor in aging and Alzheimer's disease

In aging, cognitive abilities are compromised as a result of altered function of the hippocampus and synapse dysfunction and loss (Henley and Wilkinson, 2013). Among the glutamate receptors, NMDARs are particularly vulnerable to aging. Some studies show that mRNA and protein levels of GluN1 subunits are decreased in old mice compared with young adults (Magnusson et al., 2002, Magnusson, 2000). Although, this effect has also been observed in other species, there is still controversy about GluN1 subunit decline in different brain region during aging (Magnusson et al., 2010). For this reason, it has been proposed that GluN1 decline could be due to environmental factor and experiences during aging (Magnusson et al., 2010). While there is no effect of aging on GluN2A expression, GluN2B mRNA and protein levels are reduced (Magnusson, 2000, Clayton and Browning, 2001, Bai et al., 2004, Ontl et al., 2004). Because of these subunit expression alterations, GluN2A/GluN2B ratio is increased in aged animals, leading to NMDARs that have decreased agonist affinity and reduced LTP (Magnusson, 2000, Billard and Rouaud, 2007). Moreover, GluN2B protein levels at synaptic fraction are highly reduced compared with total tissue, suggesting that there is also a defect in subunit localization in old mice (Zhao et al., 2009). Interestingly, overexpression of GluN2B subunit in the forebrain or the hippocampus improves learning and memory of aged mice (Cao et al., 2007, Brim et al., 2013). It has also been reported that age-related changes in the neuronal redox state contributes to a decrease in CaMKII activity and, consequently, impairs NMDAR-mediated synaptic responses and LTP induction in the hippocampus (Bodhinathan et al., 2010).

Besides alterations in AMPARs trafficking and degradation, changes in NMDAR subunit expression, localization and internalization was associated with neuropathological stages in AD. Analyses of brain samples from AD patients revealed that GluN2A and GluN2B mRNA and protein levels are reduced in the hippocampus and the entorhinal cortex, as well as phosphorylated GluN2B (Bi and Sze, 2002, Sze et al., 2001). However, it is still unknown whether these declines are due to synaptic or neuronal loss. The proportion of GluN1 subunit transcripts containing the N-terminal cassette is also lowered in brain regions of AD patient, which could affect the responsiveness of neurons (Hynd et al., 2001). Interestingly, several single nucleotide polymorphisms (SNPs) in the coding regions of *GRIN2B* and *GRIN3A* genes are linked to AD (Stein et al., 2010, Andreoli et al., 2014, Liu et al., 2009). Experiments with Aβ-treated cultured neurons or neuronal cultures of APP_{Swe} mice demonstrated that Aβ promoted a reduction in GluN1 and GluN2B subunit expression at the cell surface that may contribute to synaptic dysfunction (Snyder et al., 2005, Goto et al., 2006). Further experiments have confirmed that Aβ specifically reduced the expression of GluN2B subunit at synaptic and not at

extrasynaptic sites (Li et al., 2011a). The excessive activation of GluN2B-containing extrasynaptic NMDARs by Aβ leaded to hippocampal LTP inhibition and LTD facilitation (Li et al., 2009, Li et al., 2011a, Rönicke et al., 2011, Ferreira et al., 2012). These studies suggest that aberrant activation of extrasynaptic NMDARs may be responsible of glutamate excitotoxicity and neurodegeneration in AD. Indeed, the activation of GluN2B-containing NMDARs in cultured neurons evoked an immediately increase in calcium that disturbed intracellular calcium homeostasis (Ferreira et al., 2012). So, the internalization of synaptic but not extrasynaptic NMDARs may alter the balance between the pro-survival synaptic and the pro-death extrasynaptic signaling leading to neuronal death (Hardingham, 2006, Hardingham et al., 2002, Li et al., 2011a, Ferreira et al., 2012).

3. cAMP-response element-binding protein (CREB) signaling

The cAMP-response element binding protein (CREB) is a transcription factor ubiquitously expressed in the nervous system that belongs to the bZIP superfamily of transcription factors. The CREB structure consists of a central kinase-inducible domain (KID) flanked by two glutamine rich domains, and a C-terminal basic leucine zipper (bZIP) domain (Altarejos and Montminy, 2011). In response to cAMP levels, calcium influx or growth factors, CREB is phosphorylated at Ser133, localized in the KID domain, by several activity-inducible kinases (PKA, PKC, CaMKII, CaMKIV and MAPK) [(Brindle et al., 1995, West et al., 2001), **Figure 8B**]. Phosphorylated CREB at Ser 133 (pCREB) results in the recruitment of transcription coactivators such as CREB-binding protein (CBP) and p300, allowing CREB-dependent gene expression by acetylating histones and recruiting RNA polymerase II complexes (Goodman and Smolik, 2000, Ogryzko et al., 1996, Kee et al., 1996). CREB dephosphorylation and inactivation is also regulated in an activity-dependent manner by the protein phosphatase type 1 (PP1) and 2A (PP2A) [(Alberts et al., 1994, Wadzinski et al., 1993), **Figure 8B**]. CREB activity is also controlled by other posttranslational modifications (glycosylation, ubiquitination and acetylation), indicating that CREB-dependent transcription is finely regulated (Rexach et al., 2012, Comerford et al., 2003, Lu et al., 2003). CREB specifically binds to DNA through its bZIP domain to the highly conserved palindromic CRE sequence (5'-TGACGTCA-3') present in promoter regions of hundreds of genes (Impey et al., 2004). These genes codify for neurotransmitters, growth factors, transcription factors, signal transduction factors and metabolic enzymes, which have a role in neuronal development, plasticity and neuroprotection (Impey et al., 2004).

De novo mRNA and protein synthesis are required for memory consolidation (Kandel, 2001). CREB is indispensable for the regulation of gene transcription involved in the formation of long-term

memories in different species (Yin et al., 1994, Bourtchuladze et al., 1994, Josselyn et al., 2001). In addition, CREB is essential for the stability of memories after retrieval, known as reconsolidation (Kida et al., 2002). Memory acquisition is thought to be achieved by the coordinated activity of subsets of neurons referred as engram cells (Tonegawa et al., 2015), and indeed CREB activity is critical for memory consolidation and retrieval engrams (Zhou et al., 2009, Matos et al., 2019). Alternatively, CREB deregulation results in memory impairments and degeneration in aging and neurodegenerative disorders [for a review, (Saura and Valero, 2011)].

In non-pathological aging there is a downregulation of neuronal genes associated with synaptic function that contribute to cognitive impairments (Loerch et al., 2008). Reduced levels of total or pCREB are associated with memory deficits in old animals, suggesting that this transcriptional factor is critical for the transcription of neuroplasticity genes (Brightwell et al., 2004, Kudo et al., 2005, Porte et al., 2008). In Huntington's disease (HD), a neurodegenerative disease characterized by motor and cognitive deficits, CREB phosphorylation is repressed, CBP expression and function is reduced and, consequently, CREB-dependent gene transcription is inhibited (Wyttenbach et al., 2001, Gines et al., 2003, Choi et al., 2009, Giralt et al., 2012). On the other hand, in postmortem brain samples of AD patients, pCREB levels are reduced whereas total CREB levels remain constant (Yamamoto-Sasaki et al., 1999). This decline in pCREB levels has also been observed in Aβ-treated neurons and neurons from APP/PS1 mouse model prior to neurodegeneration, indicating that there is a failure in the cAMP/PKA/CREB signaling pathway in early phases of AD (Tong et al., 2001, Vitolo et al., 2002, Gong et al., 2004, Liang et al., 2007, Ma et al., 2007). Although under basal or FSK-stimulated conditions Aβ does not affect pCREB levels in cultured neurons, NMDA-dependent CREB phosphorylation is inhibited by Aβ supporting the hypothesis of a deregulation in the cAMP/PKA/CREB signaling pathway (Snyder et al., 2005, España et al., 2010). Interestingly, the potentiation of this signaling pathway with the phosphodiesterase inhibitor type 4, Rolipram, restored the hippocampal function in mouse models of AD (Vitolo et al., 2002, Gong et al., 2004).

4. Synapse-to-nucleus signaling

Learning and memory rely on the coordinated communication between neurons and among the different neuronal compartments. Glutamate binding to postsynaptic receptors, specifically to NMDARs, leads to an increase in intracellular Ca^{2+} that produces short- and long-term changes in synaptic function. On the one hand, rises in synaptic Ca^{2+} leads to local changes such as insertion and removal of glutamate receptors, posttranslational modifications of synaptic proteins, and stimulation of protein translation or degradation. On the other hand, Ca^{2+} influx at synapses or

cytosol also has distal effects at the nucleus by activating signaling pathways that end up in the expression of genes involved in long-term synaptic responses (Greer and Greenberg, 2008). So, synapse-to-nucleus signaling is essential for neuronal development, plasticity and repair. Signals can be transmitted rapidly through electrochemical signals or calcium waves (Markram et al., 1995, Watanabe et al., 2006), which induce the immediate early gene expression (Murphy et al., 1991); or slowly via synaptonuclear factors that regulate more specific genetic programs involved in neuronal development, repair and plasticity [for a recent review, (Parra-Damas and Saura, 2019), **Figure 8**].

4.1. Synaptonuclear factors

Synaptonuclear factors are synaptic proteins that contain a nuclear localization sequence (NLS) that allows their translocation from synapses to the nucleus upon an increase in intracellular Ca^{2+} [(Kaushik et al., 2014), **Figure 7**]. There are a dozen of characterized synaptonuclear factors, including: cAMP-response element binding protein 2 (CREB2), CREB-regulated transcriptional coactivator 1 (CRTC1), Jacob, amyloid beta protein precursor intracellular domain associated protein-1 (AIDA1), nuclear factor kappa-light-chain-enhancer of active B cells (NF-κB), SH3 and multiple ankyrin repeat domains 3 (Shank3), RING finger protein 10 (RNF10), extracellular signal-regulated kinase (ERK), and Ca^{2+}/calmodulin dependent protein kinase II gamma (γCaMKII) [(Parra-Damas and Saura, 2019), **Figure 7**]. Translocation of these factors to the nucleus is a highly regulated process and can occur through an energy-dependent retrograde transport along microtubules or through protein diffusion [(Jordan and Kreutz, 2009, Ch'ng and Martin, 2011), **Figure 7**]. These synaptonuclear factors are essential for synaptic plasticity, learning and memory, and neuronal survival. In contrast, dysregulation or mutations of some of these factors lead to synaptic dysfunction, dendritic degeneration, and memory loss observed in neurodegenerative and neuropsychiatric disorders (Parra-Damas and Saura, 2019). Importantly, the mechanisms modulated by synaptonuclear factors at synapses during synaptic plasticity and learning and memory remain poorly understood.

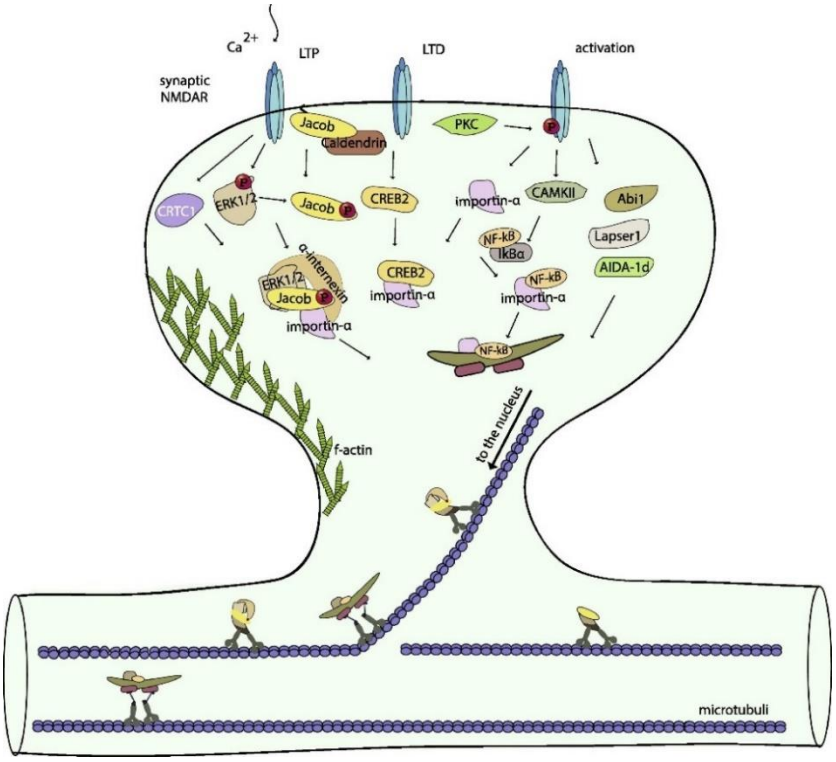

Figure 7. Synaptonuclear factors shuttle from synapse to nucleus in an activity-dependent manner. Activation of NMDARs and the consequent increase in intracellular Ca^{2+} triggers the activation of synaptic factors localizing at synapses and dendritic shafts, such as CRTC1, ERK1/2 or Jacob. These factors are retrogradely transport to the nucleus by diffusion or active transport, where they regulate gene programs essential for long-term synaptic plasticity. Abi1: Abelson interacting protein 1; AIDA1: amyloid beta protein precursor intracellular domain associated protein-1; CRTC1: CREB-regulated transcription coactivator 1; ERK1/2: extracellular signal-regulated kinase 1/2; LTD: long-term depression; LTP: long-term potentiation; NMDAR: N-methyl-D-aspartate receptor. Image modified from (Kaushik et al., 2014).

4.1.1. CREB-regulated transcription coactivator 1 (CRTC1)

The family of CREB-regulated transcription coactivators (CRTCs) are composed of three isoforms: CRTC1, CRTC2 and CRTC3 (Altarejos and Montminy, 2011). CRTC1 is the most abundant CRTC isoform found in the brain, being mainly detected in neurons of the hippocampus, cerebral cortex and cerebellum (Zhou et al., 2006). As a synaptonuclear factor, CRTC1 connects synaptic activity to CREB-dependent genetic programs at the nucleus, contributing to neuronal development, plasticity and survival (Cohen and Greenberg, 2008, Saura and Cardinaux, 2017, Parra-Damas and Saura, 2019). CRTC1 structure consists of: a coiled-coil N-terminal CREB binding domain (CBD), a central regulatory domain, a splicing domain (SD) and a C-terminal transactivation domain (TAD) [(Altarejos and Montminy, 2011), **Figure 8A**]. In the regulatory domain are located an arginine-rich NLS as well as the nuclear export sequences (NES1 and NES2) (Ch'ng et al., 2015). Mass spectrometry experiments have shown that CRTC1 has 11 Ser/Thr phosphorylation sites, indicating that CRTC1 is finely regulated by phosphorylation (Nonaka et al., 2014). Among these phosphorylation sites,

Ser64, Ser151, Ser145 and Ser245 have been reported to be responsible of CRTC1 subcellular localization [(Nonaka et al., 2014, Ch'ng et al., 2015), **Figure 8A**].

In basal conditions, CRTC1 is phosphorylated and sequestered at the cytoplasm and dendritic compartments by 14-3-3 proteins [(Ch'ng et al., 2012), **Figure 8B**]. NMDARs and L-type voltage-gated calcium channels activation upon synaptic activity leads to an increase in intracellular calcium and, consequently, CRTC1 dephosphorylates, dissociates from 14-3-3 proteins and shuttles to the nucleus. The Ca^{2+}-dependent phosphatase calcineurin is in charge of this activity-dependent dephosphorylation of CRTC1 (Ch'ng et al., 2012). Furthermore, rises in intracellular cyclic adenosine monophosphate (cAMP) inhibits AMP kinases (AMPKs) and salt-inducible kinases (SIKs), preventing CRTC1 rephosphorylation and prolonging its nuclear localization (Ch'ng et al., 2012, Nonaka et al., 2014). The motor protein dynein drives CRTC1 translocation from active synapses to the nucleus along microtubules (Ch'ng et al., 2015). Once at the nucleus, CRTC1 binds to the bZIP domain of CREB, facilitating the recruitment of the transcriptional machinery (Conkright et al., 2003, Bittinger et al., 2004). Thus, following neuronal activity, the complex CREB/CREB binding protein (CBP)/CRTC1 is recruited to the cAMP-response element (CRE)-containing promoters and along with histone acetylation induces the transcription of neuroplasticity genes, such as *Arc*, *Bdnf*, *Fgf1b* or *Fos* among others (Nonaka et al., 2014, Parra-Damas et al., 2017b, Uchida et al., 2017).

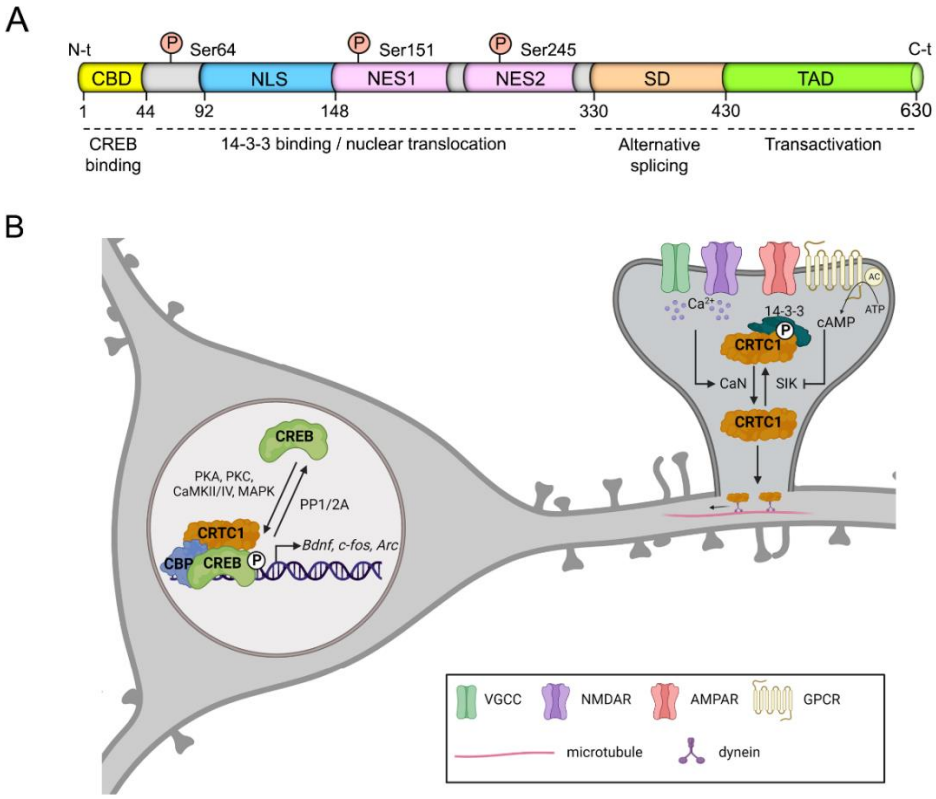

Figure 8. Structural domains and activity-dependent nuclear shuttling of CRTC1. (**A**) CRTC1 contains a N-terminal CBD followed by the NLS and NES sequences, which comprise the regulatory domain of CRTC1, a SD and a C-terminal TAD. CRTC1 dephosphorylation at one or several Ser residues (Ser 64, 151, 145 and 245) mediates CRTC1 dissociation from 14-3-3 proteins and translocation to the nucleus. CBD: CREB binding domain; NLS: nuclear localization sequence; NES: nuclear export sequence; SD: splicing domain; TAD: transactivation domain. (**B**) Stimulation of VGCC and NMDAR increase intracellular Ca^{2+} levels, which activates the phosphatase calcineurin (CaN) responsible of CRTC1 dephosphorylation. In addition, activation of GPCRs increases cAMP levels and primes PKA activation, which inhibits SIK, the CRTC1 kinase. Dephosphorylated CRTC1 is delivered to the nucleus along microtubules by the motor protein dynein. At the nucleus CRTC1 interacts with the CREB/CBP complex to potentiate the transcription of neuroplasticity genes. AC: adenylate cyclase; CaMKII and IV: Ca^{2+}/calmodulin-dependent protein kinase II and IV; CaN: calcineurin; CREB: cAMP-response element-binding protein; CBP: CREB binding protein; GPCR: G protein-coupled receptor; MAPK: mitogen-activated protein kinase; PKA: protein kinase A; PKC: protein kinase C; PP1 and PP2A: protein phosphatase type 1 and 2A; SIK: salt-inducible kinase; VGCC: voltage-gated calcium channels. Created with BioRender.

4.1.2. Physiological function of CRTC1 in the brain

CRTC1 plays important roles in neuronal development, function and plasticity. CRTC1 mRNA and protein are enriched in developing cortical neurons, suggesting that it may have a role in dendrite morphology and branching, which is important for the establishment of a functional neuronal network (Li et al., 2009). In agreement, CRTC1 is involved in BDNF-induced dendritic growth in developing neurons *in vitro* and *in vivo* (Li et al., 2009, Finsterwald et al., 2010). Furthermore, dendritic and axonal growth is negatively affected when the CRTC1/CREB interaction is disrupted (Rexach et al., 2012).

During L-LTP gene transcription and protein translation are needed for transforming transient stimuli into long-lasting effects that contribute to memory consolidation (Kandel, 2001). CRTC1 contributes to L-LTP maintenance at the Schaffer collateral-CA1 synapses in the hippocampus, whereas a dominant negative form of CRTC1 suppresses L-LTP (Zhou et al., 2006, Kovacs et al., 2007). On the contrary, CRTC1 inactivation in the hippocampus leads to long-term memory deficits that are rescued when overexpressing CRTC1 but not when a cytosolic CRTC1 is overexpressed (Uchida et al., 2017). This indicates that CRTC1 nuclear translocation and CRTC1-mediated transcription is essential for long-term synaptic plasticity. Overall, spatial and context associative learning paradigms as well as LTP-eliciting stimuli, triggers CRTC1 shuttling to the nucleus enhancing the transcription of synaptic and memory-related genes (Zhou et al., 2006, Nonaka et al., 2014, Parra-Damas et al., 2014, Uchida et al., 2017).

CRTC1 has recently emerged as a central brain-body regulator by modulating brain physiology, including metabolism, circadian rhythms, synaptic plasticity, memory and behavior (Saura and Cardinaux, 2017). In the hypothalamus, leptin acting through its receptor promotes CRTC1 dephosphorylation and the transcription of the CREB-dependent genes *Cartpt* and *Kiss1*, which encode neuropeptides that mediate satiety and fertility respectively (Altarejos et al., 2008, Rossetti et al., 2017). Mice lacking CRTC1 in the hypothalamus are sensitive to high-fat diet and exhibit hyperphagia and increased body weight (Matsumura et al., 2021). In *Drosophila*, CRTC also plays a crucial role in energy homeostasis by regulating lipid and glycogen metabolism (Choi et al., 2011, Shen et al., 2016). Fasting induces CRTC dephosphorylation and translocation to the nucleus in *Drosophila* neurons, mediating appetitive long-term memory (Hirano et al., 2013). In *Drosophila*, CRTC coordinates molecular rhythms with circadian behavior by regulating the transcription of *timeless* (*tim*) gene in a light-independent manner (Kim et al., 2016). In mammals, CRTC1 is highly expressed in the suprachiasmatic nucleus (SCN) of the hypothalamus, which is the brain region acting as the master circadian clock (Sakamoto et al., 2013). In the SCN, CRTC1 levels are increased during daytime contributing to the expression of the CREB-dependent genes *Sik1* and *Per1*, being the last one a clock gene (Sakamoto et al., 2013, Jagannath et al., 2013). SIK1 suppresses the effect of light by phosphorylating CRTC1 and repressing further expression of *Per1* (Jagannath et al., 2013). Therefore, the SIK1-CRTC1 pathway adjusts the light/dark cycle by regulating the expression of CREB-dependent genes, a transcriptional program conserved along evolution (Sakamoto et al., 2013, Jagannath et al., 2013, Kim et al., 2016).

4.1.3. CRTC1 dysfunction in brain pathologies

CRTC1 dysregulation leads to altered neuronal plasticity and cognitive impairments, which are common features of neuropsychiatric and neurodegenerative disorders (España et al., 2010, Breuillaud et al., 2012, Chaturvedi et al., 2012, Parra-Damas et al., 2014, Won et al., 2016). Depression-like behavior induced by prenatal stress in rats is accompanied by a reduction in total CRTC1 levels and consequently a decrease in the expression of downstream-dependent genes (Si et al., 2021). Mice lacking CRTC1 ($Crtc1^{-/-}$) exhibit altered social-related behaviors and depressive-like symptoms associated with depression and bipolar disorder (Breuillaud et al., 2012). These mutant mice have reduced levels of several CREB-regulated neuroplasticity genes in different regions of the limbic system, which has been shown to be critical for mood regulation (Price and Drevets, 2010, Breuillaud et al., 2012, Ni et al., 2019). These results suggest that CRTC1 has an important role modulating expression of genes involved in emotional responses (Breuillaud et al., 2012, Ni et al., 2019). Interestingly, lipopolysaccharide-induced depressive-like behaviors can be reverted by the overexpression of CRTC1 in the dentate gyrus (Ni et al., 2019).

CRTC1 has been shown to be deregulated in Alzheimer's disease (AD), Huntington's disease (HD) and Parkinson's disease (PD). Deficient CRTC1 dephosphorylation, nuclear translocation and transcription of CREB-dependent genes are observed in $APP_{Swe,Ind}$ and presenilin conditional double knockout (PS cDKO) mice and APP transgenic rats at early pathological stages (España et al., 2010, Parra-Damas et al., 2014, Parra-Damas et al., 2017a, Wilson et al., 2017). CRTC1 dysfunction occurs in response to intraneuronal Aβ accumulation that impairs calcineurin-mediated CRTC1 dephosphorylation (España et al., 2010, Wilson et al., 2017). Also, CRTC1-BDNF signaling pathway is affected by soluble oligomeric Aβ42 leading to L-LTP and memory impairments (Yan et al., 2021). Interestingly, a gene therapy approach based on CRTC1 overexpression in the hippocampus ameliorates transcriptional deficits, memory impairments and dendritic degeneration in the aforementioned mouse models, indicating that increasing CRTC1 mitigates cognitive decline (Parra-Damas et al., 2014, Parra-Damas et al., 2017a, Yan et al., 2021). In agreement with these findings, CRTC1 levels and CRTC1-dependent gene transcription are reduced in the human hippocampus at intermediate AD stages (Parra-Damas et al., 2014). Altered CRTC1 gene expression can be due to a decrease in the methylation of CRTC1 promoter regions, which correlate with phospho-tau deposition in the hippocampus of AD patients (Mendioroz et al., 2016). CRTC1 expression levels are also reduced in the striatum of transgenic HD mouse models as well as in postmortem tissue from HD patients (Chaturvedi et al., 2012). CRTC1 inactivation in HD results in a repression of neuroplasticity genes such as *Bdnf* that can contribute to neurodegeneration (Jeong et al., 2011,

Giralt et al., 2012). CRTC1 also has a neuroprotective role in PD. In the substantia nigra of PD patients, p21-activated kinase 4 (PAK4) activity is decreased and, consequently, the levels of the phosphorylated active form of CRTC1 (pCRTC1 Ser215) is decreased leading to a reduction in the expression of CRTC1-dependent genes (Won et al., 2016).

Despite the strong evidence of CRTC1 deregulation in neuropsychiatric and neurodegenerative disorders, further studies are needed to better understand the CRTC1-dependent molecular mechanisms modulating neuronal function and plasticity.

Hypothesis and objectives

The general hypothesis of this doctoral thesis is that synaptic proteome is essential for synaptic plasticity and its deregulation contributes to synapse dysfunction and cognitive decline in dementia. We first hypothesize that synaptonuclear factors, such as CRTC1 that shuttles from synapses to the nucleus to regulate gene expression, mediate synaptic plasticity acting locally at synapses and distally at the nucleus. The second hypothesis is that CRTC1 deregulation is associated with neuropathological changes in tauopathy dementias. Therefore, the main goals and their specific objectives of this doctoral thesis are:

Aim 1: To investigate the synaptic CRTC1-dependent molecular mechanisms involved in synaptic plasticity.

1.1. To investigate the role of CRTC1 in glutamatergic neurotransmission.
1.2. To examine the function of CRTC1 in neuronal proteostasis, including mRNA localization, local protein synthesis and protein degradation.

Aim 2: To study the function of presenilins (PS) in CRTC1 deregulation and pathological tau accumulation at synapses during neurodegeneration.

2.1. To study the link between abnormal synaptic accumulation of tau and autophagy deregulation in tauopathies.
2.2. To analyze synapse pathology caused by hyperphosphorylated and aggregated tau protein.

Materials and methods

1. Animal model and cell culture

1.1. Mouse models

PS1 conditional knockout (cKO) mice, lacking *PS1* specifically in forebrain glutamatergic neurons, were previously generated in Dr Jie Shen laboratory at Harvard Medical School (Yu et al., 2001). Briefly, to overpass embryonic lethality due to *PS1* deficiency, floxed *PS1* (*PS1* f/f) mice were crossed with CaM-Cre transgenic mice. PS1 inactivation starts at postnatal day 18 (P18) when Cre-recombinase is expressed. We generated PS1 cKO;Tau mice by crossing PS1 cKO mice with tau transgenic mice expressing FTD-linked P301S *tau* (isoform 4R) under the neuron-specific prion protein promoter (Soto-Faguás et al., 2021). The genetic background of all mice is C57BL6/129 hybrid. Mice were maintained in standard conditions at the Animal Core facility of the Universitat Autònoma de Barcelona, on a 12 h light/dark cycle with available food and water. Animal experimental procedures were conducted according to the approved Animal and Human Ethical Committee of the Universitat Autònoma de Barcelona (protocol CEEAH 2896, Generalitat de Catalunya DMAH 8787) following the European Union guidelines (2010/63/EU).

1.1.1. Genotyping

A small portion of mouse tail was incubated with 50 mM NaOH at 95ºC for 30 min to extract genomic DNA. For genotyping, 2 µl of the extracted DNA were added to the polymerase chain reaction (PCR) mix containing: 2 mM $MgCl_2$, 0.2 mM dNTPs mix, 0.5 µM of each primer (**Table 4**) and 1U of DNA polymerase in PCR buffer. PCR products were resolved in a 2% agarose gel containing 1X SYBR® Safe at 110 V for 40 min, and DNA bands were visualized in a UV transilluminator (GeneGenius, Syngene).

1.1.2. Stereotaxic injections

For *in vivo* overexpression or silencing of murine *Crtc1*, adeno-associated virus (AAVrh.2/10) containing Crtc1-myc under the cytomegalovirus promoter (AAV-CRTC1) or a CRTC1 short hairpin (Sh) RNA under the histone 1 promoter (AAV-ShCRTC1) were used, respectively. As controls AAVs expressing GFP or an ShScramble RNA were injected. 4.5-5 month-old C57BL/6 mice were anesthetized with isofluorane and bilaterally injected in the dorsal hippocampus with AAV-GFP, AAV-CRTC1, AAV-ShScramble or AAV-ShCRTC1 (3 µl; $5.1 \cdot 10^{11}$ gc/ml; 0.5 µl/min). The stereotaxic injection coordinates, according to Paxinos and Franklin's brain atlas, were (in mm) as follows: anteroposterior: -2.0 from Bregma; mediolateral: ±1.8 from Bregma; ventral: -1.8 from dural surface. Mice were analyzed 1.5 months after injection.

1.1.3. Behavioral test: contextual fear conditioning

Mice were handled for three consecutive days (3 min/day) prior to the beginning of the test. Mice were placed in a conditioning chamber (15.9 x 14 x 12.7 cm) for 3 min, foot-shocked (1 s/1 mA) and retained in the chamber for 2 min (immediate freezing). For assessing long-term memory, 24 h after training mice were placed again in the conditioning chamber for 4 min and memory was tested as freezing behavior, defined as a complete cessation of movement except for respiration, using Video Freeze® Software.

1.2. Primary neurons

Cortical and hippocampal neurons were obtained from E15.5 mouse embryos from PS1 f/f; $PS2^{+/+}$ and PS1 f/f; $PS2^{+/+}$ crossings (control neurons), or PS1 f/f; $PS2^{+/-}$;Tau and PS1 f/f; $PS2^{-/-}$ crossings. Embryos were extracted and placed in a 100 mm dish containing cold phosphate buffer saline (PBS) supplemented with 30 mM glucose. After extracting the brains, the hemispheres were separated, the meninges were removed, and the cortices and hippocampi were dissected. Cortices or hippocampi were transferred to a sterile Falcon tube containing Solution 1 and centrifuge 1 min at 1,500 rpm. The supernatant was discarded and a trypsin solution (Solution 2) was added. Then, the tissue was incubated at 37ºC during 10 min, stirring the tube every 2 min. To stop the reaction, Solution 3, which contains trypsin inhibitor, was added. The digested tissue was centrifuge 1 min at 1,500 rpm and the supernatant was discarded. The pellet was resuspended in Solution 4, mechanically dissociated using a Pasteur pipette and filtered using a nylon mesh (40 µm pore size). The filtered cell suspension was transferred to a Falcon tube containing Solution 5, and centrifuge 5 min at 1,000 rpm. The supernatant was discarded, and the pellet resuspended in complete Neurobasal. The number of cells per milliliter was determined using Trypan Blue and a Neubauer chamber. Cortical and hippocampal neurons were seeded in poly-D-lysine coated plates or coverslips, respectively. Neurons were maintained in a humidified incubator at 37ºC and 5% CO_2, and half of de medium was changed every 4-5 days. All solutions and culture mediums composition is detailed in **Table 1**.

1.3. Primary fibroblasts

Primary human skin fibroblasts from FAD patients and healthy controls were kindly provided by Dr Carlos Vicario (Instituto Cajal, Madrid). Fibroblasts were maintained in complete Dulbecco's Modified Eagle's Medium (DMEM) at 37ºC in a humidified 5% CO_2 incubator. For subculturing, fibroblasts were washed with PBS1X and trypsinized for 5-7 min at 37ºC. Complete DMEM was

added to inactivate trypsin and cells were centrifuged 5 min at 1,000 rpm. Cells were resuspended, counted and plated at 4,000-5,000 cells/cm^2.

1.4. iPSC-derived neurons

iPSC-derived neurons lysates from control or FAD patient carrying *PSEN1* G206D mutation were kindly provided by Dr Carlos Vicario (Instituto Cajal, Madrid) (Díaz-Guerra et al., 2019). Differentiated iPSC-derived neurons at 50 days *in vitro* (DIV) were treated and lysed for biochemical analysis.

1.5. Cell lines

Human embryonic kidney 293T cells (HEK293T) were maintained in complete DMEM at 37ºC in a humidified 5% CO_2 incubator. Cells were washed with PBS1X and trypsinized for 3 min at 37ºC. Trypsinization was stopped by adding complete DMEM and cells were centrifuged 5 min at 1,000 rpm. Cells were resuspended, counted, and plated at the required density.

1.6. Cellular transduction

Cultured neurons at 3, 4 or 15 DIV were kept with half of the medium and transduced with 1-2 lentiviral particles (LV) per cell. The following day, fresh medium was added.

1.7. Cellular transfection

1.7.1. Transfection of primary neuron culture

Cultured neurons plated in 24-well plates at a cell density of 150,000 cells/well were transfected at 7 DIV using Lipofectamine 2000 reagent. To form DNA-liposome complexes, DNA was incubated with Lipofectamine 2000 (ratio 1:0.7; for each µg of DNA, 0.7 µg of Lipofectamine 2000 were used) for 20 min at RT. Half of the culture medium was removed and DNA-Lipofectamine mix was added to the neuronal culture. The mixture was incubated for 50 min and, afterwards, the medium was completely replaced with conditioned medium diluted in fresh medium (ratio 1:1). Experiments were performed 24 h after transfection.

1.7.2. Transfection of primary fibroblasts and cell lines

Primary human fibroblasts and HEK293T plated in 24-well dishes (18,000 cells/well) or 60 mm dishes ($1.2 \cdot 10^6$ cells), respectively, were transfected with Lipofectamine 2000 reagent 24 h after plating following the manufacturer's protocol. Briefly, DNA was incubated with Lipofectamine 2000 (ratio 1:2; for each µg of DNA; 2 µg of Lipofectamine 2000) for 20 min at RT. The total amount of

DNA transfected was 0.5 µg for primary fibroblasts and 2 µg for HEK293T cells. Culture medium was replaced with OptiMEM supplemented with 2 mM glutamine, and transfection mix was added to each well in a dropwise manner. 2-3 h later medium was changed to complete DMEM without antibiotics. Cells were analyzed 24-48 h after transfection.

1.8. Pharmacological treatments

Cultured neurons or primary fibroblasts were kept with half of the medium and incubated with the pharmacological reagents. Drugs working concentrations are summarized in **Table 2**, and timepoints and duration of the treatments are specified in the results section.

2. Molecular biology

2.1. Plasmid DNA amplification and purification

To amplify plasmid DNA, 25 µl of DH5α competent cells were transformed with 1 µl of purified DNA. Competent cells were kept on ice for 30 min and heat shocked at 42ºC for 45 s to facilitate the entry of the DNA. Cells were kept on ice for another 5 min, resuspended in S.O.C medium and incubated for 1 h at 37ºC in agitation. Transformed cells were plated in LB agar plates with the corresponding selection antibiotic (100 µg/ml) and incubated O/N at 37ºC.

2.1.1. Maxiprep

For high plasmid DNA yields a maxiprep was done. A positive colony was selected and grown for 8-9 h in 5 ml of LB with the corresponding selection antibiotic (100 µg/ml) and then, transferred to 250 ml of LB supplemented with the antibiotic (100 µg/ml). Bacteria were grown O/N at 37ºC in agitation. The next day, bacterial culture was harvested by centrifuging at 4,000 g for 10 min (Beckman J2-21 centrifuge, JA-14 rotor) and plasmid DNA was purified using the PureLink™ HiPure Plasmid Filter Maxiprep Kit following the manufacturer's procedure. Purified DNA was eluted in miliQ H_2O, quantified using NanoDrop™ 2000 (Thermo Scientific) and stored at -20ºC.

2.1.2. Miniprep

For lower plasmid DNA yields miniprep procedure was done. A transformed colony was selected and grown in 5 ml of LB containing the selection antibiotic (100 µg/ml) O/N at 37ºC and in agitation. 3 ml of bacterial culture was harvested, and plasmid DNA was isolated using the QIAprep® Spin Miniprep Kit according to the manufacturer's instructions. Purified DNA was eluted in miliQ H_2O, quantified using NanoDrop™ 2000 (Thermo Scientific) and stored at -20ºC.

2.2. Cloning of mutant genes

Mouse *Crtc1*-myc and *Crtc1* S64/151/245A-myc cDNAs were subcloned into the pWPI lentiviral vector using the In-Fusion® HD Cloning Kit according to the manufacturer's instructions. First, pWPI vector was linearized by restriction enzyme digestion with PmeI. Then, the insert was amplified by PCR using a high-fidelity DNA polymerase (Platinum Pfx) and specific primers with 15 bp extensions at the 5' end that were complementary to the ends of the linearized vector. Digested vector and amplified insert were verified on an agarose gel electrophoresis and purified with QIAquick Gel Extraction kit. 100 ng of insert and 100 ng of linearized vector were incubated with In-Fusion HD Enzyme Premix for 15 min at 50ºC. Finally, stellar competent cells were transformed with 2.5 µl of In-Fusion reaction mixture. The incorporation of the insert into the vector was verified by screening several positive colonies by PCR and sequencing.

2.3. Lentiviral particles generation

HEK 293T at 60-70% of confluency were transfected using the calcium phosphate transfection protocol (Jiang and Chen, 2006). Briefly, 30 µg of the lentiviral plasmid of interest, 15 µg of psPAX2 lentiviral packaging plasmid, and 10 µg of psMD2.G envelope expressing plasmid were mixed with HEPES buffered saline (HBS) containing $CaCl_2$ and incubated for 20 min at RT. HEK293T medium was replaced with DMEM supplemented with 25 µM chloroquine and transfection mixture was incubated for 7-8 h. Then, the transfection medium was replaced with complete DMEM. Medium was harvested 24 h, 36 h and 48 h after transfection, centrifuged 5 min at 1,000 rpm to discard cell debris, and filtered into an ultracentrifuge tube. The filtered medium was then centrifuged 2 h at 25,000 rpm and 4ºC (Sorvall Discovery 90SE ultracentrifuge, rotor SW28). Next, the supernatant was discarded, and the pellet was resuspended in 100 µl of cold PBS 1X and left O/N at 4ºC in agitation. The next day, lentiviruses were aliquoted and stored at -80ºC.

2.4. Lentivirus titration

HEK 293T cells plated in 24-well plates at an initial density of 30,000 cells/well were transduced with serial dilutions of the lentivirus. 72 h after transduction, cells were trypsinized and the percentage of green fluorescent protein (GFP) positive cells for each lentiviral dilution was determined by flow cytometry (Cytomics FC500, Beckman Coulter). The lentivirus titer (infective particles/µl) was determined using the following formula:

$$\mathrm{IP}/\mu\mathrm{l} = \frac{\%\ \text{of infected cells} \cdot 0.01 \cdot \text{nº of cells the day of transfection}}{\text{virus dilution}}$$

2.5. Bioluminescence resonance energy transfer (BRET)

HEK293 cells were transiently transfected using polyethylenimine (PEI) with a constant amount of donor protein fused to Renilla luciferase (RLuc) and increasing amounts of acceptor protein fused to yellow fluorescent protein (YFP). 48 h after transfection, cells were detached from the culture plate using HBSS buffer supplemented with 0.1% glucose, centrifuged 5 min at 3,200 rpm and resuspended in the same buffer. Protein concentration was adjusted to 0.2 mg/ml before BRET measurements. First, to quantify BRET-acceptor expression, cells (20 µg of protein) were distributed in 96-well microplates (Porvair Sciences, 205003) and fluorescence was measured in Mithras LB 940 (Berthold, Germany) using an excitation filter of 485 nm. BRET-acceptor fluorescence was determined as fluorescence of the sample minus the fluorescence of cells expressing BRET-donor alone. For BRET measurement, cells (20 µg of protein) were distributed in 96-well microplates (Porvair Sciences, 204003) and 5 µM Coelenterazine H was added. BRET measurement readings were collected 1 min after the addition of Coelenterazine H, which allowed the integration of the signal detected in the short-wavelength filter at 485 nm and the long-wavelength filter at 530 nm. To measure BRET-donor expression luminescence, readings were performed 10 min after adding Coelenterazine H. Net BRET ratio was defined as [(long-wavelength emission)/(short-wavelength emission)]-Cf, where Cf corresponds to [(long-wavelength emission)/(short-wavelength emission)] in the condition where BRET-donor was expressed alone. BRET values were expressed as mili BRET units (mBU: 1000 × net BRET), and BRET curves were fitted by using a non-linear regression equation.

2.6. CRE-promoter activity assay

CRE-promoter activity in cultured cortical neurons was analyzed using the commercial kit Dual-Luciferase Reporter Assay System. Neurons plated in 24-well dishes at a cell density of 150,000 cells/well were transfected using Lipofectamine 2000 with: pCRE-Luc (0.5 µg/well), which encodes the firefly (*Photinus pyralis*) luciferase gene under the control of three CRE sites; pRL-TK (0.1 µg/well), which constitutively express *Renilla reniformis* luciferase and it is used as an internal control of the technique; and the plasmid of interest (0.5 µg/well). 24 h after the transfection, neurons were treated with FSK/KCl (20 µM, 30 mM) or Bic/4-AP (50 µM, 2.5 mM) for 4 h. Next, neurons were lysed with 100 µl of Passive Lysis Buffer and lysates (20 µl) were loaded into a 96-well opaque plaque. Firefly luciferase luminescence was measured by adding 25 µl of Luciferase Assay Reagent II (LARII). Then, 25 µl of Stop & Glo® Reagent was added to quench the reaction and to simultaneously initiate *Renilla* luciferase reaction. Luminescence was measured in Varioskan™

Lux reader (Thermo Scientific) and values were represented as firefly luciferase readings normalized to *Renilla* luciferase reading.

3. Biochemical analyses

3.1. Brain and cell lysis

Mouse hippocampi were homogenized in ice-cold RIPA-DOC lysis buffer (**Table 5**) supplemented with protease and phosphatase inhibitors, using a potter homogenizer. After the dissociation, samples were kept in ice during 1 h, sonicated and stored at -80ºC.

Human hippocampi were homogenized in ice-cold O^+ lysis buffer (**Table 5**) containing protease and phosphatase inhibitors, using a potter homogenizer. After tissue dissociation, samples were boiled 5 min at 95ºC, sonicated, and centrifuged 15 min 14,000 rpm. The supernatant was stored at -20ºC for protein analysis.

Cell cultures were washed three times with ice-cold PBS 1X and lysed with a scraper in ice-cold RIPA-DOC buffer supplemented with protease and phosphatase inhibitors. The lysates were sonicated and stored at -20ºC.

3.2. Synaptosomes fractionation

Individual mouse hippocampus was homogenized with a glass homogenizer in ice-cold buffer A. The homogenate was centrifuged 10 min at 1,400 x *g* and the pellet was re-extracted with buffer A and centrifuge 10 min at 710 x *g*. The supernatants were combined and centrifuge 10 min at 13,800 x *g*. The pellet was resuspended in ice-cold buffer B and loaded at the top of a 0.85 M, 1 M, 1.2 M discontinuous sucrose gradient and centrifuge 2 h at 82,500 x *g*. The synaptosome fraction was collected from the 1 M-1.2 M sucrose interphase and diluted with an equal amount of buffer C. Purified synaptosomes were centrifuged 1 h at 32,800 x *g* to obtain the presynaptic (supernatant) and the postsynaptic (pellet) fraction. The postsynaptic fraction was resuspended in ice-cold buffer D. Samples were sonicated and stored at -80ºC. All buffers were supplemented with phosphatase and protease inhibitor, and its composition is detailed in **Table 5**.

3.3. Protein quantification

Protein concentration of tissue and cell lysates was determined using the BCA protein assay kit. In a 96-well plate, 10 µl of each sample and of the standard curve samples were loaded. Then, 100 µl of working reagents (50 parts of BCA Reagent A and 1 part of BCA Reagent B) was added. The plate

was incubated at room temperature (RT) for 15 min in agitation, and finally the absorbance at 526 nm was measured in Varioskan™ LUX reader (Thermo Scientific).

Protein concentration of human samples was quantified with Coomassie (Bradford) protein assay kit. In a 96-well plate, 5 µl of each sample and of the standard curve were loaded. Then, 250 µl of Coomassie reagent was added and incubated for 10 min at RT in agitation. Absorbance at 595 nm was measured in Varioskan™ LUX reader (Thermo Scientific).

3.4. Western blotting

The same amount of protein for each sample was diluted with loading buffer and heated at 95ºC for 5 min. Samples were loaded in acrylamide gels and electrophoresis was performed at 25 mA in running buffer. Proteins were transferred to PVDF membranes, previously activated with methanol, during 75 min at a constant voltage of 120 V in cold transfer buffer. Membranes were stained with Ponceau S to verify protein transference and, after eliminating the Ponceau stain with Tris-buffered saline-Tween (TBS-T), PVDF membranes were incubated with blocking solution for 1 h at RT. Then, the membranes were washed twice (10 min) with TBS-T and incubated with the primary antibody overnight at 4ºC or 1 h at RT (**Table 7**). Next, membranes were washed three times (10 min) with TBS-T and incubated with the secondary antibody conjugated to the horseradish peroxidase (HRP) for 1 h at RT (**Table 7**). Finally, membranes were washed twice (10 min) with TBS-T and one time (10 min) with TBS before detecting the protein bands by a chemiluminescence reaction using ECL substrate (ECL1:ECL2 1:1 ratio). Protein bands were detected on ChemiDoc MP System (Bio-Rad) and quantified with Image Lab 5.2.1 software (Bio-Rad). When needed, membranes were stripped in stripping buffer at 56ºC and agitation for 20 min. Then, membranes were washed three times with distilled water and three times (10 min) with TBS-T before blocking and reincubating with a primary antibody.

4. Immunostainings

4.1. Immunocytochemistry

For immunostaining, mouse hippocampal neurons or primary human fibroblasts were seeded in 24-well plates with coverslips at a cell density of 30,000 cells/well or 18,000 cells/well, respectively. Cells were washed with PBS 1X and fixed with 4% PFA for 15 min at RT. Then, cells were permeabilized and blocked with blocking solution for 30 min at RT and incubated with the primary antibody O/N at 4ºC (**Table 7**) in a humidified chamber. Next, neurons were incubated with the secondary antibody for 1 h at RT in a humidified chamber (**Table 7**). Finally, nuclei were stained

with Hoechst (1 µg/ml) for 10 min at RT and coverslips were mounted using FluorSave™ Reagent or Mowiol. Images were acquired on a Zeiss LSM 700 confocal microscope and analyzed using ImageJ (NIH) and Imaris 8.3.4 (Bitplane) software.

4.1.1. Colocalization analysis

4.1.1.1. GluN1/PSD95 colocalization

GluN1 and PSD95 colocalization analysis in primary and secondary dendrites was performed using the spots and ImarisColoc tool from Imaris software. GluN1 and PSD95 puncta were considered positive when the spot diameter was ≥ 0.4 µm or ≥ 0.7 µm, respectively. Dendrite length was also measured using the filament tool. Results are represented as total puncta number relative to dendrite length, or as percentage of GluN1/PSD95 colocalized spots relative to total GluN1 spots.

4.1.1.2. Autophagic flux analysis

Autophagic flux was monitored with the use of the mCherry-EGFP-LC3B vector. mCherry and EGFP puncta were defined using the spots tool from Imaris software and considered positive when the spot diameter was ≥ 0.5 µm. To discriminate between autophagosomes (mCherry- and EGFP-positive) from autolysosomes (mCherry-positive and EGFP-negative), mCherry and EGFP colocalization was calculated with the ImarisColoc tool. Autophagosomes corresponded to mCherry puncta colocalizing with EGFP, and autolysosomes to mCherry puncta that did not colocalized with EGFP. Data are represented as autophagosomes or autolysosomes per cell.

4.1.2. CRTC1 subcellular localization analysis

CRTC1 subcellular localization was quantified with ImageJ software. Nuclear and cytosolic regions of interest (ROIs) were established, and CRTC1 intensity was calculated as integrated density (IntDen). Data are represented as nuclear to cytoplasmic ratio of CRTC1 intensity.

4.2. Fluorescence *in situ* hybridization (FISH)

For FISH experiments, neurons were fixed with 4% PFA and permeabilized with 0.2% Tx-100 in RNAse free PBS for 5 min at RT. Then, the coverslips were washed with RNAse free PBS and Wash buffer A, and incubated O/N at 37ºC in a humidified chamber with the hybridization solution containing the Fluo®Red 590 Oligo-dT probe (1:100) and a chicken anti-MAP2 antibody (**Table 7**). Next, the coverslips were rinsed with Wash buffer A and incubated with Wash buffer A plus the secondary antibody AMCA anti-chicken (**Table 7**) 30 min at 37ºC. Finally, the coverslips were washed with Wash buffer B and RNAse free PBS, and mounted with Mowiol. Images were acquired

on a Zeiss AxioObserver microscope at 63x. Dendrites of GFP positive neurons were straightened and the intensity of total mRNA levels were measured using ImageJ software (NIH).

4.3. Puromycylation

Neurons were incubated with 10 µM puromycin for 10 min prior to fixation. As a negative control, neurons were pretreated with 200 µM cycloheximide for 1 h. Before cell fixation with 4% PFA, coverslips were washed with 0.01% Tx-100 in PBS to remove the excess of puromycin. Neurons were permeabilized with 0.15% Tx-100 in PBS for 5 min at RT and blocked with 5% BSA in PBS for 1 h at RT. Neurons were incubated with mouse anti-puromycin antibody and chicken anti-MAP2 antibody (**Table 7**) O/N at 4ºC in a humidified chamber. Lastly, the coverslips were incubated 1 h at 37ºC with the corresponding secondary antibodies (**Table 7**) and mounted with Mowiol. Images were acquired on a Zeiss AxioObserver microscope at 63x. Dendrites of GFP positive neurons were straightened and the intensity of total puromycin levels were measured using ImageJ software (NIH).

5. Statistical analysis

GraphPad Prism 8 software was used to perform the statistical analyses. For multiple comparison, data was analyzed by one- or two-way analysis of variance (ANOVA) followed by Tukey's post hoc test or by Dunnett's post hoc when comparing to control group. Two-tailed unpaired Student *t* test was used for analyzing differences between two groups. When values were not normally distributed, the non-parametric Kruskal-Wallis' test was used. Values identified as outliers by Grubbs' test were not included in the analysis. Data is represented as the mean ± standard error of the mean (SEM). Significant differences were considered when the $P < 0.05$.

6. List of materials

Table 1. List of reagents, buffers and culture mediums used in cell cultures.

Reagent	Source	Identifier
B27	Thermo Fisher Scientific	17504-044
Bovine serum albumin (BSA)	Sigma-Aldrich	A7906
Deoxyribonuclease I from bovine pancreas (DNAse)	Sigma-Aldrich	D5025
Dulbecco's Modified Eagle's Medium (DMEM)	Thermo Fisher Scientific	41965-039
Dulbecco's phosphate buffered saline (PBS) 10X	Sigma-Aldrich	D1408
Fetal bovine serum (FBS)	Thermo Fisher Scientific	10270-106
Lipofectamine 2000 reagent	Thermo Fisher Scientific	11668-027
L-Glutamine (200 mM)	Thermo Fisher Scientific	25030-081
Neurobasal medium	Thermo Fisher Scientific	21103-049
OptiMEM medium	Thermo Fisher Scientific	31985-070
Penicillin/Streptomycin (500 U/ml)	Thermo Fisher Scientific	15140-122
Poly-D-lysine (PDL)	Sigma-Aldrich	P7658
Trypsin	Sigma-Aldrich	T9201
Trypsin inhibitor	Thermo Fisher Scientific	17075-029
Trypsin/EDTA	Thermo Fisher Scientific	5200-056
X-tremeGENE 9 DNA transfection reagent	Roche	XTG9-RO
Commercial kit	**Source**	**Identifier**
CalPhos™ mammalian transfection kit	Takara Bio	631312
Buffer	**Composition**	
Krebs-Ringer buffer (1X)	120 mM NaCl, 4.8 mM KCl, 1.2 mM KH_2PO_4, 25 mM $NaHCO_3$ and 14.3 mM glucose, pH 7.4	
Solution 1	Krebs-Ringer buffer, 0.3% BSA, 0.03% $MgSO_4$	
Solution 2	Solution 1, 0.025% trypsin	
Solution 3	Solution 1, 0.052% trypsin inhibitor, 0.008% DNAse and 0.03% $MgSO_4$	
Solution 4	Solution 1 and 16% solution 3	
Solution 5	Solution 1, 0.03% $MgSO_4$, 0.0014% $CaCl_2$	
Culture medium	**Composition**	
Complete DMEM medium	DMEM, 1% Penicillin/Streptomycin and 10% FBS	
Complete Neurobasal medium	Neurobasal medium, 2% B27, 0.5% Penicillin/Streptomycin, 1% glutamine	

Table 2. List of pharmacological treatments and their working concentration used in primary neuronal cultures.

Reagent	Source	Identifier	Dose
4-aminopyridine (4-AP)	Sigma-Aldrich	275875	2.5 mM
Actinomycin D (ActD)	Thermo Fisher Scientific	11805-017	2 µg/ml
1(S),9(R)-(-)-Bicuculline methiodide (Bic)	Sigma-Aldrich	14343	50 µM
Chloroquine (CQ)	Sigma-Aldrich	C6628	10-20 µM
Cycloheximide	Sigma-Aldrich	01810	200 µM
Forskolin (FSK)	Sigma-Aldrich	F6886	20 µM
GF-109203X hydrochloride (GF)	Sigma-Aldrich	B6292	10 µM
L-Glutamic acid (Glut)	Sigma-Aldrich	G1626	100 µM
MG132	Tocris	1748	1 µM
Potassium chloride (KCl)	Sigma-Aldrich	P9333	30 mM
Phorbol-12-myristate 13-acetate (PMA)	Sigma-Aldrich	P1585	5 µM
Puromycin dihydrochloride	Santa Cruz	58-58-2	10 µM
Tetrodotoxin citrate (TTX)	Tocris	1069	1 µM

Table 3. AAVs, bacterial strains, reagents, commercial kits and recombinant DNA used in molecular biology experiments.

AAVs	**Source**	
AAV2/10-CMV-GFP	UPV CBATEG	
AAV2/10-CMV-CRTC1-myc-IRES-GFP	UPV CBATEG	
AAV2/10-H1-Scramble-RSV-GFP	UPV CBATEG	
AAV2/10-H1-ShCRTC1-RSV-GFP	UPV CBATEG	
Bacterial strains	**Source**	**Identifier**
DH5α competent cells	Invitrogen	18265-017
Stellar competent cells	Takara Bio	636766
Reagents	**Source**	**Identifier**
1 Kb Plus DNA Ladder	Invitrogen	10787-018
Agarose	Condalab	8019
Ampicillin sodium salt	Sigma-Aldrich	A0166
Coelenterazine H	Invitrogen	C6780
DNA polymerase 5U/µl	Biotools	10049-4111
dNTPs mix 10 mM	Biotools	20038
Kanamycin	Sigma-Aldrich	K1876
Luria Broth base (LB)	Invitrogen	12795-027
Luria Broth agar	Invitrogen	22700-025
Polyethylenimine (PEI)	Sigma	408727
Platinum Pfx DNA Polymerase	Invitrogen	11708-013
S.O.C. medium	Invitrogen	15544-034
SYBR® Safe DNA gel stain	Invitrogen	S33102
Commercial kit	**Source**	**Identifier**
Dual-Luciferase Reporter Assay System	Promega	E1910
In-Fusion® HD Cloning Kit	Clontech	011614
PureLink™ HiPure Plasmid Filter Maxiprep Kit	Thermo Fisher Scientific	K210017
PureLink™ HiPure Precipitator Module	Thermo Fisher Scientific	K210022
QIAprep® Spin Miniprep Kit	Qiagen	27104
QIAquick® Gel Extraction Kit	Qiagen	28704
Recombinant DNA	**Source**	**Identifier**
pCDH-EF1a-mCherry-EGFP-LC3B	Addgene	170446
pcDNA3.1-CRTC1-myc	Dr. Jean-René Cardinaux	
pcDNA3.1-CRTC1S64/151/245A-myc	Saura Lab	
pcDNA3.1-GluN2B	Dr. Rafael Franco	
pCre-Luc	Stratagene	
pEYFP-N1-Cald	Dr. Rafael Franco	
pEYFP-N1-Caln	Dr. Rafael Franco	
pEYFP-N1-CaM	Dr. Rafael Franco	
pHA-CRTC1	Dr. Toh Hean Ch'ng	
pHA-CRTC1mNLS1	Dr. Toh Hean Ch'ng	
pHA-CRTC1mNLS2	Dr. Toh Hean Ch'ng	
pRL-TK control reporter vector	Promega	E2241
pRLuc-N1-GluN1	Dr. Rafael Franco	
psMD2.G	Addgene	12259
psPAX2	Addgene	12260
pWPI	Addgene	12254
pWPI-CRTC1-my	This thesis	
pWPI-CRTC1(S64,151,245A)-myc	This thesis	
Restriction enzymes	**Source**	**Identifier**
PmeI	NEB	R0560S

Primers used for cloning	Sequence (5' to 3')
Fw_CRTC1_pWPI	CTAGCCTCGAGGTTTGGATCCACCATGGCGACTTC
RV_CRTC1-myc_pWPI	TGCAGCCCGTAGTTTTCACAGATCTTCCTCGCTGA
Buffer	**Composition**
HBSS	137 mM NaCl, 5 mM KCl, 0.34 mM Na_2HPO_4×$12H_2O$, 0.44 mM KH_2PO_4, 1.26 mM $CaCl_2$×2 H_2O, 0.4 mM $MgSO_4$×$7H_2O$, 0.5 mM $MgCl_2$

Table 4. Primers used for genotyping.

Gene	Primer	Sequence (5' to 3')
Cre	P156	GCCTGCATTACCGGTCGATGCAACGA
	P157	GTGGCAGATGGCGCGGCAACACCATT
PS1	P139	GGTTTCCCTCCATCTTGGTTG
	P140	TCAACTCCTCCAGAGTCAGG
	P158	TGCCCCCTCTCCATTTTCTC
PS2	P162	CATCTACACGCCCTTCACGG
	P163	CACACAGAGAGGCTCAAGATC
	P164	AAGGGCCAGCTCATTCCTCC
Tau	P16134	GGCATCTCAGCAATGTCTCC
	P12473	GGTATTAGCCTATGGGGGACAC
	OIMR8744	CAAATGTTGCTTGTCTGGTG
	OIMR8745	GTCAGTCGAGTGCACAGTTT

Table 5. Reagents, commercial kits and buffers used for biochemical experiments.

Reagents	Source	Identifier
30% Acrylamide/Bis Solution 37.5:1	Bio-Rad	1610158
Ammonium persulfate	Sigma-Aldrich	A3678
cOmplete™ Protease Inhibitor Cocktail	Roche	11697498001
Immuno-Blot® PVDF membrane	Bio-Rad	1620177
Luminol	Sigma-Aldrich	09253
p-Coumaric acid	Sigma-Aldrich	28200
PhosSTOP™ Phosphatase Inhibitor Cocktail	Roche	04906837001
Ponceau S	Sigma-Aldrich	81462
Precision Plus Protein All Blue Standards	Bio-Rad	1610373
TEMED	Sigma-Aldrich	T9281
Tween® 20	Sigma-Aldrich	P2287
Commercial kit	**Source**	**Identifier**
Coomassie Protein Assay Kit	Thermo Fisher Scientific	1856209
Pierce™ BCA Protein Assay Kit	Thermo Fisher Scientific	23225
Buffer	**Composition**	
Blocking solution	10% nonfat powdered milk, 0.1% BSA in TBS 1X	
Buffer A	5 mM HEPES pH 7.4, 0.32 M sucrose, 1 mM $NaHCO_3$, 1 mM $MgCl_2$, 0.5 mM $CaCl_2$	
Buffer B	6 mM Tris-HCl pH 8, 0.32 M sucrose, 1 mM $NaHCO_3$	
Buffer C	12 mM Tris-HCl pH 8, 1% Triton X-100	
Buffer D	40 mM Tris-HCl, 1% NP-40	
ECL1	1 M Tris-HCl pH 8.5, 0.5 M luminol, 79.2 mM p-Coumaric acid	
ECL2	1 M Tris-HCl pH 8.5, 8.8 M H_2O_2	
Loading buffer 1X	0.5 M Tris-HCl pH 6.8, 10% glycerol, 2% SDS, 0.01% bromophenol blue, 5% β-mercaptoethanol	
O^+ lysis buffer	62.5 mM Tris-HCl pH 6.8, 5% β-mercaptoethanol, 10% glycerol, 2.3% SDS, 5 mM NaF, 100 µM Na_3VO_4, 1 mM EDTA, 1 mM EGTA	

Primary antibody solution	0.1% BSA, 0.02% thimerosal in TBS 1X
RIPA-DOC lysis buffer	50 mM Tris-HCl pH 7.4, 150 mM NaCl, 2.5 mM EDTA, 1 mM Na_3VO_4, 25 mM NaF, 0.1% SDS, 1% NP-40, 0.5% Na-deoxycholate
Running buffer 1X	25 mM Tris base, 200 mM glycine, 0.1% SDS
Separating buffer 4X	1.5 M Tris base pH 8.8, 0.4% SDS
Stacking buffer 4X	0.5 M Tris base pH 6.8, 0.4% SDS
Stripping buffer	0.5 M Tris-HCl pH 6.8, 10% SDS and 0.7% β-mercaptoethanol
Transfer buffer 1X	10 mM Tris base, 100 mM glycine
Tris-buffered saline 1X (TBS 1X)	20 mM Tris base, 137 mM NaCl, pH 7.6
TBS-Tween (TBS-T)	TBS 1X, 0.1% Tween-20

Table 6. List of reagents and buffers required for immunostaining experiments.

Reagents	**Source**	**Identifier**
Cy™3 Streptavidin	Jackson ImmunoResearch	016-160-084
FluorSave™ Reagent	Calbiochem	345789
Hoechst 34580	Invitrogen	H21486
Mowiol 4-88	Sigma-Aldrich	81381
Normal Goat Serum (NGS)	Sigma-Aldrich	S26-M
Paraformaldehyde (PFA) 16%	Thermo Fisher Scientific	28908
Stellaris® Fluo®Red 590 Oligo-dT probe	Biosearch Technologies	
Stellaris® RNA FISH Hybridization Buffer	Biosearch Technologies	SMF-HB1-10
Stellaris® RNA FISH Wash Buffer A	Biosearch Technologies	SMF-WA1-60
Stellaris® RNA FISH Wash Buffer B	Biosearch Technologies	SMF-WB1-20
Triton X-100	VWR	0694
Buffer	**Composition**	
Blocking solution	2% NGS, 2% BSA, 0.2% Tx-100 in TBS 1X	

Table 7. List of antibodies and working dilutions used for western blot (WB) and immunocytochemistry (ICC).

Antibody	**Host**	**Source**	**Identifier**	**Application and dilution**	
				WB	**ICC**
AMCA anti-chicken	Donkey	Jackson ImmunoResearch	703-155-155		1:1,000
Anti-chicken IgY Alexa Fluor® 488	Goat	Invitrogen	A11039		1:300
Anti-mouse IgG Alexa Fluor® 488	Goat	Invitrogen	A11001		1:300
Anti-mouse IgG Alexa Fluor® 568	Goat	Invitrogen	A11031		
Anti-mouse IgG Alexa Fluor® 647	Goat	Invitrogen	A32728		1:300
Anti-rabbit IgG Alexa Fluor® 568	Goat	Invitrogen	A11036		1:300
Biotin-SP Fab anti-mouse IgG	Goat	Jackson ImmunoResearch	115-067-003		1:300
β-tubulin	Mouse	Sigma Aldrich	T7816	1:20,000	
c-myc	Rabbit	Santa Cruz	sc-789 A-14	1:1,000	
CP13 [pTau(Ser202)]	Mouse	P. Davies		1:250	

CRTC1	Rabbit	Cell Signaling	2587	1:10,000	
D1M9X (Tau)	Rabbit	Cell Signaling	46687	1:1,000	
DyLight™ 405 anti-mouse IgG	Goat	Jackson ImmunoResearch	115-475-003		1:300
GAPDH	Mouse	Ambion	AM4300	1:100,000	
GFP	Chicken	Abcam	ab13970		1:1,000
GluA1	Rabbit	Chemicon	AB1504	1:2,000	
GluA2	Mouse	Merck Millipore	MABN1189	1:1,000	
GluN1	Mouse	Sigma	MAB363	1:1,000	1:200
GluN2A	Rabbit	Merck Millipore	AB1555	1:2,500	
GluN2B	Rabbit	Merck Millipore	AB1557	1:1,000	
HA-tag	Mouse	Santa Cruz	sc-7392	1:1,500	1:500
Homer 1	Rabbit	Synaptic Systems	160 003	1:1,000	
HRP anti-mouse	Goat	Bio-Rad	1706516	1:3,000	
HRP anti-rabbit	Goat	Bio-Rad	1706515	1:3,000	
LC3B	Rabbit	Abcam	ab48394	1:1,000	
MAP2	Chicken	EnCor Biotechnology	CPCA-MAP2		1:1,000
Myc-tag	Mouse	Abcam	ab32		1:200
p62/SQSTM1	Mouse	Abcam	ab56416	1:1,000	
pGluA1(Ser831)	Rabbit	Santa Cruz	sc-16313-R	1:1,000	
pGluA1(Ser845)	Rabbit	Merck Millipore	04-1073		
pGluN1(Ser890)	Rabbit	Cell Signaling	3381	1:1,000	
pGluN1(Ser897)	Rabbit	Cell Signaling	3385	1:1,000	
pGluN2B(Ser1303)	Rabbit	Merck Millipore	07-398	1:500	
PHF1 [pTau(Ser396/404)]	Mouse	P. Davies		1:250	
pPSD95(Ser295)	Rabbit	Abcam	ab76108	1:20,000	
PSD95	Rabbit	Cell Signaling	3450	1:1,000	1:200
Puromycin	Mouse	Kerafast	EQ0001		1:10,000
Synaptophysin	Mouse	Sigma	S5768	1:1,000,000	
Syntaxin-1	Mouse	Santa Cruz	sc-12736	1:3,000	
TG5 (Tau)	Mouse	P. Davies		1:500	

Table 8. Software used for data analysis.

Software	Source
GraphPad Prism 8	GraphPad Software
ImageJ Software	NIH
Image Lab 5.2.1	Bio-Rad
Imaris 8.3.4 Software	Bitplane
Video Freeze®Software	Med Associates

Results

CHAPTER 1:

CRTC1-dependent molecular mechanisms involved in synaptic plasticity

1. CRTC1 is essential for hippocampal-dependent memory

CRTC1 is required for induction and/or maintenance of LTP (Zhou et al., 2006, Kovacs et al., 2007, Uchida et al., 2017), but the underlying mechanisms are still unclear. To better understand the role of CRTC1 in hippocampal-dependent synaptic plasticity and memory, we investigated the effect of CRTC1 inactivation and overexpression in contextual fear memory and glutamatergic neurotransmission.

We injected intrahippocampally 6 month-old mice (C57BL/6 background) with adeno-associated viral (AAV) vectors containing empty vector (GFP or scramble) or that overexpress (AAV-CRTC1-myc) or inactivate (AAV-ShCRTC1) *Crtc1* specifically in neurons. One month later, mice were trained in the contextual fear conditioning (CFC) and hippocampi were analyzed biochemically (**Figure 9A,B**). In CFC, mice learn to associate a specific context (chamber) with an aversive stimulus (footshock). During training, mice were exposed to the context for 3 min and freezing behavior was considered a measurement of neophobia. Mice were then foot-shocked (1 sec/1 mA) and kept in the conditioning chamber for 2 min (immediate freezing). Long-term associative memory was assessed, 24 h later by exposing the mice to the chamber (4 min) without shock (**Figure 9A**). All experimental groups showed a freezing time effect ($P < 0.0001$) with no significant group differences in basal (context) and immediate freezing ($P > 0.05$). However, compared to GFP- or scramble-injected mice, freezing responses at 24 h were significantly increased and reduced by CRTC1 overexpression or silencing, respectively ($P < 0.05$, **Figure 9C**). AAVs transduction was efficient as tested by measuring total CRTC1 and myc-tag protein levels. Total CRTC1 levels were slightly increased but not significantly ($P = 0.113$), but there was a significant increase in myc-tag levels in AAV-CRTC1-myc injected mice ($P = 0.02$, **Figure 9D**). In addition, endogenous CRTC1 levels were significantly reduced (~ 45%) in mice injected with AAV-ShCRTC1 ($P = 0.004$, **Figure 9E**). These behavioral results indicate that CRTC1 is critical for long-term associative memory.

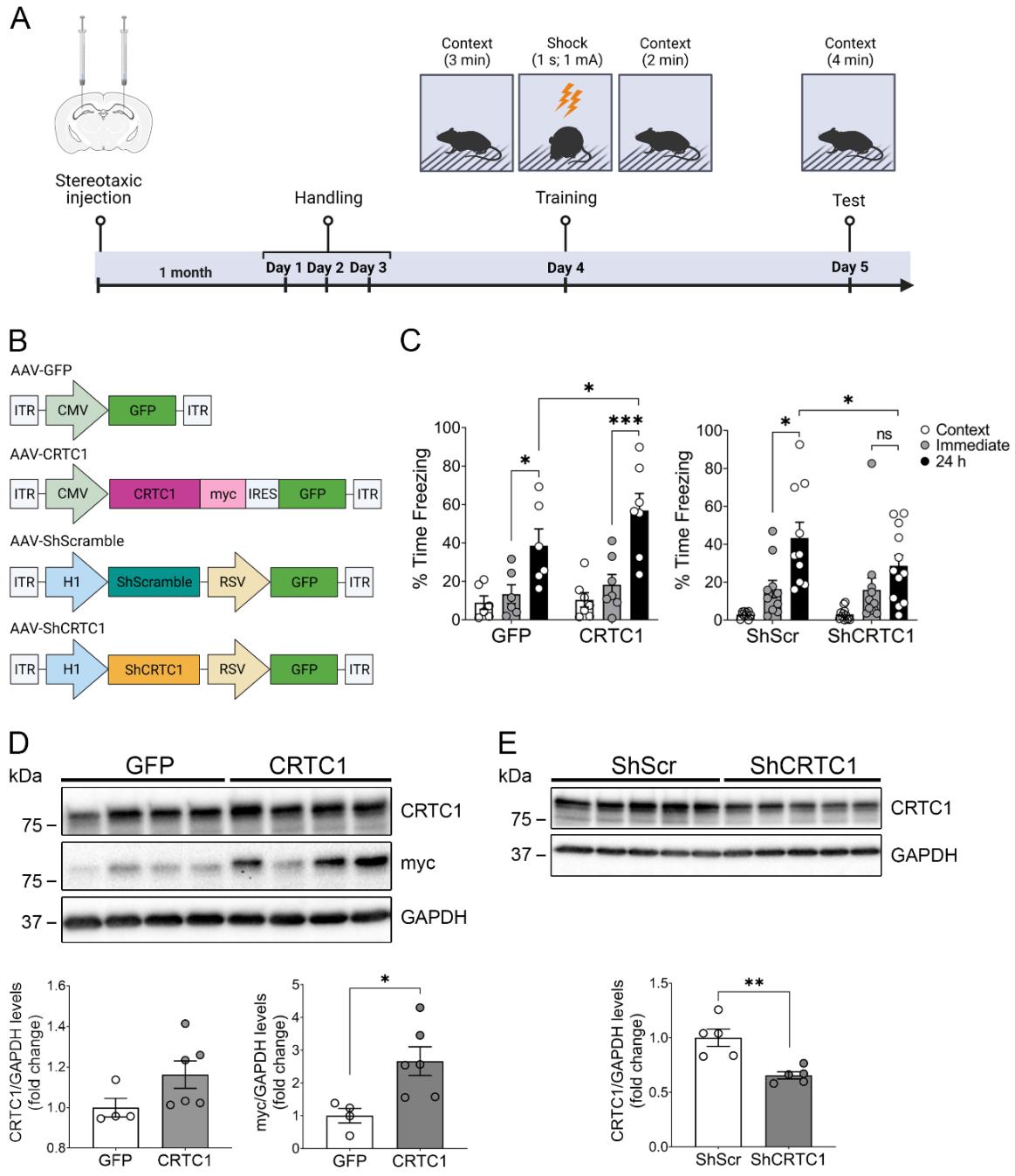

Figure 9. CRTC1 is required for associative memory. (A) CFC behavioral paradigm used to assess associative memory. C57BL/6 adult mice (6 month-old) were bilaterally injected in the dorsal hippocampus and tested before (context), immediately and 24 h after contextual fear conditioning. **(B)** Schematic representation of AAV2/10 vectors engineered to overexpress (AAV-CRTC1) or silence (AAV-ShCRTC1) CRTC1 and the respective controls (AAV-GFP or AAV-ShScramble). ITR: inverted terminal repeat; CMV: cytomegalovirus promoter; IRES: internal ribosome entry site; GFP: green fluorescent protein, H1: histone 1 promoter; RSV: Rous sarcoma virus promoter. **(C)** Percentage of time freezing in AAV-GFP- and AAV-CRTC1-injected mice (left) or AAV-ShScramble- and AAV-ShCRTC1-injected mice (right). Values represent mean percentage of freezing ± SEM of multiple mice (n = 6-12) per group. **(D,E)** Western blot images and quantification analysis of CRTC1 and myc-tag protein levels. Protein levels were normalized to GAPDH. Data represent mean ± SEM of multiple mice (n = 4-6) per group. Two-way ANOVA followed by Scheffé's post hoc test or unpaired Student t test were used as a statistical test. **P* < 0.05, ***P* < 0.01, ****P* < 0.001.

2. CRTC1 regulates glutamate receptors in neurons

2.1. CRTC1 does not affect AMPAR levels or phosphorylation

To investigate the CRTC1-dependent molecular mechanisms underlying associative memory, we first examined whether CRTC1 regulated expression and/or activation of AMPA receptors (AMPARs), which are key players in fast excitatory neurotransmission. We biochemically analyzed GluA1 and GluA2 subunits of AMPARs in hippocampal lysates from AAV-GFP or AAV-CRTC1-injected mice tested in the CFC (**Figure 9A,C**). As controls, naïve non-injected mice were used. Total GluA1 and GluA2 levels were unchanged after CRTC1 overexpression (GluA1: $P = 0.774$; GluA2: $P = 0.069$), whereas phosphorylated GluA1 at Ser 831 and Ser 845 relative to total GluA1 levels were not affected (pGluA1(Ser831)/GluA1: $P = 0.42$; pGluA1(Ser845)/GluA1: $P = 0.968$, **Figure 10A**). To further confirm these results, hippocampal lysates from mice stereotaxically injected with AAV-ShScr or AAV-ShCRTC1 were analyzed (**Figure 10B**). Only a statistically significant difference among groups was observed in phosphorylated GluA1 at Ser 831 relative to total GluA1 (pGluA1(Ser831)/GluA1: $P = 0.013$; pGluA1(Ser845)/GluA1: $P = 0.132$; GluA1: $P = 0.1$; GluA2: $P = 0.076$, **Figure 10B**).

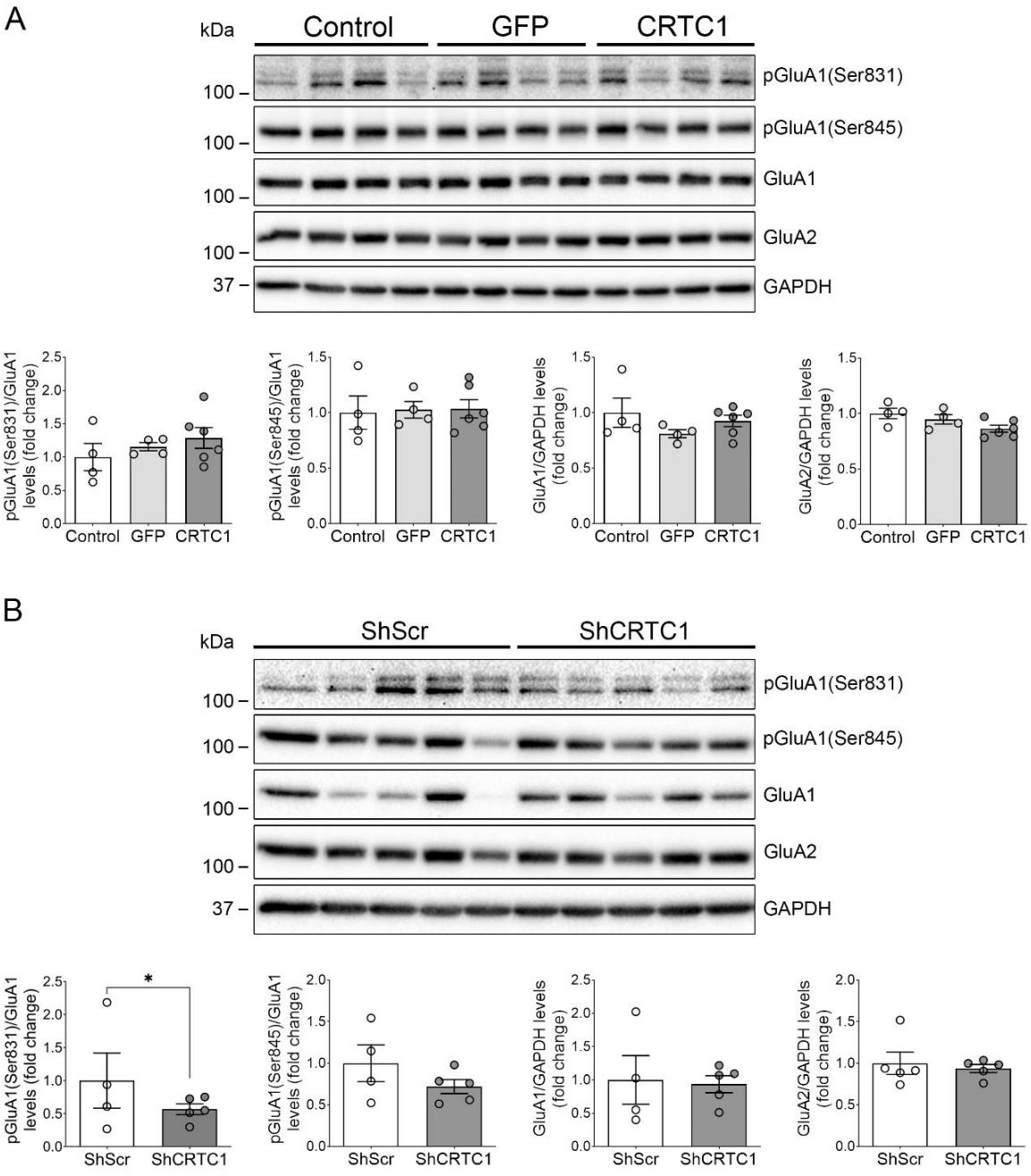

Figure 10. CRTC1 overexpression or inactivation do not affect total and phosphorylated AMPARs in the mouse hippocampus. Western blot images and quantification analysis of phosphorylated (p) and/or total GluA1 and GluA2 levels in hippocampal lysates of naïve (control) and GFP- or CRTC1-injected mice **(A)**, and ShScr- or ShCRTC1-injected mice **(B)**. Protein levels were normalized to GAPDH or total GluA1. Data represent mean ± SEM of multiple mice (n = 4-6) per group. One-way ANOVA followed by Tukey's post hoc test or wo-tailed unpaired Student t test were used as a statistical test. **P* < 0.05.

2.2. CRTC1 modulates NMDAR levels and phosphorylation

To examine whether CRTC1 regulates NMDARs subunit composition and/or phosphorylation, I next analyzed total and phosphorylated NMDARs subunits levels in the above lysates. Western blot and quantification analyses showed that GluN1 subunit levels remained constant between groups (*P* =

0.605). However, CRTC1 overexpression increased phosphorylated GluN1 at two different residues, Ser 890 (P = 0.05) and Ser 897 (P = 0.009), reported to be phosphorylated by PKCγ and PKA, respectively [(Sánchez-Pérez and Felipo, 2005, Zou et al., 2002), **Figure 11A**]. Considering that phosphorylated GluN1 (Ser 890) levels are similar in naïve (control) and AAV-GFP-injected mice (P = 0.591), memory-induced GluN1 phosphorylation at Ser 890 seems to be dependent on CRTC1 (**Figure 11A**). Conversely, increased pGluN1 at Ser 897 is like due to CFC training as revealed by a significant increase in both AAV-GFP- (P = 0.021) and AAV-CRTC1-injected mice (P = 0.008, **Figure 11A**). To further corroborate whether CRTC1 regulates GluN1 levels and phosphorylation, hippocampus of mice stereotaxically injected with AAV-ShScr or AAV-ShCRTC1 were analyzed. Notably, AAV-ShCRTC1-mediated CRTC1 inactivation reduced significantly total GluN1 (P = 0.015), without significant changes in phosphorylated GluN1 normalized to total GluN1 (pGluN1(Ser890)/GluN1: P =0.209; pGluN1(Ser897)/GluN1: P = 0.162, **Figure 11B**).

Next, I analyzed total and phosphorylated GluN2 subunits in control and AAV-injected groups. Mice overexpressing CRTC1 showed a slight non-significant reduction of GluN2A and increase of GluN2B levels (GluN2A: P = 0.069; GluN2B: P = 0.099, **Figure 12A**). Interestingly, CRTC1-injected mice showed an increase of GluN2B/GluN2A levels (P = 0.002) without significant changes in PKC-dependent GluN2B phosphorylation (Ser 1303) (pGluN2B(Ser1303)/GluN2B: P = 0.979, **Figure 12A**). In AAV-ShCRTC1-injected mice, there was not any change in GluN2 subunit expression levels (GluN2A: P = 0.404; GluN2B: P = 0.722; pGluN2B(Ser1303)/GluN2B: P = 0.14, **Figure 12B**). This result is interesting because it suggests that CRTC1 could mediate a shift in GluN2 subunits of NMDARs favoring GluN2B instead of GluN2A subunits. Our biochemical analyses suggest that CRTC1 may be critical for glutamatergic neurotransmission by regulating GluN1 levels and promoting PKCγ-mediated GluN1 phosphorylation at Ser 890.

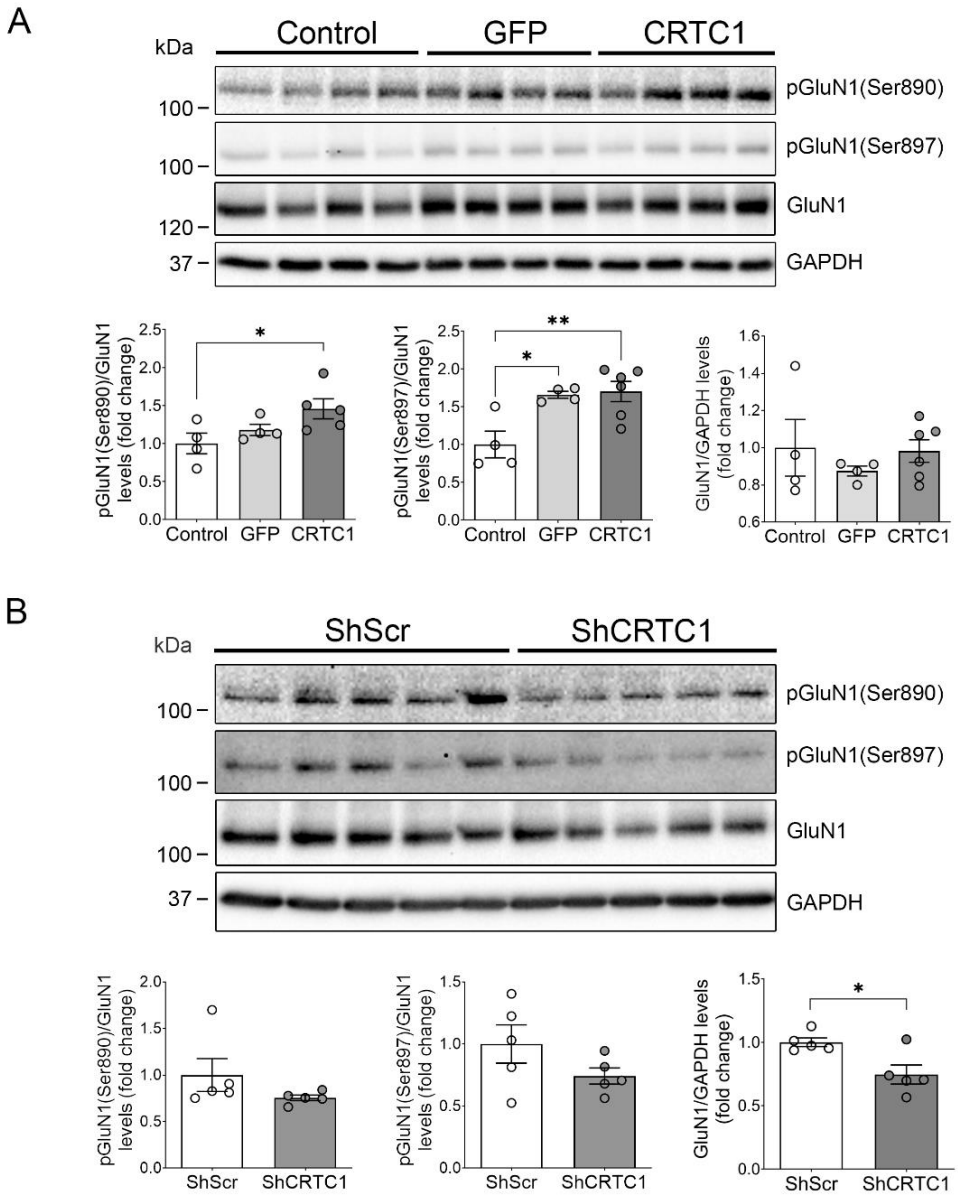

Figure 11. CRTC1 potentiates total and phosphorylated GluN1 in the mouse hippocampus. Western blot images and quantification analysis of phosphorylated (p) and total GluN1 levels in hippocampal lysates of naïve (control) or AAV-GFP- or AAV-CRTC1-injected mice **(A)**, and AAV-ShScr- or AAV-ShCRTC1-injected mice **(B)**. Protein levels were normalized to GAPDH or total GluN1. Data is represented as mean ± SEM of multiple mice (n = 4-6) per group. One-way ANOVA followed by Tukey's post hoc test or two-tailed unpaired Student t test were used as statistical tests. **P* < 0.05, ***P* < 0.01.

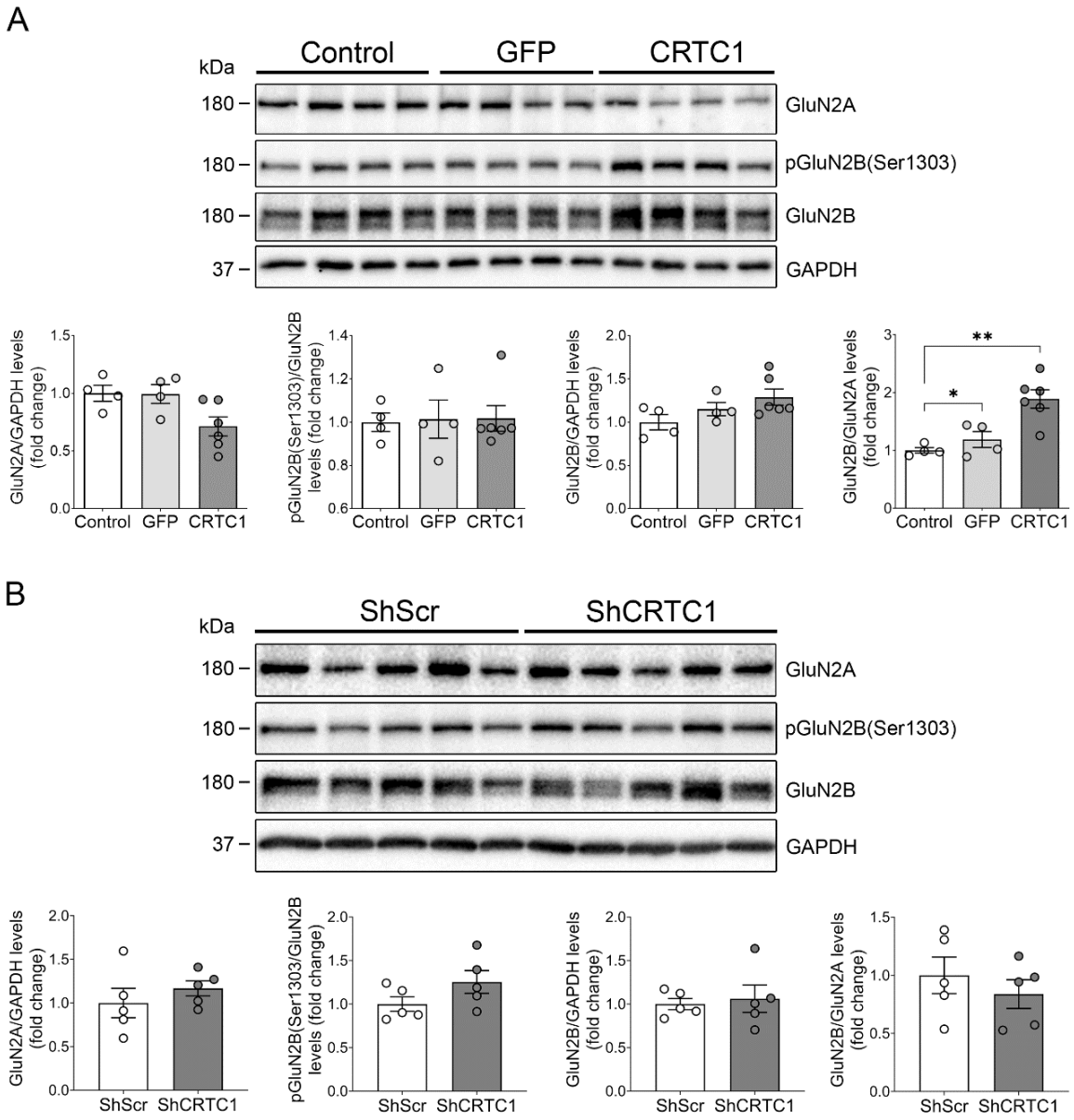

Figure 12. Effect of CRTC1 overexpression on GluN2 subunits in the mouse hippocampus. Western blot and quantitative analyses of phosphorylated (p) and/or total GluN2A and GluN2B levels in hippocampal lysates of naïve (control) or AAV-GFP- or AAV-CRTC1-injected mice **(A)**, and AAV-ShScr- or AAV-ShCRTC1-injected mice **(B)**. Protein levels were normalized to GAPDH or total GluN2B. Data represent mean ± SEM of multiple mice (n = 4-6) per group. One-way ANOVA followed by Tukey's post hoc test or two-tailed unpaired Student t test were used as statistical tests. **P* < 0.05, ***P* < 0.01.

2.3. PKC-mediated GluN1 phosphorylation at Ser 890 enhances GluN1 synaptic localization

Protein phosphorylation is a reversal post-translational modification that regulates a wide range of biological processes, including glutamate ionotropic receptor cell surface localization and gating (Lee, 2006, Salter et al., 2009). To evaluate whether CRTC1 was potentiating GluN1 phosphorylation at Ser 890 through PKC activation, cultured cortical neurons (20 DIV) were pharmacologically

treated with phorbol-12-myristate 13-acetate (PMA) and GF-109203X hydrochloride (GF), which activates and inhibits PKC, respectively. Biochemical analyses revealed that PMA increases GluN1 phosphorylation (Ser 890), which was decreased by the presence of GF (P = 0.024), indicating that GluN1 phosphorylation at Ser 890 is PKC-dependent (**Figure 13**). Total GluN1 levels were unaffected by PMA in the presence or absence of GF (**Figure 13**). Interestingly, induction of synaptic activity via network disinhibition through the stimulation with Bicuculline methiodide (Bic), a GABAA receptor antagonist, and 4-aminopyridine (4-AP), a K^+ channel blocker, also potentiated GluN1 phosphorylation at Ser890 (P = 0.019, **Figure 13**).

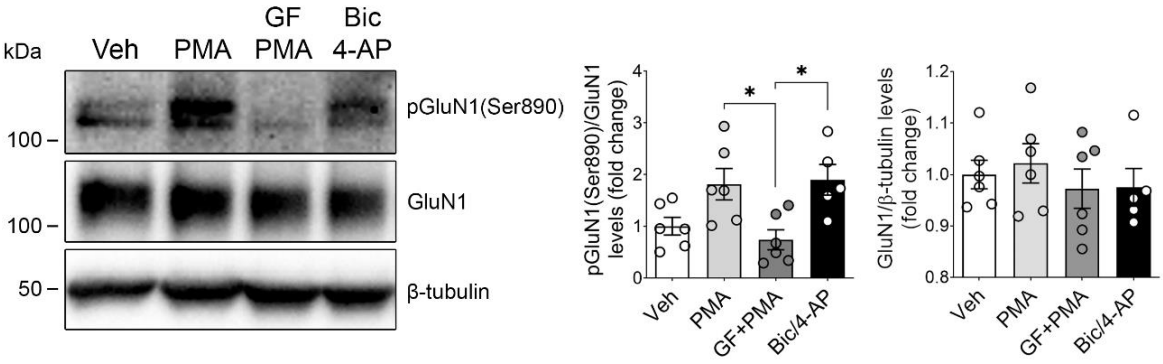

Figure 13. GluN1 phosphorylation at Ser 890 is dependent on PKC and synaptic activity. Western blot and quantification analysis of phosphorylated (p) and total GluN1 in cultured cortical neurons (20 DIV). Neurons were pretreated with 1 µM tetrodotoxin (TTX; 16 h) and treated with phorbol-12-myristate 13-acetate (PMA, 5 µM; 15 min) in the presence or absence of GF-109203X hydrochloride (GF, 10 µM; 30 min), or Bic/4-AP (50 µM, 2.5 mM; 15 min). Protein levels were normalized to β-tubulin or total GluN1. Data represent mean ± SEM of independent cultures (n = 6). One-way ANOVA followed by Tukey's post hoc test was used as a statistical test. *P < 0.05.

To investigate if under our experimental conditions, PKC activation increases GluN1 synaptic localization, mature hippocampal neurons (20 DIV) were treated with the PKC activator PMA for 15 min. Hippocampal neurons were then fixed and immunostained for GluN1 and the postsynaptic scaffolding protein PSD95. After confocal microscope imaging, GluN1/PSD95 colocalization was quantified using the Imaris 8 software. In primary dendrites, PMA treatment did not affect GluN1 synaptic colocalization as not significant differences were observed in GluN1/PSD95 puncta (P = 0.325, **Figure 14A**). By contrast, PKC activation increased the number of PSD95 puncta (P = 0.041) and the percentage of GluN1/PSD95 puncta (P = 0.014) in secondary dendrites (**Figure 14B**). These results indicate that PKC activation potentiates PSD95 accumulation at postsynapses in secondary dendrites and, consequently, the recruitment of NMDARs.

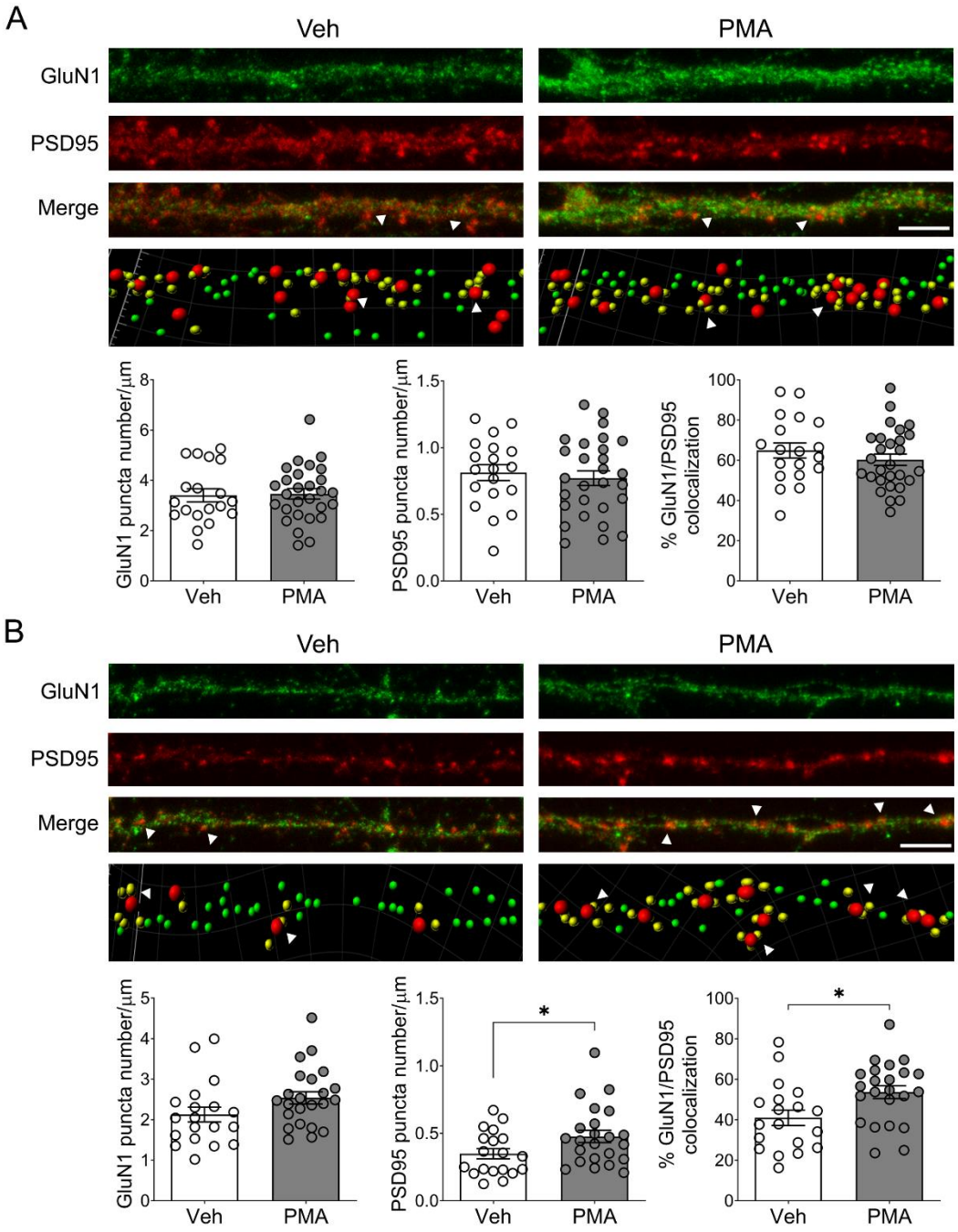

Figure 14. PKC activation potentiates GluN1/PSD95 colocalization in secondary dendrites of hippocampal neurons. Confocal images of primary **(A)** and secondary **(B)** dendrites of hippocampal neurons (20 DIV) treated with vehicle (Veh) or PMA (5 µM, 15 min). Neurons were imaged for GluN1 (green) and PSD95 (red). Total GluN1 (green spots) and PSD95 (red spots) puncta per µm, and GluN1/PSD95 colocalization (arrowheads/yellow spots) were quantified. Data represent mean ± SEM (n = 19-28 dendrites from two biological replicates). Statistical analysis was determined by two-tailed t-test. **P* < 0.05. Scale bar: 5 µm.

2.4. GluN1 phosphorylation is independent of transcription

As protein kinase activity is a reversible and dynamic process (Gelens and Saurin, 2018), we investigated whether GluN1 phosphorylation at Ser 890 was dependent on transcriptional activity.

Transcriptional blockade with actinomycin D (ActD) did not prevent GluN1 phosphorylation at Ser 890 upon synaptic stimulation with Bic/4-AP (P = 0.002) in cultured cortical neurons (**Figure 15**). This pharmacological treatment did not significantly affect total GluN1 levels (**Figure 15**). This suggests that PKC-dependent GluN1 phosphorylation at Ser 890 is independent of gene transcription.

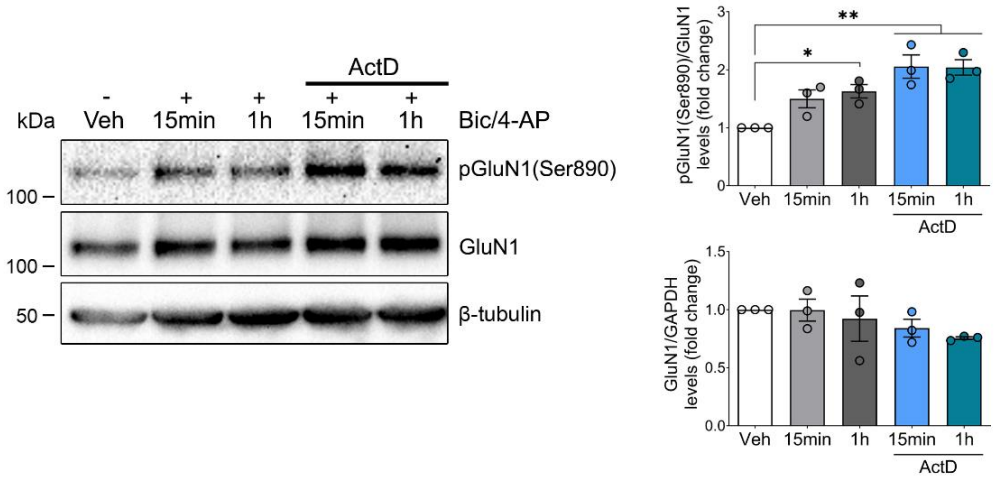

Figure 15. GluN1 phosphorylation at Ser 890 is independent of transcription. Western blot and quantification analyses of phosphorylated (p) GluN1 and total GluN1 protein levels of cultured cortical neurons (20 DIV). Neurons were treated with Actinomycin D (2 µg/ml; 1 h) to block gene transcription before synaptic stimulation with Bic/4-AP (50 µM, 2.5 mM; 15 min or 1 h). Protein levels are normalized to β-tubulin or total GluN1. Data represent mean ± SEM of independent cultures (n = 3). One-way ANOVA followed by Tukey's post hoc test was used as a statistical test. *P < 0.05, **P < 0.01.

2.5. CRTC1 locally regulates GluN1 synaptic localization

CRTC1 is critical for activity-dependent expression of neuronal gene programs (Parra-Damas et al., 2014, Parra-Damas et al., 2017b), but whether CRTC1 plays additional roles in neurons independent of transcription is still unclear. Since the above biochemical analyses suggest that CRTC1 could be mediating PKC-induced GluN1 Ser 890 phosphorylation independent of gene transcription, we next investigated whether CRTC1 could regulate GluN1 localization at synapses.

2.5.1. Effect of Ser phosphorylation-deficient CRTC1 mutants on CRTC1-mediated transcription and nuclear translocation

To gain insights into the mechanisms regulating CRTC1 expression, nuclear translocation and synaptic and transcriptional functions, expression, and nuclear translocation, I characterized distinct CRTC1 mutants (**Figure 16A**). The triple CRTC1 S64/151/245A mutant contains three serine to alanine mutations in conserved serine residues localized in the N-terminal and NES domains that are dephosphorylated by calcineurin/PP2B leading to CRTC1 nuclear localization [(Ch'ng et al., 2012, Nonaka et al., 2014, Ch'ng et al., 2015), **Figure 8A,16A**]. In addition, the CRTC1 nuclear

localization sequence (NLS) mutants mNLS1 (R103A, R106A, R108A and R110A) and mNLS2 (P114A, R116A and R117A) showed impaired activity-dependent nuclear translocation (Ch'ng et al., 2015). I first, evaluated expression of CRTC1 mutants in transiently transfected HEK293T cells. Immunoblotting against HA-tag and myc-tag showed a specific band corresponding to CRTC1 molecular weight (75 kDa), indicating that all mutants are properly expressed (**Figure 16B**). Compared to CRTC1, which was translocated to the nucleus after FSK/KCl treatment, either the triple CRTC1 S64/151/245A and NLS mutants did not translocate to the nucleus after FSK/KCl treatment (**Figure 16C,D**). NLS mutants translocation results agreed with previous studies (Ch'ng et al., 2015).

CRTC1 interacts with CREB/CBP complex to induce CRE-dependent transcription (Conkright et al., 2003, Bittinger et al., 2004). By using a CRE-dependent luciferase assay, we found that neuronal activity induced 2-fold increase in CREB-mediated transcription in control ($P < 0.001$) but not in CRTC1 inactivation (ShCRTC1) conditions ($P > 0.999$, **Figure 16E**). In LV-ShCRTC1 conditions, expression of wild-type CRTC1, but not CRTC1 S64/151/245A-myc mutant, was able to increase CREB transcriptional activity in basal and synaptic and neuronal activities conditions (**Figure 16E**). Surprisingly, although both CRTC1 mNLS mutants were unable to translocate to the nucleus in basal or neuronal activity conditions, they induced CREB-mediated transcription upon Bic/4-AP (mNLS2: $P = 0.013$) and/or FSK/KCl stimulation (mNLS1: $P = 0.004$; mNLS2: $P = 0.044$; **Figure 16E**). Considering that CREB is regulated by a wide range of signaling pathways (Alberini, 2009), it is possible that these mutants are potentiating some of these intracellular signals that lead to CREB activation.

Therefore, the phosphorylation-defective CRTC1 S64/151/245A mutant is not able to translocate to the nucleus to promote CREB-mediated transcription in response to neuronal activity.

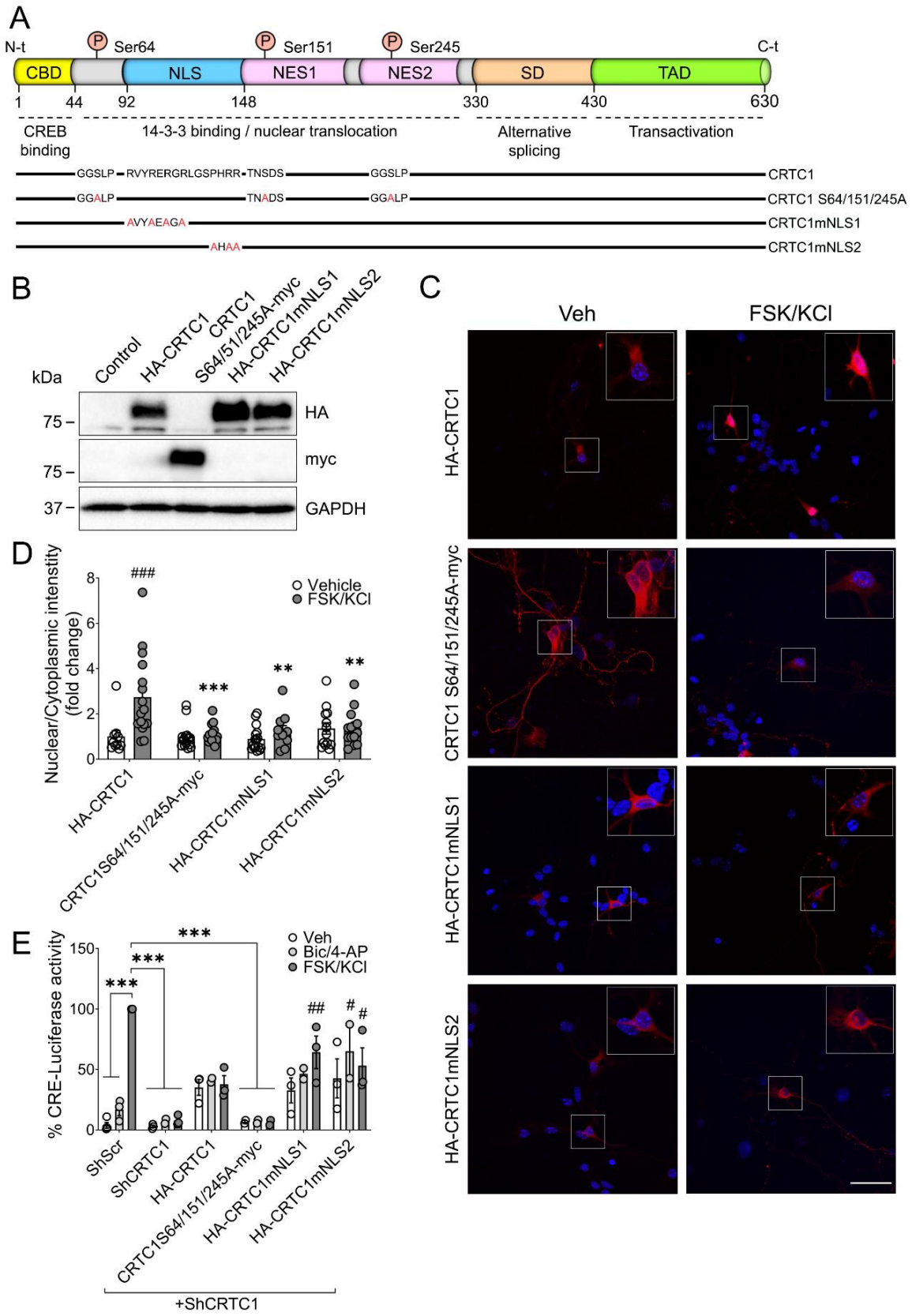

Figure 16. Point mutations in CRTC1 conserved domains impair activity-dependent CRTC1 nuclear translocation and transcriptional activity. (A) Schematic representation of mouse CRTC1 (top) and CRTC1 S64/151/245A, CRTC1mNLS1 and CRTC1mNLS2 mutants. **(B)** Western blot images of HEK293T cells transfected with wild-type and mutant CRTC1. **(C)** Confocal images of transfected hippocampal neurons (7

DIV) with HA-CRTC1, CRTC1 S64/151/245A-myc, HA-CRTC1mNLS1 or HA-CRTC1mNLS2 (in red) treated with vehicle or FSK/KCl (20 µM, 30 mM) for 15 min. Scale bar: 40 µm. **(D)** Quantification of nuclear/cytoplasmic CRTC1 intensity (n = 10-16 neurons from two independent cultures). Two-way ANOVA followed by Tukey's post hoc test was used. $^{**}P < 0.01$ and $^{***}P < 0.001$ compared to HA-CRTC1 FSK/KCl; $^{\#\#\#}P < 0.001$ compared to HA-CRTC1 Veh. **(E)** CREB transcriptional activity analysis in cortical neurons (8 DIV) transduced with LV-ShScr or ShCRTC1 and transfected with the wild-type or mutatnt CRTC1. Neurons were treated with vehicle, Bic/4-AP (50 µM, 2.5 mM) or FSK/KCl (20 µM, 30 mM) for 4 h before analyzing the CRE-promoter luciferase activity. Data represent mean ± SEM of three independent experiments. Two-way ANOVA followed by Tukey's post hoc test was used as a statistical test. $^{***}P < 0.001$; $^{\#}P < 0.05$ and $^{\#\#}P < 0.01$ compared with ShCRTC1 FSK/KCl.

2.5.2. Synaptic CRTC1 modulates activity-dependent GluN1 localization at synapses

We next analyzed the role of endogenous CRTC1 and phosphodeficient CRTC1 S64/151/245A mutant on synaptic GluN1 localization. Cultured hippocampal neurons (20 DIV) transduced with lentivirus expressing control (ShScr-GFP) or *Crtc1* (ShCRTC1-GFP) shRNA alone or in combination with CRTC1 S64/151/245A-myc mutant were analyzed for GluN1/PSD95 colocalization. Only GFP-positive or GFP- and myc-positive neurons were considered for the confocal imaging analyses. In basal vehicle (TTX) or synaptic activity (TTX plus Bic/4-AP for 1 h) conditions, CRTC1 inactivation or CRTC1 S64/151/245A overexpression did not affect GluN1 puncta number (treatment effect: $P = 0.114$; transduction effect: $P = 0.376$, **Figure 17A,B**). Interestingly, in basal conditions, CRTC1 S64/151/245A increased significantly total PSD95 puncta ($P = 0.006$) and GluN1/PSD95 colocalization ($P = 0.017$) compared to control and CRTC1-silenced neurons (PSD95 puncta: $P = 0.009$; GluN1/PSD95: $P = 0.037$, **Figure 17A,B**). Upon synaptic activity, GluN1/PSD95 colocalization was increased in control neurons compared to basal conditions ($P = 0.002$), an effect not observed in the absence of CRTC1 ($P = 0.959$) or in mutated CRTC1-overexpressing neurons ($P = 0.901$, **Figure 17A,B**). These results indicate that CRTC1 is required for synaptic activity-dependent GluN1 localization at synapses, and that CRTC1 inactivation occludes the effect of activity on synaptic GluN1/PSD95 localization. Moreover, this effect seems to be independent of CRTC1 nuclear activity as the phosphodeficient CRTC1 S64/151/245A mutant can modulate GluN1 synaptic localization.

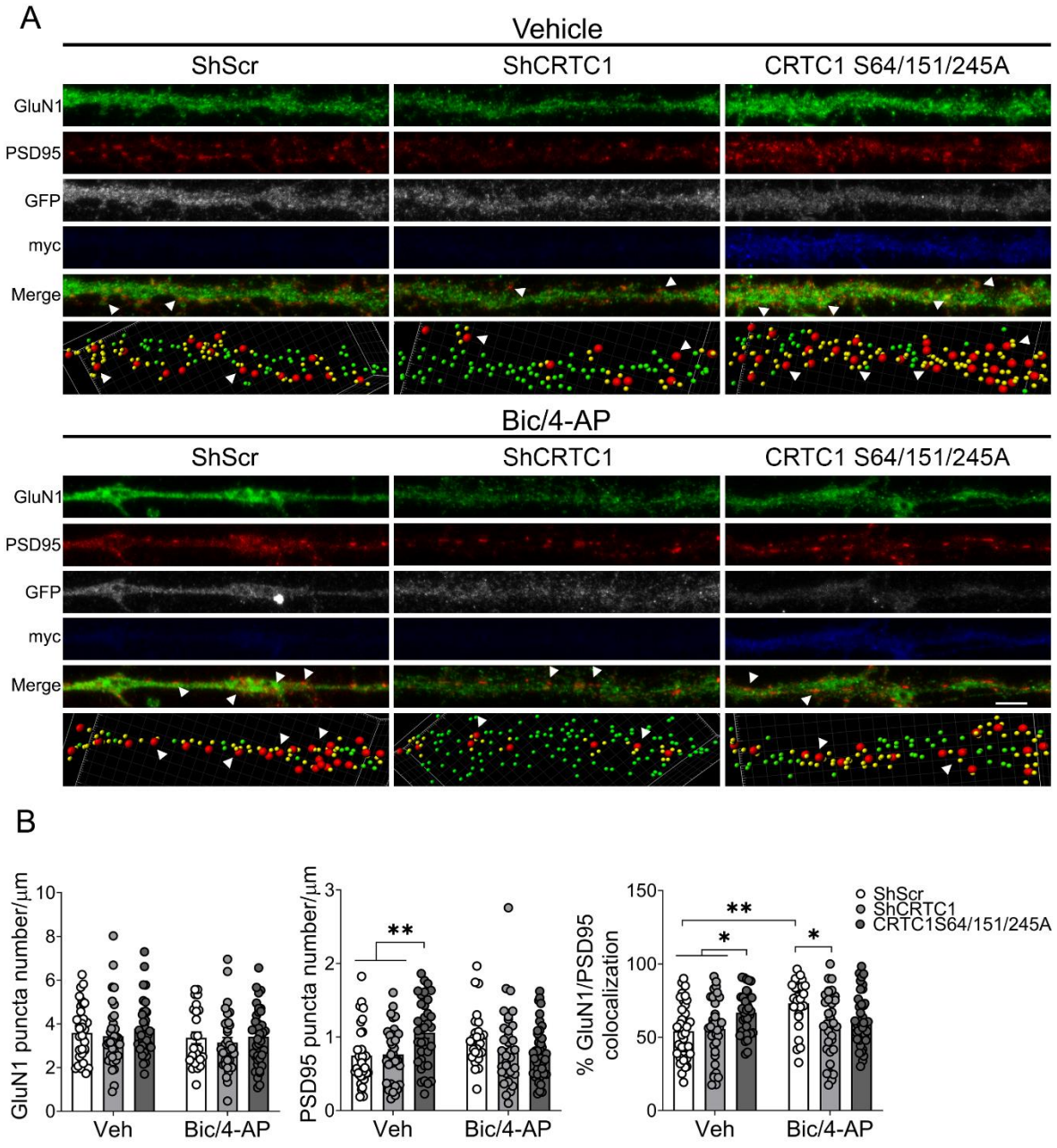

Figure 17. Activity-dependent GluN1 synaptic localization is locally regulated by CRTC1. Representative images of primary dendrites of hippocampal neurons (20 DIV) transduced with LV-ShScr or LV-ShCRTC1 alone or with LV-CRTC1S64/151/245A for 5 days, treated with TTX (1 µM for 16 h) and stimulated with Bic/4-AP (50 µM, 2.5 mM for 1 h). Neurons were imaged for GluN1 (green), PSD95 (red), GFP (grey) and myc-tag (blue). Total GluN1 (green spots) and PSD95 (red spots) puncta per µm, and GluN1/PSD95 colocalization (arrowheads/yellow spots) were quantified. Data represent mean ± SEM (n = 24-42 dendrites from three independent cultures). Statistical analysis was determined by two-way ANOVA followed by Tukey's post hoc test. **P* < 0.05, ***P* < 0.01. Scale bar: 5 µm.

2.5.3. Synaptic activity reduces PSD95 phosphorylation independently of CRTC1

GluN1 phosphorylation is important for receptor localization and gating, but PSD95 phosphorylation/dephosphorylation also regulates synaptic strength at excitatory synapses (Kim et

al., 2007, Sen et al., 2016). PKC-dependent phosphorylation of PSD95 at Ser 295 potentiates PSD95 accumulation at the postsynaptic density and the recruitment of AMPARs, while its dephosphorylation is associated with LTD (Kim et al., 2007, Sen et al., 2016). To further investigate the role of CRTC1 in NMDA-mediated synaptic plasticity, I next studied how synaptic activity affected GluN1 and PSD95 phosphorylation. Here, we analyzed total and phosphorylated levels of GluN1 and PSD95 in cultured cortical neurons (20 DIV), transduced with LV-ShScr or LV-ShCRTC1 alone or in combination with LV-CRTC1 S64/151/245, and treated with vehicle TTX (O/N) to reduce basal synaptic activity or stimulated with Bic/4-AP (15 min or 1 h). Biochemical analyses showed reduced endogenous CRTC1 after LV-ShCRTC1 silencing (transduction effect: $P < 0.0001$, **Figure 18**), which was rescued after LV-CRTC1 S64/151/245 transduction ($P = 0.003$). Interestingly, CRTC1 protein levels were increased in control neurons upon treatment with Bic/4-AP for 15 min ($P = 0.004$) or 1 h ($P = 0.002$) compared to TTX-treated neurons (**Figure 18**).

Synaptic activity induced a non-significant time-dependent increase of in control and CRTC1-silenced neurons. By contrast, neurons transduced with LV-CRTC1 S64/151/245A show higher pGluN1 in TTX conditions, an effect that decreases with time (**Figure 18**). These results agree with increased GluN1/PSD95 localization at synapses in stimulated control neurons and in TTX-treated neurons overexpressing CRTC1 S64/151/245A (**Figure 17**). On the contrary, synaptic activity caused a time-dependent reduction of pPSD95 in control and CRTC1-silenced neurons (**Figure 18**), which could result in loss of synaptic PSD95 and, consequently, internalization of glutamate receptors. This activity-dependent PSD95 dephosphorylation was lost in CRTC1 S64/151/245A-expressing neurons (**Figure 18**), suggesting that synaptic CRTC1 contributes to PSD95 clustering and stabilization at synapses.

Together, the biochemical and immunofluorescence analyses indicate that CRTC1 modulates PKC-dependent GluN1 and PSD95 phosphorylation, contributing to PSD95 reorganization and glutamate receptor stabilization at synapses. Based on the constitutively cytosolic/synaptic CRTC1 S64/151/245A mutant, we conclude that synaptic GluN1/PSD95 is stabilized by CRTC1 independently of its nuclear function.

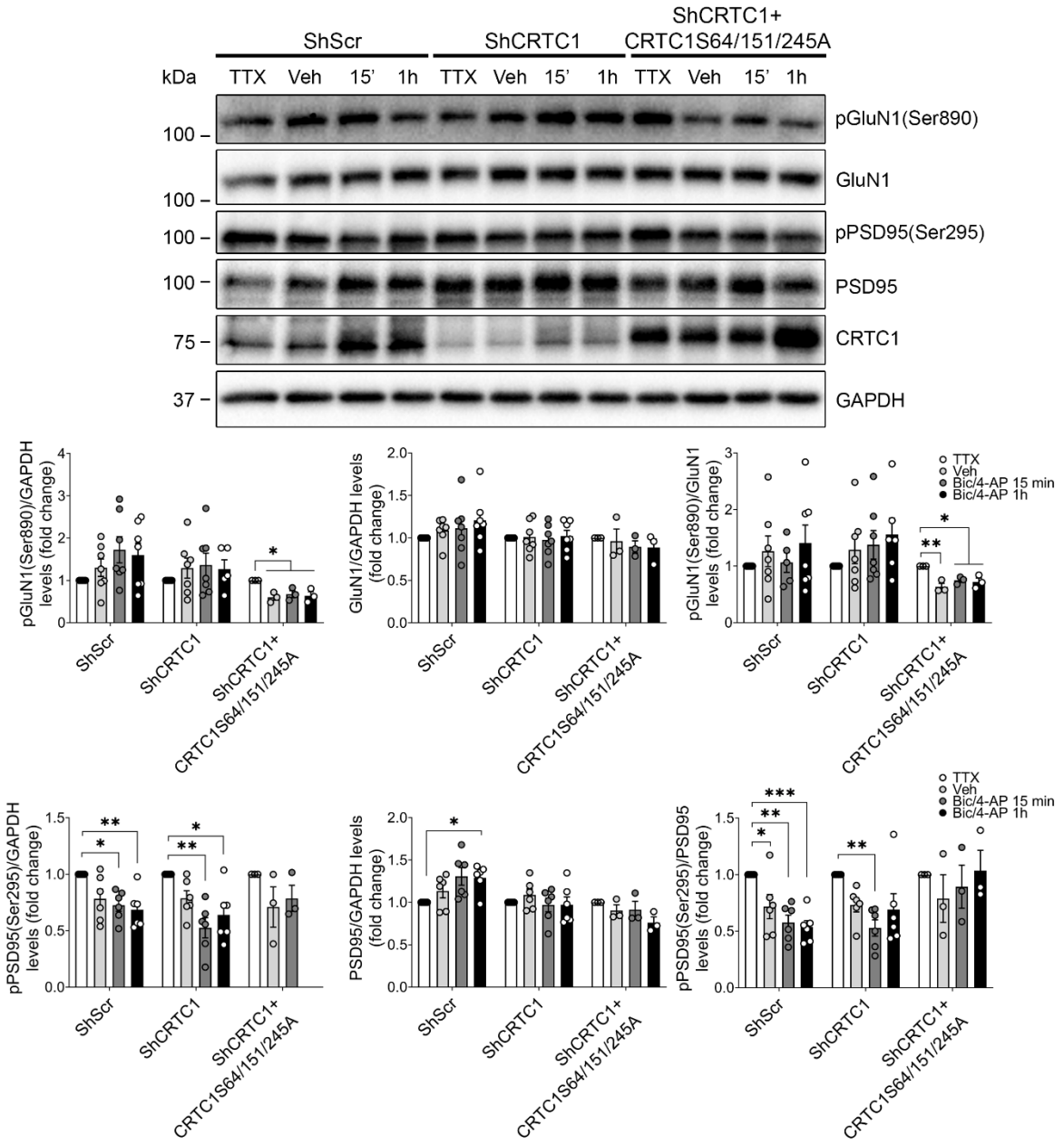

Figure 18. Synaptic activity induced PSD95 dephosphorylation is blocked by CRTC1 S64/151/245A mutant. Western blot and quantification analysis of total and phosphorylated (p) GluN1 and PSD95, and total CRTC1 of cultured cortical neurons (20 DIV), transduced with LV-ShScr or LV-ShCRTC1 alone or in combination with LV-CRTC1 S64/151/245A, pretreated with TTX (1 µM, 16 h), and stimulated with vehicle (Veh) or Bic/4-AP (50 µM, 2.5 mM; 15 min or 1 h). Protein levels were normalized to GAPDH, to total GluN1 or total PSD95. Data is represented as mean ± SEM of independent cultures (n = 3-6). One-way ANOVA followed by Tukey's post hoc test was used as a statistical test. **P* < 0.05, ***P* < 0.01, ****P* < 0.001.

2.6. CRTC1 increases GluN1 interaction with the calcium sensor calmodulin

Calcium sensors such as calmodulin, calneuron or caldendrin are classical Ca^{2+} signaling mediators in neurons (Burgoyne et al., 2019). Ca^{2+} influx through activated NMDARs results in the activation of a wide range of signaling pathways that modulate neuronal function. Calmodulin and calneuron

directly interact with GluN1 subunit coupling NMDARs activation to the MAPK signaling pathway (Franco et al., 2018). To investigate whether CRTC1 modulates the interaction of GluN1 subunit and calcium sensors, bioluminescence resonance energy transfer (BRET) assays were performed in an heterologous expression system. HEK293T cells were transfected with GluN1 fused to Renilla Luciferase (RLuc) and GluN2B for a correct NMDAR assembling and activity, as well as with the calcium sensors calmodulin (CaM), calneuron (Caln) or caldendrin (Cald) fused to YFP (**Figure 19**). BRET signal between the donor (GluN1-RLuc) and the acceptor (calcium sensor-YFP) was measured in the presence or absence of CRTC1. A saturation curve demonstrating a specific interaction was obtained in BRET assays using GluN1-RLuc and CaM-YFP, and GluN1-RLuc and CaM-YFP (**Figure 19A,B**). The linear non-specific signal observed in cells transfected with GluN1-RLuc and Cald-YFP indicates a lack of interaction between NMDARs and this calcium sensor (**Figure 19C**). Interestingly, a significant change in GluN1-Rluc and CaM-YFP interaction in the presence of CRTC1 was detected (P = 0.009), suggesting that CRTC1 potentiates GluN1 and CaM interaction. This effect seems specific for GluN1-CaM since it was not observed with GluN1-Caln partner (P = 0.686). These results indicate that CRTC1 potentiates specifically the interaction between GluN1 and CaM in heterologous cells system.

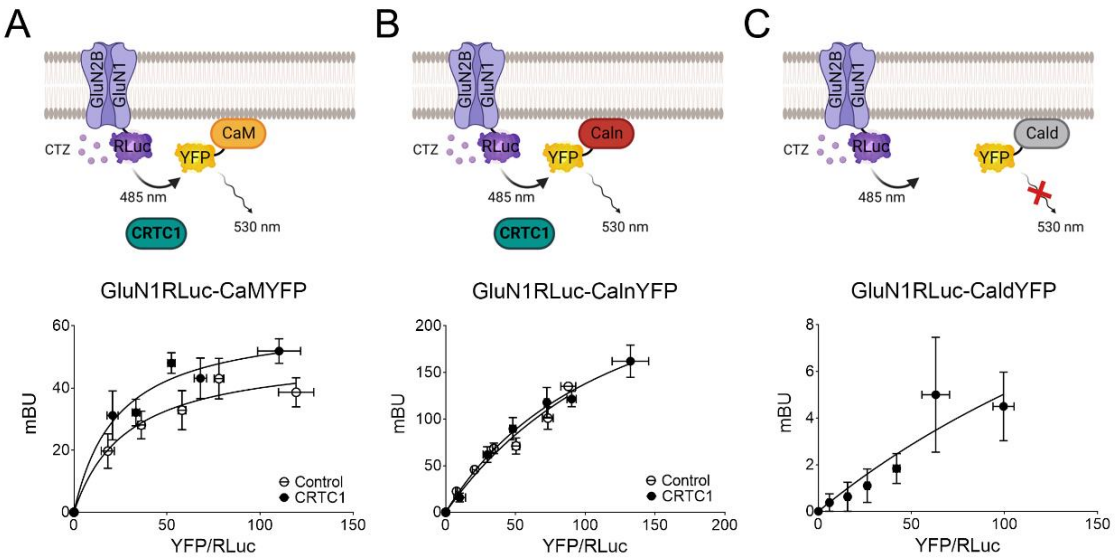

Figure 19. CRTC1 enhances GluN1 interaction with calmodulin. BRET saturation experiments in HEK293T cells transfected with cDNAs for GluN1-RLuc (0.3 µg), GluN2B (0.3 µg), empty vector (Control; 0.5 µg), CRTC1 (0.5 µg) and increasing amounts of cDNAs for CaM-YFP (0.2-1.5 µg) **(A)**, Caln-YFP (0.25-2 µg) **(B)**, or Cald-YFP (0.25-2 µg) **(C)**. Data represent mean ± SEM of independent experiments (n = 3-4). Curves were statistically compared with extra sum of squares F test. RLuc: Renilla Luciferase; YFP: yellow fluorescent protein; CTZ: coelenterazine H; CaM: calmodulin; Caln: calneuron; Cald: caldendrin; mBU: milli BRET units.

3. CRTC1 modulates mRNA localization and protein synthesis at dendrites

The localization of transcripts at specific cellular compartments is critical in compartmentalized cells such as neurons. mRNA pools at dendritic compartments allows neurons to finely tune the responses upon a local stimulus by rapidly synthesizing proteins and incorporating them into postsynaptic sites (Miller et al., 2002, Bradshaw et al., 2003). Here, we studied if CRTC1 could modulate the dendritic localization and/or abundance of mRNAs in cultured hippocampal neurons by using fluorescence in situ hybridization (FISH). Neurons overexpressing CRTC1 showed, independently of the treatment, an increase of total mRNAs levels at MAP2-stained dendrites compared with neurons transduced with empty vector (pWPI) ($P < 0.001$, **Figure 20A,B**). Blockade of synaptic activity with 1 µM TTX did not affect dendritic mRNA levels whereas glutamate (100 µM) stimulation induced a modest, although non-significant, reduction in total mRNAs at dendrites of control and CRTC1 overexpressing neurons (**Figure 20A,B**). Interestingly, glutamate significantly reduced dendritic mRNAs in LV-ShScr transduced neurons ($P = 0.018$), whereas a similar reduction was detected in the absence of CRTC1 (LV-ShCRTC1) independently of the treatment ($P < 0.001$, **Figure 20A,B**). Indeed, the effect of glutamate on dendritic mRNA levels was occluded in ShCRTC1-transduced neurons (**Figure 20A,B**). These results suggest that CRTC1 regulates the localization and/or stability of mRNAs at dendritic compartments in primary hippocampal neurons.

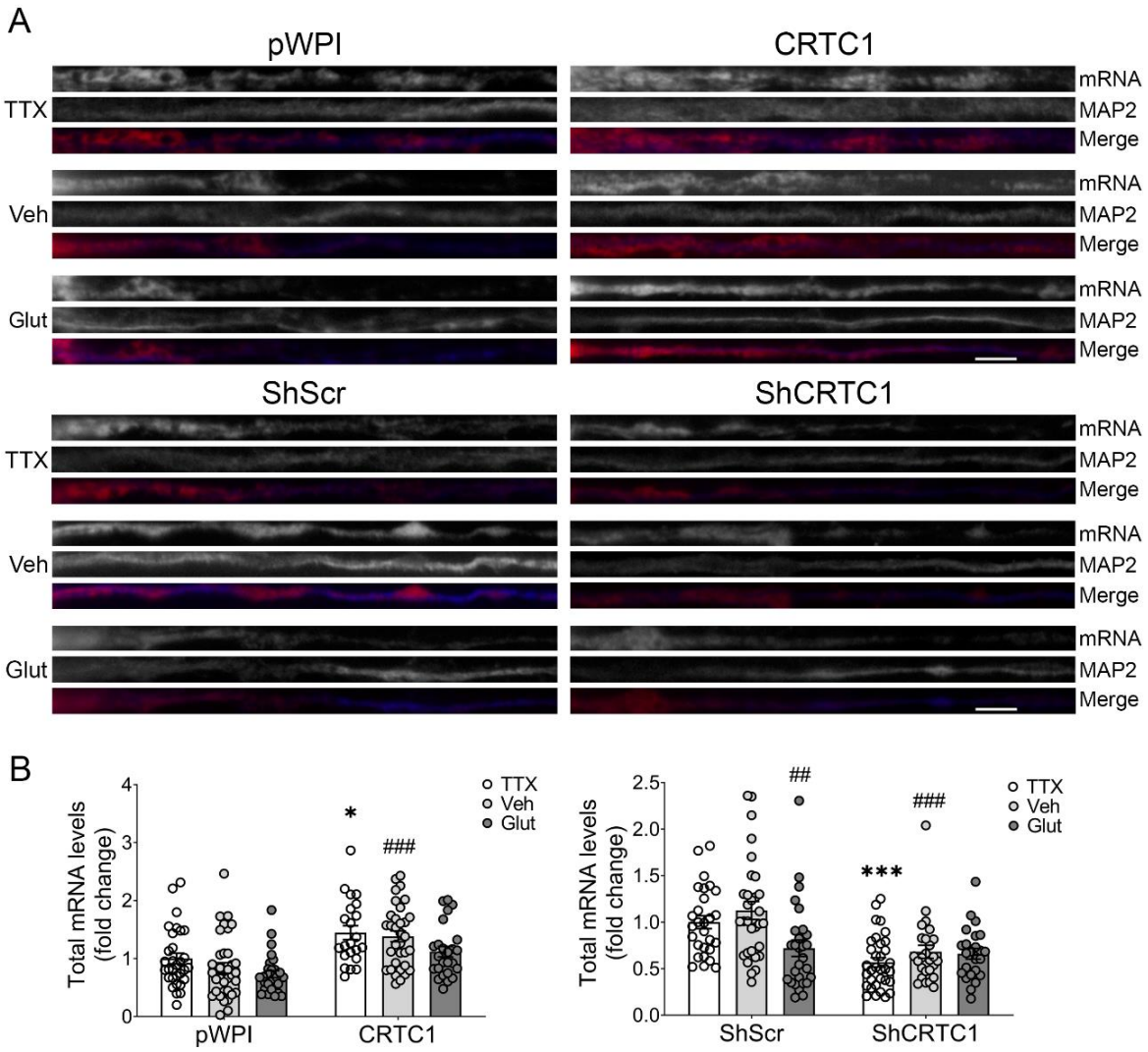

Figure 20. Levels of dendritic mRNAs are positively regulated by CRTC1. (A) Straighten dendrites of cultured hippocampal neurons (11 DIV) transduced with LV-CRTC1 (top) or LV-ShCRTC1 (bottom) and their respective controls LV-pWPI or LV-ShScr. Neurons were treated with 1 µM TTX or 100 µM glutamate for 30 min and imaged for total mRNAs (red) and MAP2 (blue). Scale bar: 5 µm. **(B)** Total mRNA levels were quantified by measuring total mRNA intensity and normalized with control neurons (pWPI or ShScr) treated with TTX. Data represent mean ± SEM of multiple dendrites (n = 24-33) of two biological replicates. Two-way ANOVA followed by Tukey's post hoc test was used as a statistical test. *$P < 0.05$, ***$P < 0.001$ compared with control TTX; $^{\#\#}P < 0.01$, $^{\#\#\#}P < 0.001$ compared with control Veh.

Besides mRNA localization at dendritic compartments, local protein synthesis in neurons is key to modulate synaptic plasticity by synthesizing, in a fast and localized manner, proteins involved in synaptic responses (Miller et al., 2002, Bradshaw et al., 2003, Yoon et al., 2016). To investigate whether CRTC1 controls protein synthesis in dendrites, puromycylation assays were performed in cultured hippocampal neurons transduced with vector, CRTC1 or ShCRTC1 lentiviral vectors. Immunostaining using an anti-puromycin antibody revealed no changes in overall protein synthesis following CRTC1 overexpression ($P = 0.324$), whereas CRTC1 silencing induced a decrease in total

protein synthesis (*P* = 0.039, **Figure 21**). These results indicate that CRTC1 positively regulate local mRNA levels and protein synthesis at dendrites in cultured hippocampal neurons.

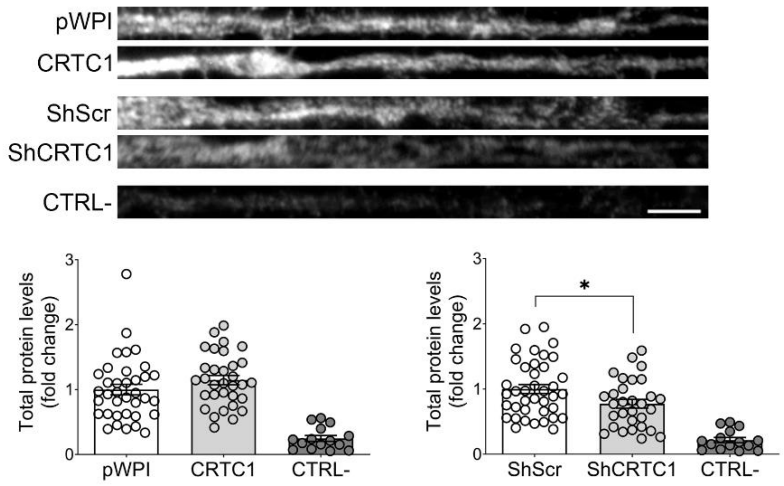

Figure 21. CRTC1 is required for local protein synthesis at dendrites. Straighten dendrites of cultured hippocampal neurons (11 DIV) transduced with LV-CRTC1 or LV-ShCRTC1 and their respective controls LV-pWPI and LV-ShScr. As a negative control (CTRL-), neurons were treated with 200 µM cycloheximide for 1 h prior the incubation with 10 µM puromycin. Total protein levels were quantified by measuring puromycin intensity. Data represent mean ± SEM of multiple dendrites (n = 15-39) of two biological replicates. One-way ANOVA followed by Tukey's post hoc test was used as a statistical test. **P* < 0.05. Scale bar: 5 µm.

CHAPTER 2:

Molecular mechanisms underlying synapse pathology in tauopathies

Presenilin 1 (PSEN1/PS1) and presenilin 2 (PSEN2/PS2) are the catalytic components of the γ-secretase complex, an aspartyl protease responsible of APP processing and Aβ generation. Mutations in *PS1* and *PS2* genes cause early-onset FAD by promoting Aβ and tau pathologies (De Strooper et al., 2012). Mouse model of neurodegeneration lacking both presenilin (PS cDKO) show disrupted CRTC1 phosphorylation, nuclear translocation, and transcription of CREB-dependent genes (Parra-Damas et al., 2014, Parra-Damas et al., 2017a). The tauopathy mouse model PS1 cKO;Tau expressing FTD-linked P301S human Tau and lacking PS1 in glutamatergic neurons exhibits age-dependent tau phosphorylation and aggregation, neurodegeneration and memory deficits (Soto-Faguás et al., 2021). However, the molecular mechanisms linking PS, tau and synaptic pathologies in tauopathies remain unclear.

1. CRTC1 is downregulated at hippocampal synapses of PS1 cKO;Tau mice

To analyze the link between CRTC1 and PS1 and tau, I studied total hippocampal lysates and purified synaptosomes, and pre- and postsynaptic fractions of hippocampus of 11-12 month-old WT, PS1 cKO, Tau and PS1 cKO;Tau mice. At this age, Tau and PS1 cKO;Tau mice develop cerebral tau pathology and neurodegeneration (Soto-Faguás et al., 2021). First, the efficiency of the synaptosomes purification was validated by immunoblotting with antibodies against the postsynaptic marker PSD95 and the presynaptic marker synaptophysin (**Figure 22A**). An enrichment of PSD95 and synaptophysin in the postsynaptic and presynaptic fraction, respectively, certified the correct isolation of purified synaptic fractions (**Figure 22A**).

Total tau was similarly and significantly increased in total hippocampal lysates and purified synaptosome fractions in Tau and PS1 cKO;Tau transgenic mice at 11-12 months of age (lysate: $P < 0.001$; synaptosomes: $P < 0.001$, **Figure 22B-D**). Interestingly, tau phosphorylation at Ser 202 was exacerbated in hippocampal lysates ($P = 0.033$) and synaptosome fraction (not significant) of PS1 cKO;Tau mice compared to Tau mice (**Figure 22B-D**). Compared to control and PS1 cKO mice, tau accumulation in Tau and PS1 cKO;Tau mice was linked to a downregulation of CRTC1 in lysates (Tau: $P < 0.01$; PS1 cKO;Tau: $P < 0.05$) and purified synaptosomes (Tau: $P < 0.05$; PS1 cKO;Tau: $P < 0.05$, **Figure 22B-D**).

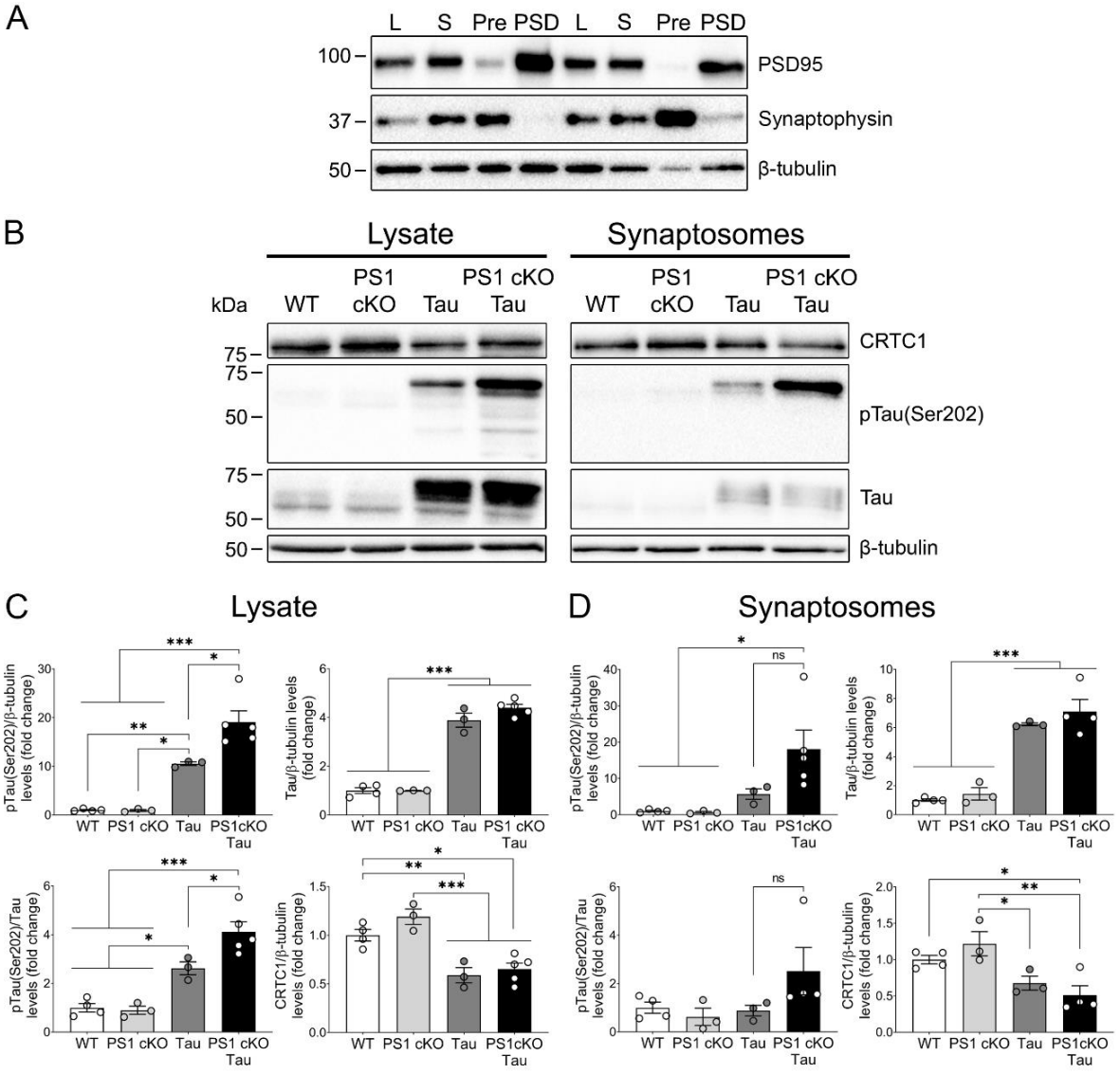

Figure 22. Tau accumulation and CRTC1 downregulation in hippocampal synapses of PS1 cKO;Tau mice. (A) Western blot images of PSD95 and synaptophysin of total lysate (L), synaptosomes (S), pre- (Pre) and post-synaptic (PSD) fractions obtained from mouse hippocampus. **(B)** Western blot images of phosphorylated (p) Ser 202 (CP13) and total tau (TG5), and CRTC1 of hippocampal lysates (left) and purified synaptosomes (right) of WT, PS1 cKO, Tau and PS1 cKO;Tau mice at 11-12 months. Quantitative analysis of protein levels from total hippocampal lysates **(C)** and synaptosome fractions **(D)**. Protein levels were normalized to β-tubulin or total tau. Data represent mean ± SEM of multiple mice (n = 3-5) per group. One-way ANOVA followed by Tukey's post hoc test was used as a statistical test. **P* < 0.05, ***P* < 0.01, ****P* < 0.001, ns: not significant.

Total tau was increased in pre- and postsynaptic fractions in tau transgenic groups (Tau Pre: *P* = 0.005; PS1 cKO;Tau Pre *P* = 0.021; Tau PSD: *P* = 0.006; PS1 cKO;Tau PSD: *P* = 0.001) but it was differentially distributed among synaptic compartments, so that was more enriched at postsynaptic compartments (~5-13 fold) than presynaptic fractions (~2-4 fold, **Figure 23A-C**). Also, phosphorylated tau at Ser 202 was significantly increased in postsynaptic fractions of PS1 cKO;Tau mice compared to WT and PS1 cKO (*P* < 0.001), and Tau mice (*P* = 0.01, **Figure 23A,C**). These results suggest that pathological tau mislocalizes to dendritic compartments where may contribute to

synaptic dysfunction in Tau and PS1 cKO;Tau transgenic mice, as previously reported in other experimental models (Hoover et al., 2010). Pre- (*P* = 0.04) and postsynaptic (not significant) CRTC1 was also downregulated in tau transgenic groups (**Figure 23A-C**), but to elucidate whether it is the cause or consequence of pathological tau accumulation further research is needed.

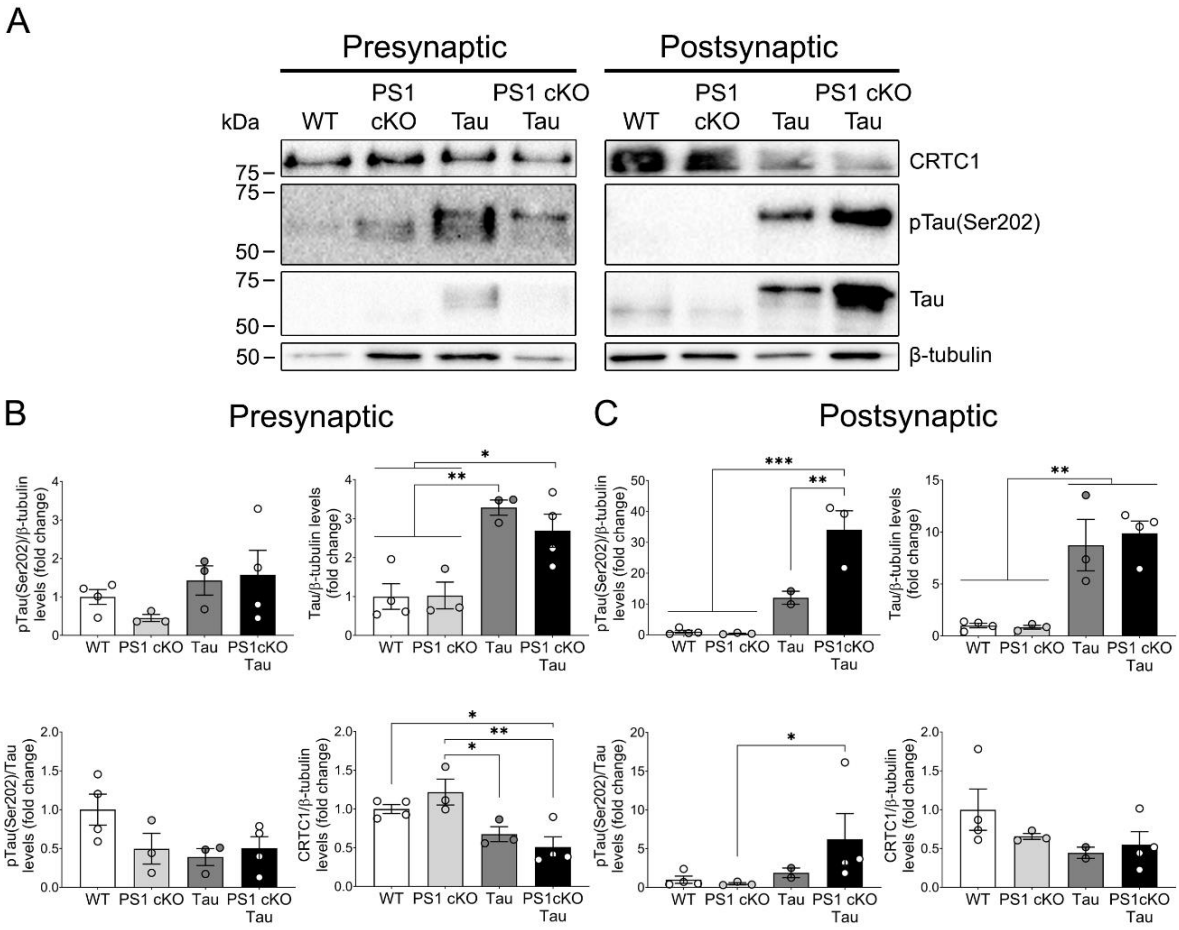

Figure 23. Increased pTau and reduced CRTC1 levels in hippocampal synaptic compartments of PS1 cKO;Tau mice. (A) Western blot images of phosphorylated (p) Ser 202 (CP13) and total tau (TG5), and CRTC1 of purified pre- (left) and post-synaptic fractions (right) of WT, PS1 cKO, Tau and PS1 cKO;Tau mice at 11-12 months. Quantitative analysis of pre- **(B)** and post-synaptic protein levels **(C)** normalized to β-tubulin or total tau. Data represent mean ± SEM of multiple mice (n = 3-5) per group. One-way ANOVA followed by Tukey's post hoc test was used as a statistical test. **P* < 0.05, ***P* < 0.01, ****P* < 0.001.

2. Synaptic tau accumulation is associated with decreased synaptic markers

Mislocalization of phosphorylated tau into dendritic spines is associated with early synaptotoxicity in mouse models of tauopathies (Yoshiyama et al., 2007, Hoover et al., 2010). Here, we analyzed synaptic proteins in hippocampal lysates, synaptosomes and postsynaptic fractions of WT, PS1 cKO, Tau and PS1 cKO;Tau mice at 11-12 months. There were not synaptic protein alterations in PS1 cKO mice compared with WT (**Figure 24**). However, glutamate ionotropic receptors subunits GluA1 and GluN1 were significantly reduced in lysates and synaptosomes of Tau and PS1 cKO;Tau mice (*P* <

0.05, **Figure 24**). The same tendency was observed in the postsynaptic fractions but was not statistically significant. There was also a decrease of PSD95 in total lysates (*P* = 0.03) and synaptosomes (*P* = 0.033) of tau transgenic groups (**Figure 24**). These results suggest that tau mislocalization in Tau and PS1 cKO;Tau mice leads to a decrease of synaptic proteins that could contribute to deficits in synaptic plasticity, learning and memory.

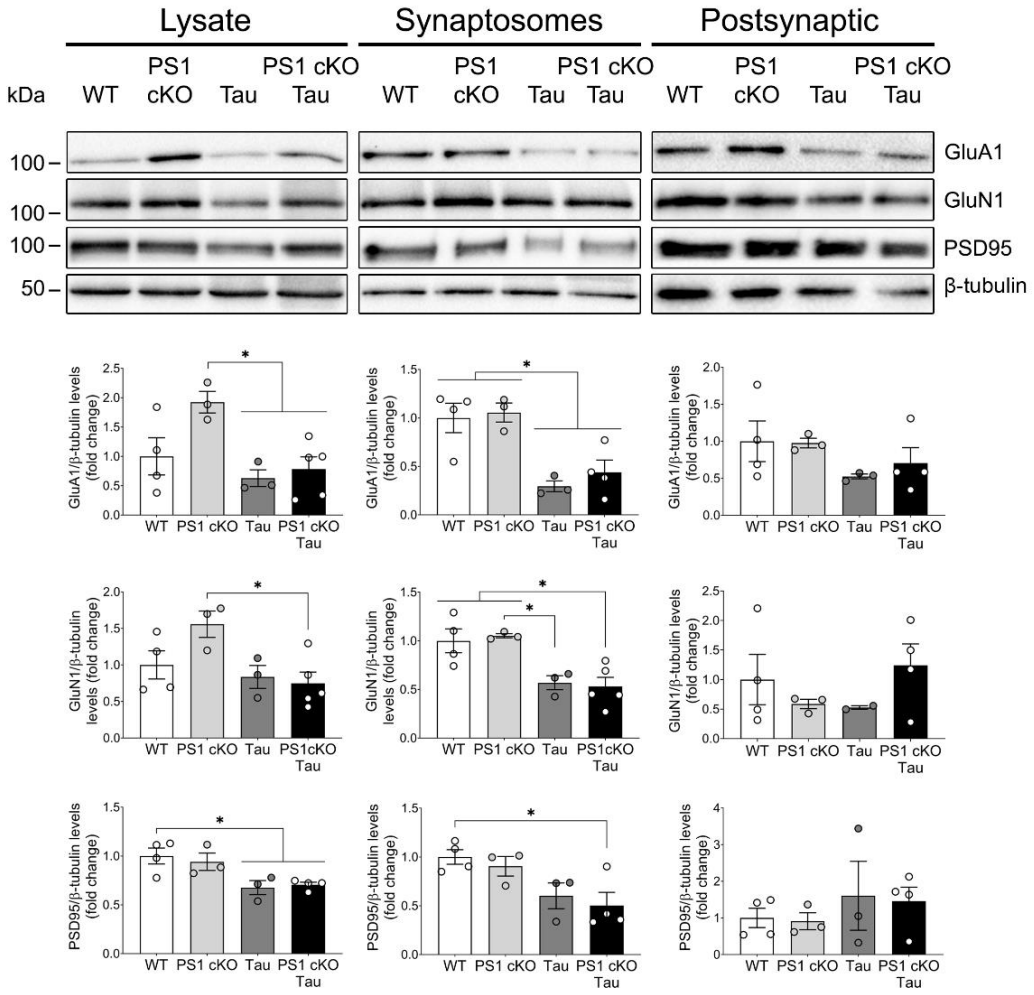

Figure 24. Accumulation of pathological tau and decreased synaptic proteins in hippocampus of Tau and PS1 cKO;Tau mice. Western blot images and quantification analysis of synaptic proteins of hippocampal lysates, and purified synaptosomes and postsynaptic fractions of WT, PS1 cKO, Tau and PS1 cKO;Tau mice at 11-12 months. Protein levels were normalized to β-tubulin. Data represent mean ± SEM of multiple mice (n = 3-5) per group. One-way ANOVA followed by Tukey's post hoc test was used as a statistical test. **P* < 0.05, ***P* < 0.01, ****P* < 0.001.

3. Increased levels of autophagosomes at hippocampal synapses of PS1 cKO;Tau mice

To elucidate whether tau accumulation could be associated with autophagic flux failure, levels of microtubule-associated protein light chain 3 (LC3) and sequestome 1 (SQSTM1), also known as p62, were analyzed. Number of autophagosomes was assessed by measuring LC3-I conversion to LC3-II.

Additionally, LC3-II and p62 turnover were quantified to evaluate autolysosomes degradative efficiency (Mizushima et al., 2010). Compared with non-transgenic (control) and PS1 cKO mice, PS1 cKO;Tau mice displayed increased p62 levels in hippocampal lysates (P = 0.006), synaptosomes (P = 0.05) and postsynaptic fractions (P = 0.019, **Figure 25A-C**). Intriguingly, there was a significant decrease in LC3-I protein levels, without changes in LC3-II, in synaptosome fraction of Tau (P = 0.045) and PS1 cKO;Tau (P = 0.025) transgenic mice (**Figure 25B**). LC3-II/LC3-I ratio was increased in total lysates (P = 0.229) and synaptosomes (P = 0.017) of PS1 cKO;Tau mice (**Figure 25A,B**). The increase in p62 levels and LC3-II/LC3-I ratio in hippocampal synaptosomes of PS1 cKO;Tau mice suggests either accumulation of synaptic autophagosomes caused by synaptic tau pathology and/or inappropriate tau degradation or synaptic accumulation of pathological tau due to disrupted synapse autophagy.

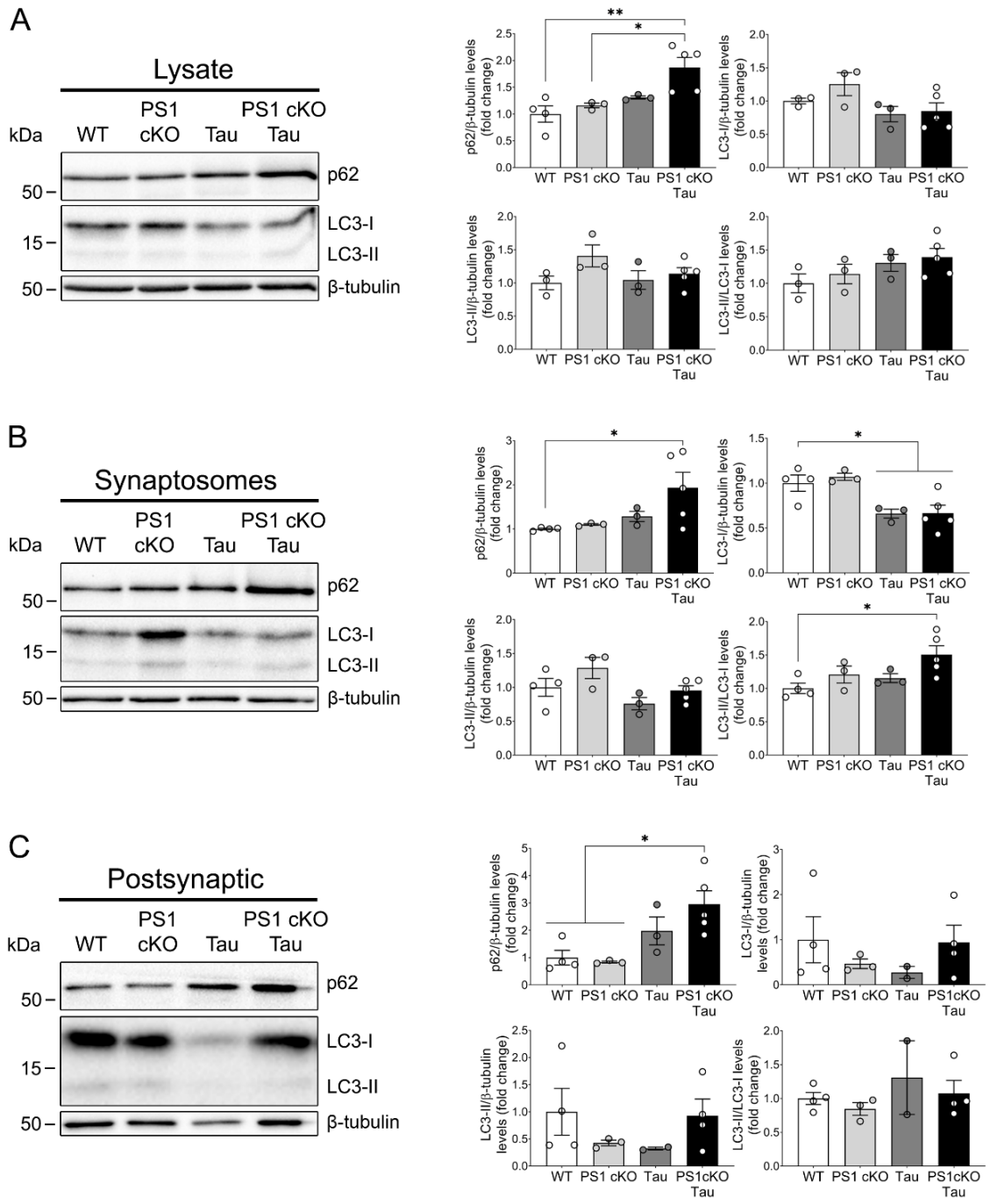

Figure 25. Altered autophagy markers in hippocampal synapses of PS1 cKO;Tau mice. Western blot images and quantification analysis of p62 and LC3 protein levels of total lysate **(A)**, synaptosomes **(B)** and postsynaptic **(C)** fractions obtained from WT, PS1 cKO, Tau and PS1 cKO;Tau mouse hippocampus. Protein levels were normalized to β-tubulin. Data are mean ± SEM of multiple mice (n = 3-5) per group. One-way ANOVA followed by Tukey's post hoc test was used as a statistical test. **P* < 0.05, ***P* < 0.01.

4. Autophagy marker LC3 is increased by CRTC1 silencing in the mouse hippocampus

Recent reports have shown that genes necessary for autophagy induction (*Ulk1*), phagophore expansion (*Atg5*) and autophagosome assembly (*Atg7* and *LC3*) contain CREB binding sites and that

CRTC1-CREB complex drives their activity-dependent upregulation (Seok et al., 2014, Pan et al., 2021). To address the effect of CRTC1 inactivation in the expression of autophagy markers, hippocampal lysates of AAV-ShScr- amd AAV-ShCRTC1-injected mice were biochemically analyzed. Contrary to what was previously described in the literature (Pan et al., 2021), we found that CRTC1 silencing leads to increased LC3-I and LC3-II levels along with an increase in LC3-II/LC3-I ratio, without changes in p62 levels (**Figure 26**). This result suggests that long-term CRTC1 downregulation *in vivo* contributes to the induction of autophagy flux.

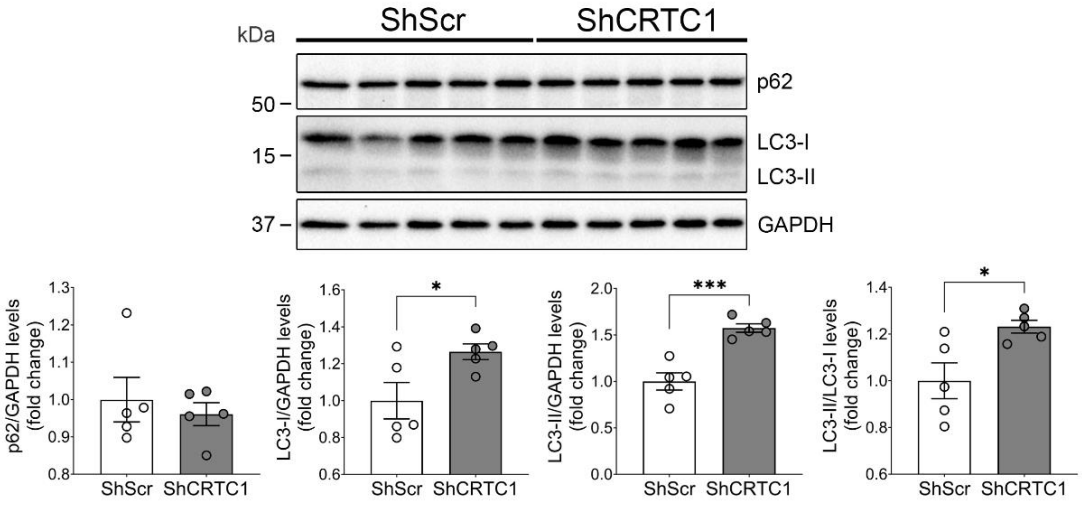

Figure 26. CRTC1 silencing upregulates LC3-I and LC3-II protein levels in the mouse hippocampus. Western blot images and quantitative analysis of autophagy markers p62 and LC3. Protein levels were normalized to GAPDH. Data represent mean ± SEM of multiple mice (n = 5) per group. Two-tailed unpaired Student t test was used as statistical tests. **P* < 0.05, ****P* < 0.001.

5. FAD-linked *PSEN1* mutations potentiate autophagy initiation in human primary fibroblasts

To examine the role of PS1 in autophagy, we monitored autophagy dynamics in primary human skin fibroblasts from healthy controls and patients with FAD-linked *PSEN1* mutations. We used two independent primary fibroblasts lines from controls (CTRL 1 and 2) and two from patients harboring missense mutations G206D (*PSEN1* exon 7) or L286P (*PSEN1* exon 8) causing early-onset autosomal dominant AD (Sánchez-Valle et al., 2007, Wu et al., 2011, Díaz-Guerra et al., 2019).

Autophagic flux was evaluated by assessing LC3 and p62 protein levels in the presence or absence of chloroquine (CQ), a chemical that blocks autophagosome-lysosome fusion, making it a good pharmacological tool to study the autophagic pathway (Mauthe et al., 2018). Treatment of fibroblasts with CQ (10 µM) for 24 h increased autophagic vacuoles visualized under a bright-field microscope (**Figure 27A**). Biochemical analysis showed a significant increase in p62 (*P* < 0.001), LC3-

II (P < 0.001) and LC3-II/LC3-I ratio (P < 0.001) in CQ-treated fibroblast compared with vehicle-treated controls (**Figure 27B,C**). These results indicated that CQ treatment caused an efficient impairment of autophagosomes clearance in human primary fibroblasts.

Levels of p62 were not affected in fibroblasts with G206D and L286P PSEN1 mutations indicating no change of autophagosome-lysosome fusion in basal conditions (P > 0.05, **Figure 27B,C**). Interestingly, both FAD-linked *PSEN1* mutant fibroblasts in basal conditions showed higher LC3-I levels (PS1 G206D: P = 0.002; PS1 L286P: P = 0.029) and a slight, although non-significant, increase of LC3-II compared with control fibroblasts (**Figure 27B,C**). These changes between controls and FAD-linked *PSEN1* fibroblasts disappeared in CQ-treated conditions (**Figure 27B,C**). The increase of LC3 levels and unchanged p62 suggest potentiation of autophagosomes formation and/or altered autophagic flux by FAD-linked *PSEN1* mutations.

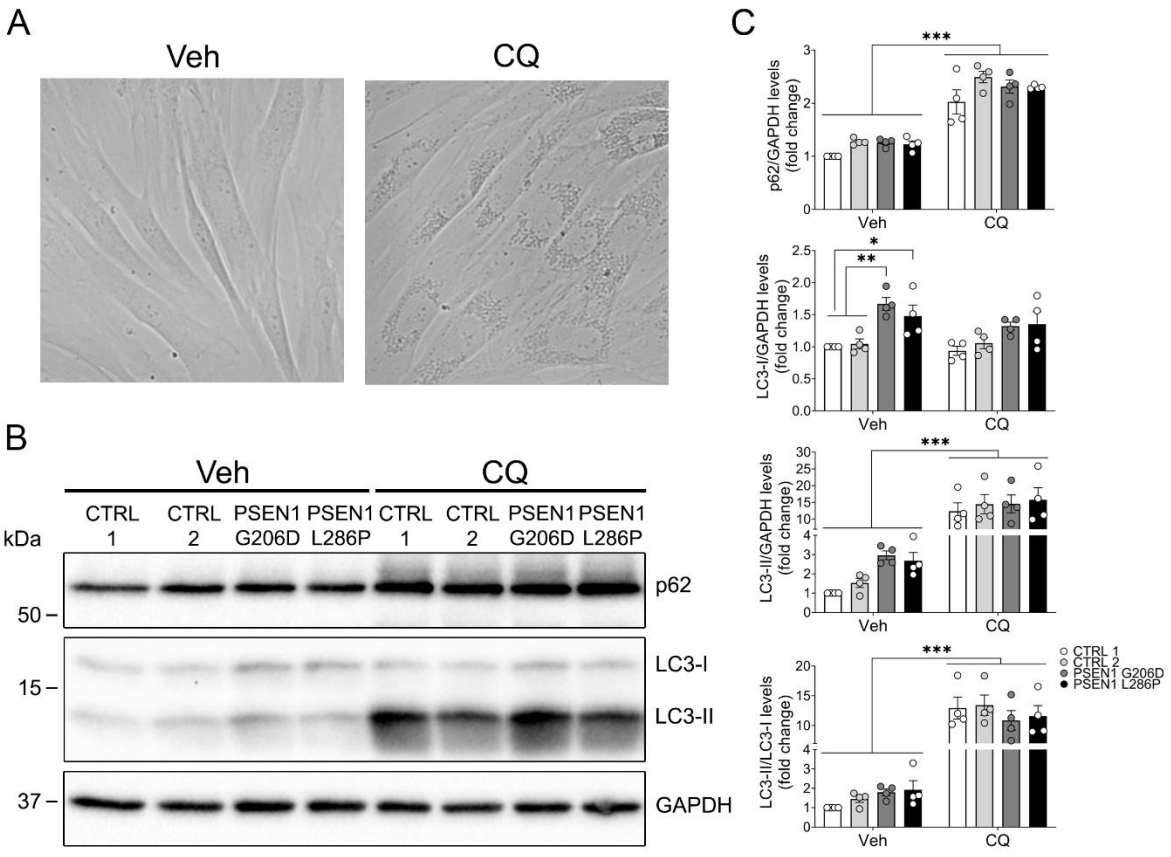

Figure 27. FAD-linked *PSEN1* G206D and L286P mutations potentiates autophagy flux in primary human fibroblasts. (A) Bright-field microscopy images of fibroblasts treated with vehicle or chloroquine (CQ, 10 µM) for 24 h. Western blot **(B)** and quantification analysis **(C)** of p62, LC3-I and LC3-II protein levels of fibroblasts treated with vehicle or CQ (10 µM) for 24 h. Protein levels were normalized to GAPDH or LC3-I, as indicated. Data are mean ± SEM of independent cultures (n = 4). Two-way ANOVA followed by Tukey's post hoc test was used as a statistical test. *P < 0.05, **P < 0.01, ***P < 0.001.

To confirm these results, we monitored autophagy in primary fibroblasts by transiently expressing a mCherry-EGFP-LC3 reporter. Analysis of fluorescence staining of this probe allows to discriminate autophagosomes (mCherry- and EGFP-positive puncta) from more acidic autolysosomes (mCherry-positive and EGFP-negative puncta) (**Figure 28A**). The differential staining allows to distinguish between the inhibition of the biogenesis of autophagosomes and the blockade of autophagosome-lysosome fusion. A significant accumulation of autophagosomes (yellow puncta) was observed in CQ-treated fibroblasts (P = 0.008), although control 2 fibroblasts were unresponsiveness to CQ as the number of autophagosomes remained constant compared with basal condition (**Figure 28B,C**). These agreed with what was previously seen in the biochemical experiments (**Figure 27**). Autophagosome number was unchanged between control 1 and FAD-linked *PSEN1* fibroblasts independently of the treatment, indicating that initial steps of autophagy were not affected by *PSEN1* mutations (**Figure 28B,C**). In basal conditions, autolysosomes (red puncta) were significantly increased in fibroblasts with G206D (P = 0.054) and L286P (P = 0.001) PSEN1 mutations compared to control 1, an effect lost after CQ treatment (**Figure 28B,C**). Unexpectedly, red puncta number was unchanged with CQ treatment (P = 0.893). This indicates that other intermediate acidic degradative organelles, such as amphisomes, are being labeled. The increase in LC3-I and LC3-II levels (**Figure 28B,C**) and mCherry single-positive puncta (**Figure 28B,C**) in fibroblasts with G206D and L286P PSEN1 mutations suggest an enhancement of autophagy flux and decreased lysosomal activity.

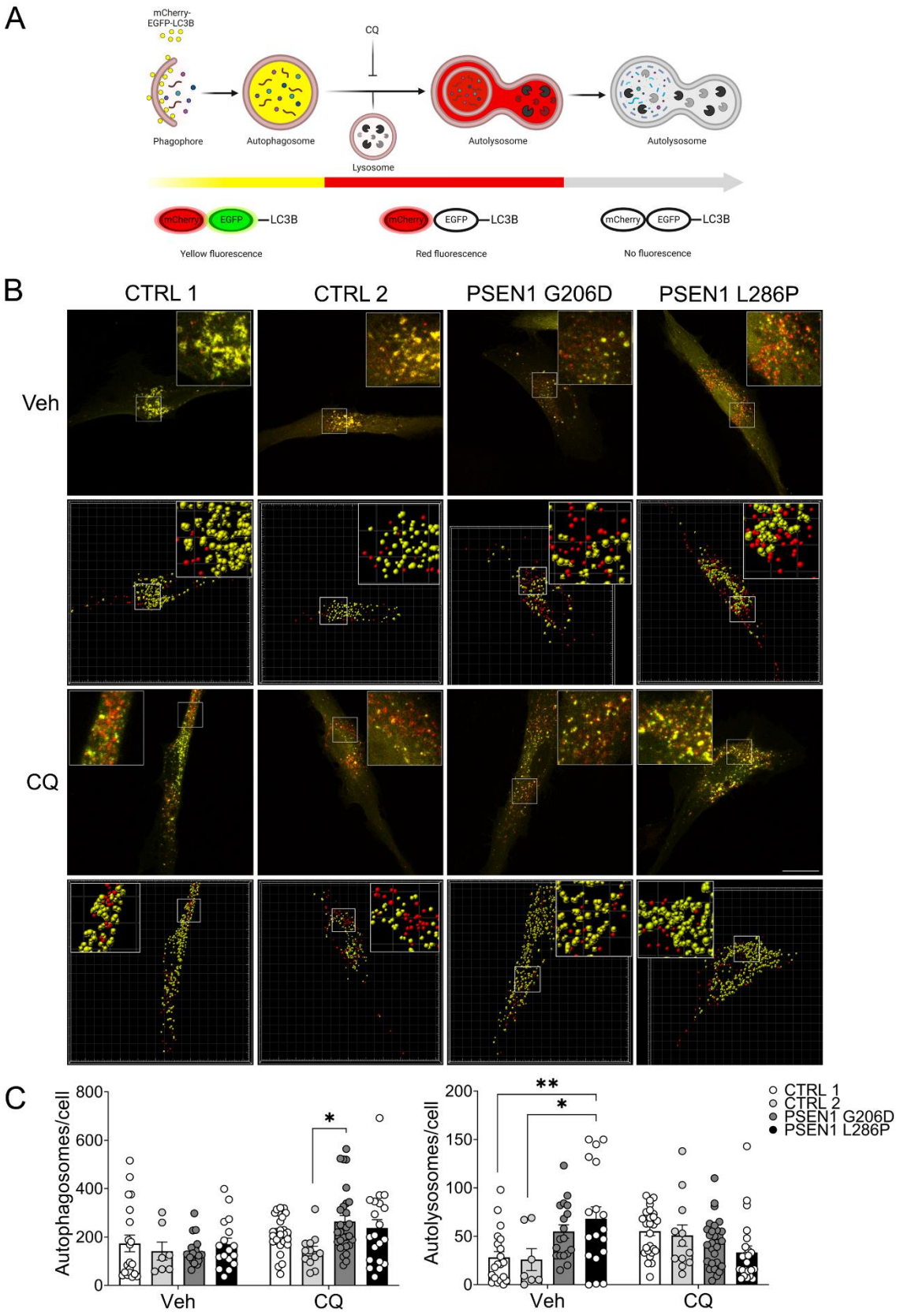

Figure 28. Autolysosomes clearance is impaired in primary human fibroblast harboring PSEN1 G206D and L286P mutations. (A) Scheme of the autophagy tandem sensor mCherry-EGFP-LC3B construct. Autophagosomes are stained in yellow as mCherry/EGFP co-staining. When autophagosomes fuse with lysosomes, EGFP expression is quenched by the acidic pH and, consequently, autolysosomes are stained only

in red (mCherry+). Fluorescence is completely lost when autolysosomes are degraded. Image created with BioRender. **(B)** Representative images of primary human fibroblasts transfected with mCherry-EGFP-LC3B vector (0.5 µg) and treated with CQ (10 µM) or vehicle for 24 h (top), and images used for quantification obtained with Imaris software (second and fourth rows). Scale bar: 20 µm. **(C)** Quantification analysis of autophagosomes (yellow puncta) and autolysosomes (red puncta) per cell. Data are mean ± SEM of multiple cells per condition (n = 7-29) from 6 independent cultures. Two-way ANOVA followed by Tukey's post hoc test was used as a statistical test. **P* < 0.05, ***P* < 0.01.

6. PSEN1 G206D increases LC3-I and tau aggregation in iPSC-derived neurons

Primary human fibroblasts do not express endogenous tau protein, so we analyzed autophagy flux and tau phosphorylation and aggregation in iPSC-derived neurons harboring PSEN1 WT or G206D mutation (Díaz-Guerra et al., 2019). In basal (vehicle) conditions, no significant changes in autophagy markers were observed between control and PSEN1 G206D iPSC-derived neurons (**Figure 29**). Treatment with CQ (25 µM) for 24 h induced a significant increase in p62 (*P* = 0.001), LC3-II (*P* < 0.001) and LC3-II/LC3-I ratio (*P* < 0.001, **Figure 29**), indicating efficient blockade of autophagosomes clearance. However, whereas LC3-I was decreased in control cells (*P* = 0.05), LC3-I levels remain unchanged and significantly higher in CQ-treated PSEN1 G206D iPSC-derived neurons (*P* = 0.015), suggesting an induction of the autophagy flux by this FAD-linked mutation when autophagosomes degradation is blocked.

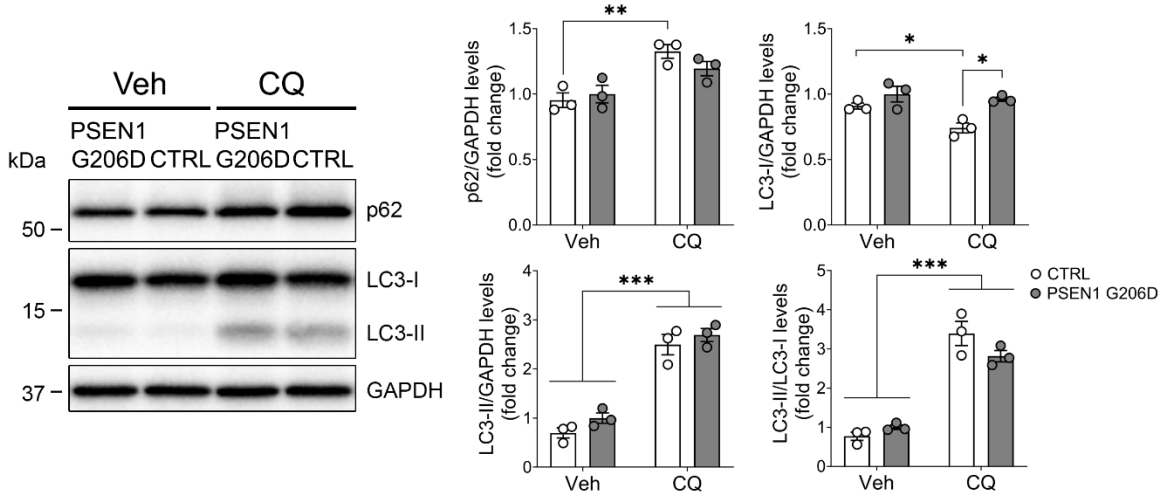

Figure 29. LC3-I levels are increased in iPSC-derived neurons with the FAD-linked *PSEN1* G206D mutation. Western blot images and quantification analysis of p62, LC3-I and LC3-II protein levels of iPSC-derived neurons (50 DIV) treated with vehicle or CQ (25 µM) for 24 h. Protein levels were normalized to GAPDH or LC3-I, as indicated. Data represent mean ± SEM of three biological replicates per condition. Two-way ANOVA followed by Tukey's post hoc test was used as a statistical test. **P* < 0.05, ***P* < 0.01, ****P* < 0.001.

To evaluate tau phosphorylation and aggregation in iPSC-derived neurons, band patterns of total and phosphorylated (Ser396/404) tau were analyzed in vehicle and CQ-treated cells. It should be noticed that bands of similar molecular weights were found with both antibodies, but the band

profiles were different (**Figure 30**). We found bands of ~60-64 kDa corresponding to monomeric tau; 75-250 kDa bands of high molecular weight tau (HMW-Tau) likely corresponding to tau aggregates/oligomers; and low molecular weight tau (LMW-Tau) bands of 20-45 kDa corresponding to truncated tau protein (Santpere et al., 2006, Lasagna-Reeves et al., 2010, Patterson et al., 2011). Surprisingly, PS1 G206D (P = 0.05) and CQ treatment (P = 0.004) decreased similarly monomeric (~60-64 kDa) tau levels compared with vehicle-treated control cells (**Figure 30**). By contrast, PS1 G206D iPSC-derived neurons show an increase of HMW-Tau relative to monomeric tau in both basal and CQ conditions (P = 0.002, **Figure 30**). Interestingly, phosphorylated Ser 396/404 monomeric tau was similarly reduced in CQ-treated PS1 WT and G206D iPSC-derived neurons, but phosphorylated HMW-Tau (tau aggregates) were increased in these conditions (**Figure 30**). By contrast, levels of ~22 kDa low molecular weight tau (LWM-Tau^{22}) were unchanged by the G206D mutation or CQ treatment. ~44 kDa truncated tau (LWM-Tau^{44}) was decreased in PS1 G206D and CQ-treated iPSC-derived neurons compared with controls (**Figure 30**). These results suggest that the FAD-linked PS1 G206D mutation potentiates phosphorylated tau phosphorylation aggregation likely contributing to increase oligomeric tau species.

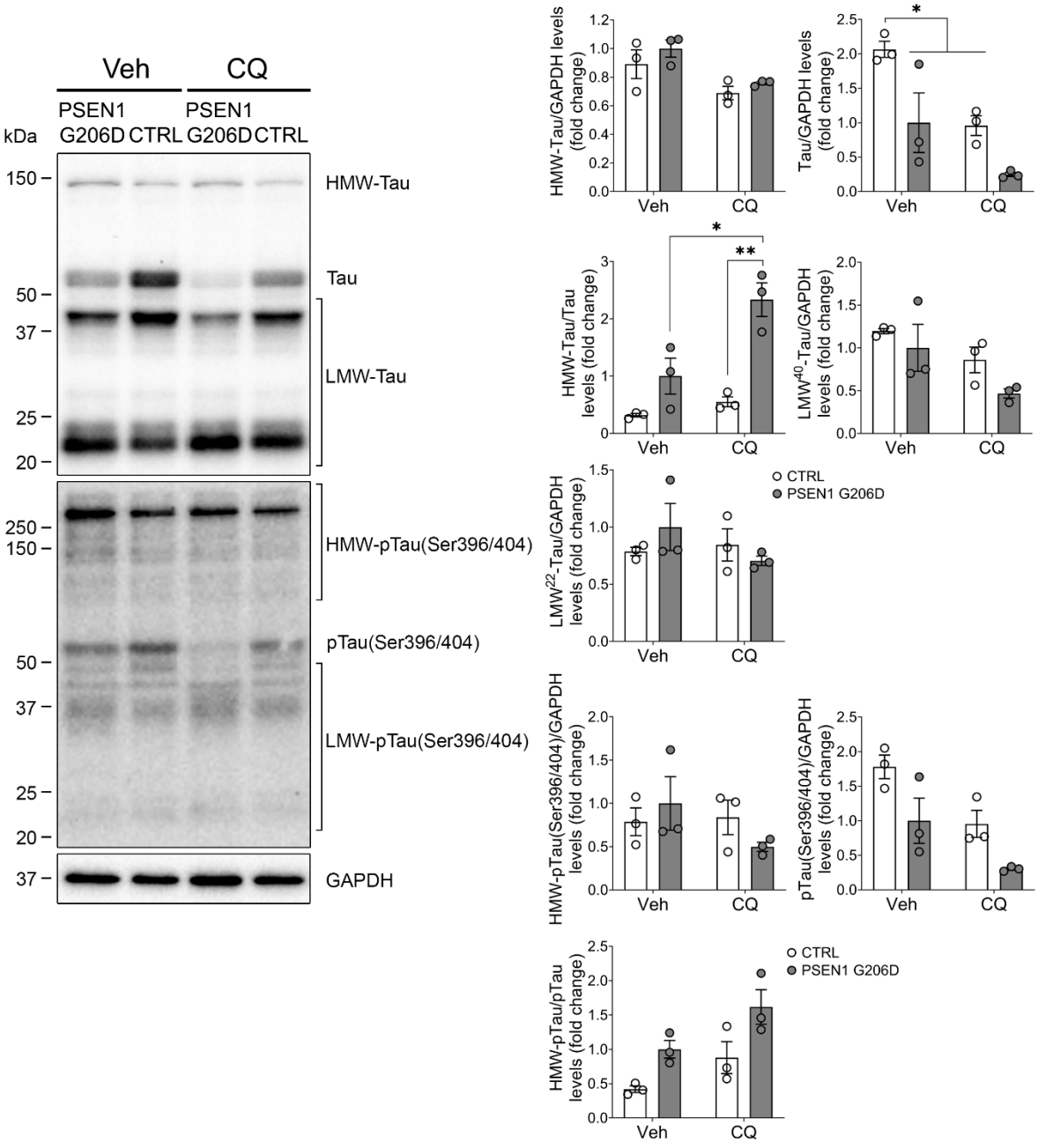

Figure 30. Intracellular tau aggregates accumulate in iPSC-derived neurons carrying the FAD-linked PSEN1 G206D mutation. Western blot images and quantification analysis of phosphorylated (p) Ser 396/404 (PHF-1) and total tau (D1M9X) of iPSC-derived neurons (50 DIV) treated with vehicle or CQ (25 µM) for 24 h. Protein levels were normalized to GAPDH or ~60-64 kDa tau band. Data represent mean ± SEM of three biological replicates per condition. Two-way ANOVA followed by Tukey's post hoc test was used as a statistical test. *P < 0.05, **P < 0.01. HMW: high molecular weight; LMW: low molecular weight.

7. Altered autophagy markers in familial Alzheimer's disease and other tauopathies

To further investigate the link between autophagy dysfunction and tau accumulation in tauopathies, hippocampus of 28 individuals clinically diagnosed with PS-linked FAD (n = 7; mean age: 53.1 ± 5.7), CBD (n = 8; mean age: 70.5 ± 6.6), PiD (n = 6; mean age: 68.3 ± 13.7) and age and

sex-matched controls (mean age = 51.4 ± 7.6: ; 3 females/4 males; n = 7) were analyzed (**Table 9**). In contrast with other studies, we used young control samples of similar age that tauopathies samples. Biochemical analysis showed elevated total and phosphorylated (Ser 202 and Ser 396/404) tau levels characteristic of these pathologies (**Figure 31A**). Interestingly, total and phosphorylated tau were significantly accumulated in patients with FAD compared with controls (pTau(Ser202): $P < 0.001$; pTau(Ser396/404): $P < 0.001$; Tau: $P < 0.0001$; pTau(Ser396/404)/Tau: $P = 0.014$, **Figure 31A**). The biochemical profile of tau bands was different among groups. In agreement with previous studies in AD (Greenberg and Davies, 1990, Lee et al., 1991), three bands of approximately 72, 68 and 60-64 kDa were detected with total tau antibody in FAD samples (**Figure 31A**). In CBD, 68 and 60-64 kDa bands were observed, while in PiD only the lower bands were detected [(Ksiezak-Reding et al., 1994, Buée Scherrer et al., 1996, Delacourte et al., 1996), **Figure 31A**].

Table 9. Human hippocampus samples used in biochemical experiments. Samples are classified according to the clinical and neuropathological diagnosis. FAD: Familial Alzheimer's disease; CBD: corticobasal degeneration; PiD: Pick's disease; F: female; M: male; PMD: postmortem delay.

Sample ID	Gender	Age	Clinical Diagnosis	PMD (h:min)	Mutation
A08-42	F	64	Control	5:00	
A06-189	F	46	Control	9:35	
A08-54	F	55	Control	8:30	
A07-128	M	43	Control	4:35	
A07-5	M	56	Control	5:00	
A10-17	M	52	Control	3:00	
A09-145	M	44	Control	6:40	
929	F	56	FAD	6:00	*PSEN1* P264L
1241	F	48	FAD	16:41	*PSEN1* M139T
1846	F	61	FAD	7:00	*PSEN2* R62H
2082	F	53	FAD	7:15	*PSEN1* L286P
898	M	57	FAD	15:25	*PSEN1* M139T
935	M	44	FAD	5:30	*PSEN1* E120G
1134	M	53	FAD	5:25	*PSEN1* M139T
1058	F	69	CBD	12:10	
1291	F	79	CBD	10:30	
1359	F	67	CBD	6:45	
1798	F	78	CBD	5:30	
1204	M	74	CBD	14:30	
1356	M	72	CBD	7:00	
1518	M	66	CBD		
1751	M	59	CBD	7:00	
1248	F	41	PiD	11:10	
1493	F	75	PiD	13:00	
1681	F	69	PiD	3:00	
1352	M	74	PiD	13:00	
1719	M	73	PiD	9:15	
1789	M	78	PiD	11:00	

Notably, p62 was significantly increased in FAD (P = 0.047), CBD (P = 0.054) and PiD (P < 0.001) compared with control group (**Figure 31B**). An increase in p62 levels could suggest that autophagosome clearance is impaired in patients with tauopathies. No changes in total LC3-I and LC3-II protein levels or LC3-II/LC3-I ratio were detected in tauopathies samples (**Figure 31B**). However, levels of the LC3 precursor (proLC3) relative to LC3-I were slightly increased in patients with FAD (P = 0.068, **Figure 31B**), indicating a possible impairment in the initial step of autophagy flux. These results suggest that different steps of autophagy could be compromised in patients with FAD-linked PS1 mutations, which in turn could contribute to the accumulation of hyperphosphorylated/total tau.

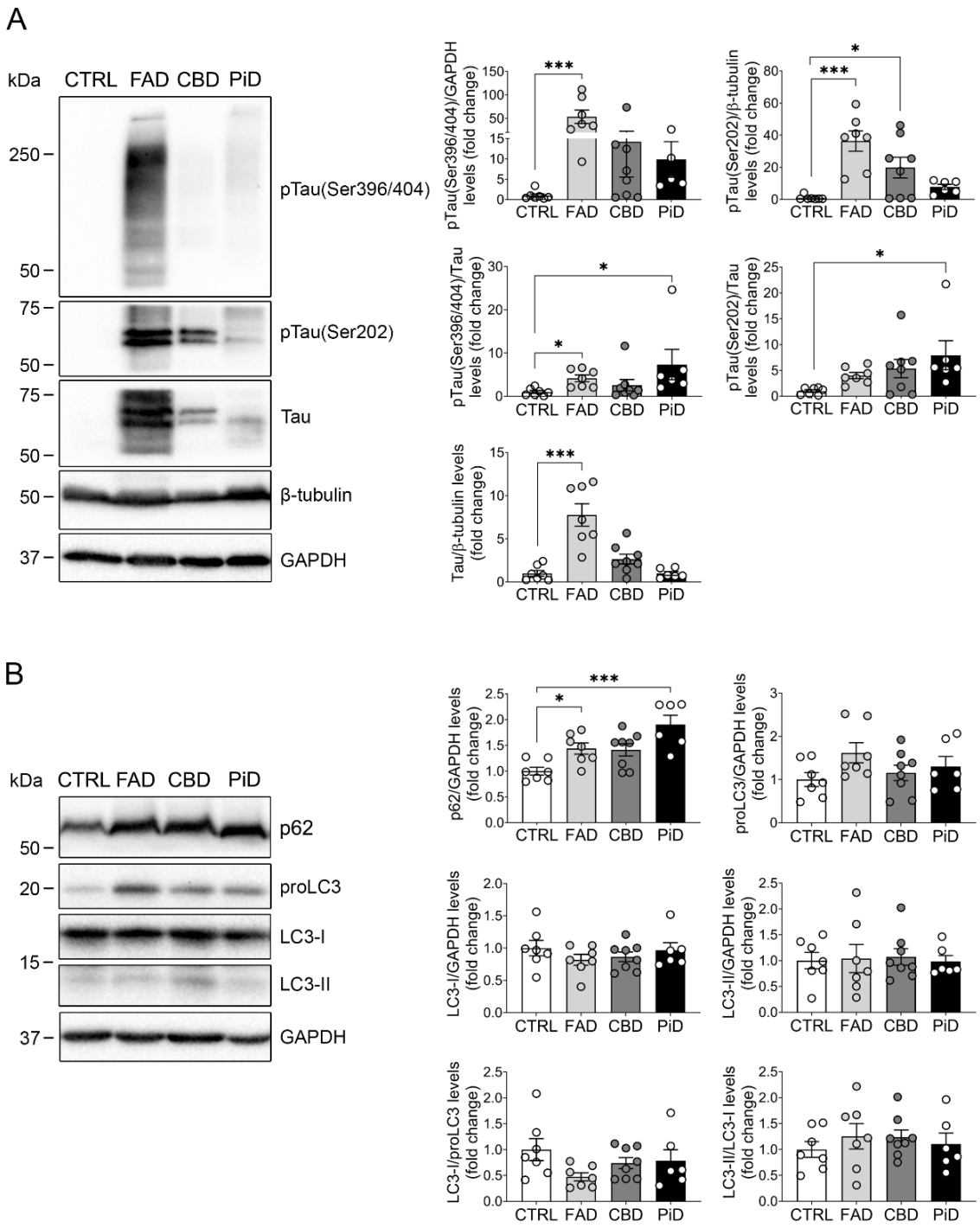

Figure 31. Increases p62 levels are associated with accumulation of total and phosphorylated tau in hippocampus of tauopathies. Western blot images and quantification analysis of phosphorylated (p) Ser 396/404 (PHF-1) and Ser 202 (CP13), and total tau (D1M9X) **(A)**, and autophagic markers p62 and LC3 **(B)** in hippocampal lysates from controls (CTRL) and patients with FAD, CBD and PiD. Protein levels were normalized to β-tubulin, GAPDH or total tau. Data represent mean ± SEM of multiple individuals (n = 6-8) per group. One-way ANOVA followed by Dunnett's post hoc test or Kruskal-Wallis followed by Dunn's post hoc test was used as statistical test. **P* < 0.05, ****P* < 0.001. CTRL: control; FAD: familial Alzheimer's disease; CBD: corticobasal degeneration; PiD: Pick's disease.

8. Tau accumulation and reduced synaptic proteins in patients with tauopathies

Accumulation of pathological tau in patients with tauopathies correlates with impaired synaptic plasticity and cognitive decline (Koch et al., 2016, de Wilde et al., 2016). To evaluate synaptic dysfunction in hippocampal samples from patients with tauopathies, synaptic markers, including the synaptonuclear factor CRTC1, were analyzed. A decrease in GluA1 levels was found in patients with FAD (P = 0.004), CBD (P = 0.011) and PiD (P = 0.007) compared with control group, whereas there was not significant changes in GluN1, PSD95, CRTC1, Homer 1 or the presynaptic proteins syntaxin and synaptophysin (**Figure 32**). These results indicate that patients with FAD, CBD and PiD show specific reduction of GluA1 levels likely leading to deficits in AMPAR-mediated neurotransmission.

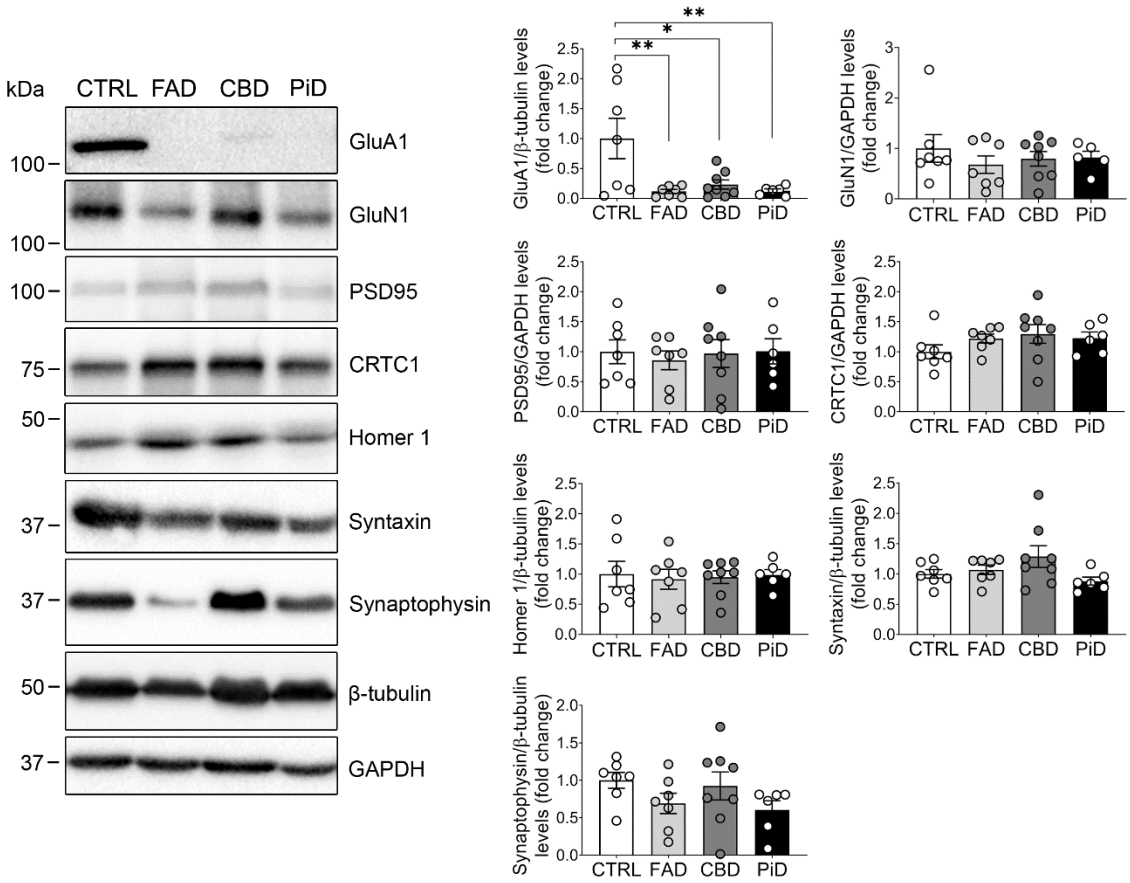

Figure 32. Reduced GluA1 levels in hippocampus of patients with tauopathies. Western blot images and quantification analysis of synaptic proteins in hippocampal lysates from controls (CTRL) and patients with FAD, CBD and PiD. Protein levels were normalized to β-tubulin or GAPDH. Data represent mean ± SEM of multiple individuals (n = 6-8) per group. One-way ANOVA followed by Dunnett's post hoc test was used as statistical test. *P < 0.05, **P < 0.01. CTRL: control; FAD: familial Alzheimer's disease; CBD: corticobasal degeneration; PiD: Pick's disease.

Discussion

Brain plasticity rely in the correct connectivity between neurons conforming a neural network, and on the accurate communication among the different neuronal compartments. Synapse-to-nucleus signaling mediated by synaptonuclear factors is a novel neural mechanism that connects synaptic activity to gene expression programs at the nucleus, contributing to neuronal development, plasticity, and survival. The CREB coactivator CRTC1 is a synaptonuclear factor activated by synaptic and neuronal activities essential for long-term synaptic plasticity and memory, and its deregulation is associated to age-related neurodegenerative diseases such as AD (España et al., 2010, Parra-Damas et al., 2014, Parra-Damas et al., 2017a, Wilson et al., 2017, Yan et al., 2021). Although, progress in the understanding CRTC1 regulation of neuroplasticity genes is well documented (Nonaka et al., 2014, Parra-Damas et al., 2014, Parra-Damas et al., 2017b, Uchida et al., 2017), the CRTC1-dependent molecular mechanisms contributing to synaptic plasticity are still poorly understood. In this doctoral thesis, I provide evidence that CRTC1 regulates hippocampal-dependent memory by modulating glutamatergic neurotransmission and expression and synaptic localization of NMDA receptors. In addition, the obtained results suggest that glutamate receptor deregulation may contribute to synapse pathology in tauopathies.

CRTC1 contributes to hippocampal-dependent memory

It is well stablished that CRTC1 mediates hippocampal-dependent long-term memory in mammals and its deregulation leads to cognitive dysfunction in mouse models of neurodegeneration. Indeed, CRTC1 overexpression rescues spatial and contextual long-term memory deficits in mouse models of neurodegeneration (Parra-Damas et al., 2014, Parra-Damas et al., 2017b, Yan et al., 2021), although the underlying mechanisms are unclear. Our results show that , bilateral injection of AAV-CRTC1 or AAV-ShCRTC1 in the dorsal hippocampus enhanced or worsened contextual long-term memory, respectively (**Figure 9C**), a finding that agrees with previous reports showing that CRTC1 overexpression or a constitutively active CRTC1 mutant enhances cued and context fear memories (Sekeres et al., 2012, Nonaka et al., 2014). It is interesting that although a significant effect on behavior was observed one month after stereotaxic injection, total CRTC1 protein levels were not drastically changed by AAV-mediated CRTC1 overexpression (1.6 fold increase) or inactivation (0.6 fold decrease, **Figure 9C-E**). This could be explained because despite CMV and H1 promoter provide strong and ubiquitous transgene expression, they could be prone to silencing over time in some tissues (Gray et al., 2011b, Sekeres et al., 2012). Nevertheless, this result is interesting as it suggests that CRTC1 effect on long-term memory persists beyond high transgene expression. Although the cellular mechanisms underlying CRTC1-dependent memory are not completely clear, it has been suggested that a rise in intracellular Ca^{2+} by AMPARs and NMDARs activation triggers CRTC1 nuclear

translocation and regulation of CREB-dependent neuroplasticity genes (e.g. *Arc, Bdnf, Fgf1, Fos, Nr4a1, Nr4a2*) (Finsterwald et al., 2010, Ch'ng et al., 2015, Parra-Damas et al., 2017b, Uchida et al., 2017) The consequence of CRTC1-dependent neuroplasticity gene regulation is potentiation of synapse morphology and plasticity leading to a change in the functionality of memory-related neural circuits. Indeed, current results from our laboratory indicate that CRTC1 potentiates LTP and contributes to structural synaptic plasticity by modulating dendritic spine maintenance and morphology (Parra-Damas, del Ser-Badia et al., in preparation).

These results are important because CRTC1 activity is impaired in the hippocampus of AD patients (Parra-Damas et al., 2014, Mendioroz et al., 2016), who show impaired associative memory performance linked to reduced hippocampal activity (Hanaki et al., 2011, Oedekoven et al., 2015). It is then possible that CRTC1 dysregulation may be involved in brain plasticity changes and neural circuit dysfunction in AD or other neurodegenerative diseases. Indeed, overexpression of CRTC1 in mouse models of neurodegeneration improved long-term memory (Parra-Damas et al., 2014, Parra-Damas et al., 2017b, Yan et al., 2021). In addition, recent reports demonstrate that CRTC1 deregulation is associated with memory deficits and neural susceptibility in HD and PD (Jeong et al., 2011, Chaturvedi et al., 2012, Won et al., 2016).

CRTC1 regulates NMDAR-mediated excitatory neurotransmission

Synapses are necessary for transmission, processing, encoding and retrieval of neural information in the brain. In the hippocampus, glutamatergic synapses constitute a high proportion of excitatory synaptic inputs suggesting their important role in learning and memory. Electrophysiological experiments have shown that CRTC1 contributes to L-LTP maintenance without affecting E-LTP, synaptic transmission and presynaptic function (Zhou et al., 2006, Kovacs et al., 2007, Uchida et al., 2017). These results agree with our and previous behavioral experiments that demonstrated the importance of CRTC1 for the formation, maintenance and extinction of memory [(Parra-Damas et al., 2014, Parra-Damas et al., 2017a, Uchida et al., 2017), **Figure 9**]. Nonetheless, the CRTC1-dependent molecular mechanisms regulating synaptic plasticity and, specifically, glutamatergic neurotransmission are still unclear.

The prototypical induction of LTP requires NMDAR activation and recruitment of AMPARs to the postsynaptic membrane. Newly synthesized GluA1-containing AMPARs are delivered to mushroom-like dendritic spines in CA1 24 h after fear conditioning (Matsuo et al., 2008), and inactivation of synaptic GluA1 can erase acquired fear memories (Takemoto et al., 2017), indicating the contribution of AMPARs to the stabilization of long-term memory. Notably, we found that the

enhancement of long-term associative memory observed in AAV-CRTC1-injected mice was not associated with changes in GluA1 or GluA2 levels in the mouse hippocampus (**Figure 10**), meaning that neither CRTC1 nor CFC paradigm regulated the expression of GluA subunits. This does not rule out the possibility that AMPARs could be reorganized within neuronal compartments to potentiate synaptic transmission. Indeed, we found that CRTC1 inactivation significantly decreased phosphorylated GluA1 at Ser 831, a process critical for AMPAR localization, conductance, and open probability (Whitlock et al., 2006, Kristensen et al., 2011, Diering et al., 2016, Summers et al., 2019). Therefore, CRTC1-mediated GluA1 phosphorylation at Ser 831 could be contributing to AMPARs localization at postsynaptic sites and, consequently, improving long-term associative memory.

It was classically believed that NMDARs subunit content was only plastic during development and that their function at the adult brain was restricted to the regulation of AMPAR-mediated transmission. Increasing evidence indicates that long-lasting changes in NMDAR-mediated transmission can occur independently of AMPAR plasticity (Grosshans et al., 2002, Harney et al., 2008, Kwon and Castillo, 2008). NMDARs are heteromeric receptors constituted by two compulsory copies of GluN1 combined with two copies of GluN2 and/or GluN3 (Sheng et al., 1994), so changes in GluN1 expression will impact on total NMDARs levels independently of its subunit composition. Interestingly, we found that CRTC1 silencing leads to a reduction of GluN1 levels in the mouse hippocampus (**Figure 11**), which could contribute to long-term memory deficits observed in the behavioral test. *In silico* studies identified CREB as a possible transcription factor involved in the regulation of *Grin1* expression in humans but not in mice (Mejía-Guerra and Lareo, 2005). This raises the possibility that CRTC1 can directly bind to regulatory elements of *Grin1* promoter region regulating its expression. Additional CREB and CRTC1 ChIP analyses will be necessary to examine the possibility that CRTC1-dependent CREB signaling may be involved in *Grin1* regulation. Additionally, we detected an activity- and CRTC1-dependent shift in the content of GluN2 subunits from GluN2A- to GluN2B-containing NMDARs (**Figure 12**). During development, NMDARs switch from GluN2B- to GluN2A-containing NMDARs (Bellone and Nicoll, 2007, Gray et al., 2011a). GluN2B-NMDARs show longer currents, are more permeable to Ca^{2+} and have higher affinity for CaMKII, suggesting that they are more likely to favor LTP in comparison with GluN2A-NMDARs (Yashiro and Philpot, 2008). Indeed, pharmacological or genetic blockade of GluN2B attenuates LTP (Barria and Malinow, 2002). Thus, an increase in GluN2B/GluN2A ratio induced by CRTC1 may contribute to optimize long-term memory by favoring LTP induction and/or develop more plastic synapses. On the contrary, although CRTC1 inactivation does not affect total GluN2 levels, it slightly decreases GluN2B/GluN2A ratio without significant effects.

GluN subunits harbor a long C-terminal domain that is phosphorylated by several protein kinases regulating NMDARs trafficking, synaptic localization, and gating. Particularly, PKC has emerged as a central player in NMDAR recruitment to cell surface and NMDAR-mediated transmission (Lan et al., 2001, Grosshans et al., 2002, Lin et al., 2006, Kwon and Castillo, 2008). Thus, PKC activators enhance GluN1 synaptic localization and long-term potentiation (Lan et al., 2001, Grosshans et al., 2002, Kim et al., 2013). Of interest, we show for the first time that *in vivo* neuronal CRTC1 overexpression enhances GluN1 phosphorylation at Ser 890, whereas genetic CRTC1 inactivation lowers total and phosphorylated GluN1 levels (**Figure 11**). In agreement with previous studies (Grosshans et al., 2002, Scott et al., 2003, Sánchez-Pérez and Felipo, 2005), we demonstrate that this phosphorylation event is activity- and PKC-dependent, and that PKC activation enhances GluN1 synaptic localization in cultured hippocampal neurons (**Figure 13,14**).

Together, these results indicate that CRTC1 contributes to NMDAR-mediated neurotransmission specifically by regulating GluN1 trafficking to synaptic sites through PKC phosphorylation at Ser 890 (**Figure 33**). Further pharmacological and/or genetic experiments are, however, required to verify that PKC is indeed mediating the effect of CRTC1 on promoting GluN1 phosphorylation and synaptic localization.

Calcium influx through synaptic NMDARs activates calcium sensors, such as calmodulin (CaM), that participate in multiple synapse-to-nucleus signaling pathways critical for LTP maintenance (Xia and Storm, 2005). CaM binds specifically to the GluN1 CTD and can act as a synaptonuclear factor shuttling in an activity-dependent manner to the nucleus, regulating gene expression and contributing to NMDAR- and AMPAR-mediated neurotransmission (Zhou and Duan, 2018, Zhou and Duan, 2021). Additionally, CaM binding to GluN1 regulates the controlled entry of Ca^{2+} through NMDARs by an autoinhibitory mechanism known as calcium-dependent inactivation (Iacobucci and Popescu, 2019, Bhatia et al., 2020). Some synaptonuclear factors (e.g. Jacob, AIDA-1 and ATF4) can directly or indirectly bind to NMDARs (Gardoni and Di Luca, 2021). Here, using BRET technique we found that GluN1-CaM interaction is enhanced by CRTC1 (**Figure 19**), but whether this interaction is potentiated by a direct binding of CRTC1 requires further research. However, considering previous studies, this enhancement in GluN1-CaM interaction by CRTC1 could positively contribute to produce long-term changes in synaptic plasticity by regulating synapse-to-nucleus communication and NMDARs excitotoxicity.

Does CRTC1 regulate locally glutamatergic neurotransmission?

Synaptonuclear factors, including CRTC1, shuttle from synaptic/cytosolic compartments to the nucleus in an activity-dependent manner to modulate gene transcription (Parra-Damas and Saura, 2019). Besides its classical function as transcriptional cofactors, it is still unknown whether synaptonuclear factors play additional roles at specific neuronal compartments, such as dendritic spines, that could contribute to synaptic plasticity. Nonetheless, CRTCs can regulate RNA splicing and vesicle trafficking from the endoplasmic reticulum to the Golgi (Amelio et al., 2009, Han et al., 2015). Here, we investigated if CRTC1 could be locally modulating the synaptic proteome and, hence, contributing locally to synaptic responses. Since glutamate receptor phosphorylation and incorporation to the postsynaptic membrane is a dynamic process and dependent, in part, of already synthetized receptors, we investigated whether CRTC1-mediated GluN1 synaptic localization was independent of its nuclear function. To address this objective, different CRTC1 reported mutants and a triple phosphorylation-defective mutants were characterized. As was previously described, mutations in the nuclear localization sequence impaired CRTC1 activity-dependent nuclear translocation [(Ch'ng et al., 2015), **Figure 16C,D**]. Surprisingly, despite defective nuclear translocation, these constitutive cytosolic mutants enhance CREB-mediated gene transcription (**Figure 16**). This suggests that CRTC1 could regulate signaling cascades that leads to the upregulation of CREB-dependent gene expression independently of its nuclear translocation. For instance, if CRTC1 potentiates PKC-dependent phosphorylation of GluN1 it could also contribute to the phosphorylation of other PKC substrates such as CREB (Brindle et al., 1995).

Besides the nuclear localization sequence, CRTC1 localization is finely tuned by phosphorylation of conserved serine residues. Double and triple phosphoincompetent (serine to alanine) CRTC1 mutants previously described in the literature show enhanced nuclear localization (Ch'ng et al., 2012, Nonaka et al., 2014, Ch'ng et al., 2015). However, a triple S64/151/245A CRTC1 mutant generated in our laboratory exhibit contrary effects as it did not localize in the nucleus and was unable to induce CREB-dependent gene transcription [(Ch'ng et al., 2015), **Figure 16C-E**]. It is important to notice that our triple Ser/Ala CRTC1 mutant comprises the full length protein, whereas the triple phosphodeficient CRTC1 mutant used by Ch'ng and collaborators is truncated and comprise the first 270 amino acids. So, although the N-terminal region of CRTC1 contains the three aminoacidic residues that undergo regulated phosphorylation, the C-terminal region seems to contain additional regulatory element that negatively impact on activation and/or nuclear translocation.

Our studies involving the constitutively cytosolic CRTC1 S64/151/245A mutant revealed enhanced synaptic GluN1 localization at basal conditions. This suggests that CRTC1 can locally regulate NMDARs localization at synapses independently of its nuclear role as a transcriptional cofactor (**Figure 17, 33**). It is important to notice that inactivation of endogenous CRTC1 or overexpression of mutant CRTC1 did not alter total and dendritic GluN1 levels (**Figure 17,18**). This suggests that CRTC1 is regulating the recruitment of already synthesized NMDARs to postsynaptic sites and agrees with previous studies reporting intracellular GluN1 delivery to the synaptic membrane following LTP stimulation (Grosshans et al., 2002). Interestingly, puncta of the scaffolding protein PSD95 were significantly increased in CRTC1 mutant overexpressing hippocampal neurons and in stimulated control neurons. An increase in the abundance of PSD95 at synapses strengthens synaptic transmission by recruiting AMPARs and NMDARs and reducing receptor recycling and/or degradation (Colledge et al., 2003, Lin et al., 2004, Kim et al., 2007, Lavezzari et al., 2004). This increase in synaptic PSD95 is associated with its phosphorylation at Ser 295. Although this pPSD95 remain constant in neurons overexpressing CRTC1 S64/151/245A, biochemical analyses revealed an activity-dependent decrease in pPSD95 that is associated with loss of PSD95 clusters at dendritic spines and LTD [(Kim et al., 2007, Sen et al., 2016), **Figure 18**]. PSD95 N-terminal domain contains other phosphorylation sites that also contribute to clustering and synaptic targeting of PSD95. In fact, PSD95 Thr 19, Ser 25 and/or Ser 35 dephosphorylation enhances PSD95 and glutamate receptor stabilization at synapses (Morabito et al., 2004, Steiner et al., 2008, Nelson et al., 2013, Delgado et al., 2020). Our findings suggests that local CRTC1 regulates PSD95 reorganization at synapses contributing to GluN1-containing NMDARs stabilization at cell surface (**Figure 33**). But, to understand whether CRTC1 is positively or negatively regulating other phosphorylation sites important for PSD95 synaptic clustering, such as Thr 19, Ser 25 and Ser 35, requires further research.

CRTC1 modulates mRNA localization and local protein synthesis

Localizing population of transcripts at specific compartments has several advantages for compartmentalized cells such as neurons. mRNA pools at dendritic compartments allows neurons to efficiently respond to extracellular stimuli by rapidly synthesizing proteins for a quick incorporation into synapses. Experiments performed by locally administrating protein synthesis inhibitors or by physically isolating the compartment of interest revealed the importance of local translation in LTP (Vickers et al., 2005, Miller et al., 2002, Bradshaw et al., 2003). Intriguingly, CRTC1 overexpression or silencing in cultured hippocampal neurons increased or decreased, respectively, mRNA localization in dendrites (**Figure 20**). Although this effect can be mediated by CRTC1

transcriptional activity, it is unlikely that an effect on a specific population of mRNAs could cause such a dramatic change in total dendritic mRNA levels. Alternatively, CRTC1 could be: (1) promoting mRNA localization at dendrites by regulating RNA binding protein (RBP) expression, which are responsible of mRNA transport; or (2) interacting with RNA-containing granules enhancing its trafficking to dendrites (Fernandopulle et al., 2021). Further experiments are required to address these hypotheses. In addition to decrease dendritic mRNA localization in CRTC1-inactivated neurons, protein synthesis rate was also slightly diminished (**Figure 21**). These results indicate that CRTC1 is locally regulating mRNA localization and translation at dendritic compartment, which could also affect long-term synaptic plasticity (**Figure 33**). However, our results could not discriminate whether the decrease in local protein synthesis by CRTC1 inactivation was due to a failure of the translation machinery or to the already decreased dendritic mRNA population.

Our findings extend the functions of CRTC1 beyond its role as a transcriptional coactivator in that we have demonstrated that CRTC1 could locally contribute to synaptic plasticity by modulating NMDAR-mediated neurotransmission. We hypothesize that during synaptic transmission, Ca^{2+} influx through NMDARs activates CRTC1 that translocate to the nucleus, but some remain in postsynaptic sites. There, CRTC1 potentiates NMDAR-mediated neurotransmission by: (1) modulating PKC-dependent GluN1 phosphorylation and NMDAR trafficking to the postsynaptic membrane; (2) regulating PSD95 reorganization at postsynaptic sites to favor receptor anchoring and gating; and (3) potentiating GluN1 interaction with the calcium sensor calmodulin to enhance downstream signaling pathways involved in the maintenance of L-LTP (**Figure 33**). Additionally, CRTC1 also contributes to the modulation of synaptic responses by localizing mRNA pools at dendritic compartments and regulating its local translation (**Figure 33**).

CRTC1-dependent regulation of autophagy markers

Regulation of autophagy gene expression has been shown to depend on CRTC1/CREB transcriptional activity and it is suppressed in PS1 KO neural stem cells (Seok et al., 2014, Chong et al., 2018, Pan et al., 2021). Contrary to what has been reported, our results indicate that CRTC1 inactivation enhances autophagy flux without affecting autolysosomes clearance (**Figure 26**). Interestingly, the expression of microRNAs (miRNAs), such as miR212/132, which can negatively regulate mRNA stability and protein expression of autophagy-related markers are also regulated by CRTC1/CREB (Ucar et al., 2012, Liang et al., 2016). This could explain the increase in LC3-II/LC3-I ratio observed in AVV-ShCRTC1-injected mice and the induction of autophagy flux in human fibroblasts and iPSC-derived neurons harboring FAD-linked *PSEN1* mutations.

Synapse pathology correlates with synaptic tau accumulation in Tau and PS1 cKO;Tau mice

Tau stabilizes axonal microtubules but also regulates spine morphology and synaptic plasticity at dendritic spines (Chen et al., 2012, Frandemiche et al., 2014). In pathological conditions, including tauopathies, hyperphosphorylated tau mislocalizes to somatodendritic compartments disrupting synaptic functions and causing synapse and neuron loss (Yoshiyama et al., 2007, Hoover et al., 2010, Jackson et al., 2017). However, how pathological tau accumulation exerts synaptotoxicity remains unclear. In this doctoral thesis, we found that PS1 loss of function exacerbates phosphorylated tau accumulation at synapses of tau transgenic mice (**Figure 22,23**). This increase in pathological tau was associated with downregulation of CRTC1 at synapses, implying that tau-mediated synaptopathy leads to CRTC1 dysfunction. Deregulation of CRTC1 dephosphorylation, nuclear translocation and transcriptional activity were previously reported in the human hippocampus at early AD pathological stages and APP transgenic and PS cDKO mouse models (España et al., 2010, Parra-Damas et al., 2014, Parra-Damas et al., 2017a, Wilson et al., 2017, Yan et al., 2021). It is plausible that reduced synaptic CRTC1 could impair in synapse-to-nucleus communication leading to a decreased neuroplasticity genes expression. Notably, CRTC1 was detected at postsynapses and presynaptic terminals. Presynaptic localization of CRTC1 was not previously reported, so this finding broadens the possible roles of CRTC1 in synaptic neurotransmission to another subcellular compartment. In agreement with a quantitative proteomic analysis of PSD fractions from Tau Tg mice (Dejanovic et al., 2018), GluA1 and GluN1 glutamate receptors subunits and scaffold protein PSD95 were decreased in 11-12 month-old Tau and PS1 cKO;Tau mice suggesting failure in glutamatergic neurotransmission (**Figure 24**). A detrimental reduction in GluA1 subunit was also observed in hippocampal samples from patients diagnosed with FAD, CBD and PiD (**Figure 32**). Reduced synaptic GluN1 levels could be due to decreased total or synaptic CRTC1 described above. Alternatively, altered synapse morphology or loss in Tau Tg mice can lead to reduce synaptic GluN or CRTC1 levels. Of interest, activation of STAT1, a synaptonuclear factor, was recently reported to downregulate GluN subunits expression and NMDAR-mediated currents in mice overexpressing human tau (Li et al., 2019). Besides transcriptional deficits, pathological tau can interact with ribosomes and impair synthesis of synaptic proteins (e.g. PSD95) contributing to synaptic dysfunction (Meier et al., 2016). Future experiments are necessary to better understand whether altered synaptic proteins in our mouse model is due to transcriptional or translational failure.

PS1 regulates autophagy-mediated tau degradation

Synaptic accumulation of aggregated tau could be the result of impaired autophagy and proteasome degradation systems (Boland et al., 2018). Tau is degraded by the proteasome and disruption of proteasomal activity drives tau accumulation and aggregation (Keller et al., 2000, David et al., 2002, Keck et al., 2003, Babu et al., 2005). Tau also contains chaperone-mediated autophagy (CMA) motifs that allows its direct delivery into lysosomes (Wang et al., 2009, Caballero et al., 2021). Although proteasome and CMA could contribute to tau degradation, autophagy has also emerged as a central process regulating tau neuronal proteostasis and its alteration disrupts neural function leading to neurodegeneration (Hara et al., 2006, Komatsu et al., 2006). Interestingly, early-onset FAD-linked *PSEN1* mutations are associated with an inappropriate lysosome acidification due to failure in the delivery of v-ATPase from the ER to lysosomes (Lee et al., 2010, Neely et al., 2011), a mechanism that can lead to autophagic vacuoles accumulation in AD (Boland et al., 2008, Lee et al., 2011). In agreement, we found that PS1 loss of function in Tau Tg mice increases synaptic p62 levels, probably due to impaired autophagosomes clearance leading to exacerbated tau phosphorylation and accumulation at synapses (**Figure 25**). There is controversy whether synaptic cargoes can be locally degraded. Although lysosomes and autolysosomes are found at synapses (Goo et al., 2017, Kulkarni et al., 2021), some studies suggest that lysosomes with full degradative capability are restricted to the soma and that acidic degradative organelles at the neuron periphery correspond to endosomes and/or amphisomes (Lie et al., 2021). Therefore, it is possible that PS1 exacerbates tau pathology by failure on autophagy vesicles acidification locally at synapses or by impairing retrograde transport of autophagosomes to the soma for degradation. In support of this idea, a recent study demonstrated that deficient acidification of axonal degradative organelles in PS1 KO neurons leads to aberrant axonal retrograde transport (Lie et al., 2022). This suggest that, probably, a failure in synaptic autophagosomes acidification and maturation impairs their retrograde transport to the soma for a complete degradation leading to tau pathology. Additionally, since autophagosome retrograde and antegrade transport is dynein-dependent (Kimura et al., 2008, Katsumata et al., 2010, Farfel-Becker et al., 2019), microtubule destabilization by tau hyperphosphorylation can also be contributing to the disruption of autophagy vesicles transport.

Failure in lysosomal acidification and function has also been observed in human fibroblasts from FAD patients harboring the FAD-linked *PSEN1* A246E mutation (Coffey et al., 2014). Our results on autophagy flux monitoring in human fibroblasts carrying G206D and L286P *PSEN1* mutations revealed increased autophagy flux induction and defective autolysosomes clearance probably due

to deficient enzymatic activity (**Figure 27,28**). In fact, small rises in lysosomal pH (~0.2 pH units) have detrimental effects in the activity of cathepsin D in FAD-linked *PSEN1* human fibroblasts (Coffey et al., 2014). Altogether, these results suggests that human fibroblasts from patient with FAD-linked *PSEN1* mutations enhance the induction of autophagy flux probably to compensate the defective lysosomal acidification and degradative activity. A similar effect was also seen in iPSC-derived neurons harboring G206D PS1 mutation (**Figure 29**). Of interest, we hypothesized that FAD-linked *PSEN1* G206D mutation contributes to the accumulation of aggregated tau by inhibiting autophagosome-lysosome fusion or by altering the acidification of lysosomes/autolysosomes (**Figure 30**). These results agree with recent studies showing that iPSC-derived neurons carrying FAD-linked *PSEN1* mutations have altered autophagy flux and impaired autophagosomes clearance leading to an increase of $A\beta_{42}$ and phosphorylated tau levels (Li et al., 2020, Chong et al., 2022). Reinforcing the cell culture experiments, analysis of human hippocampal samples from patients harboring *PSEN1* mutations and clinically diagnosed with FAD revealed that impaired autophagosomes clearance, detected as elevated p62 levels, was associated with accumulation of hyperphosphorylated and aggregated tau species compared with age-matched controls (**Figure 31**). Elevated p62 levels were also detected in hippocampal samples from other tauopathy disorders (CBD and PiD). Interestingly, a slight non-significant increase in proLC3 levels were also detected. This could mean that autophagy flux is being induced by potentiating the expression of LC3 precursor or that there is a failure in the conversion of proLC3 to LC3-I. Considering that total LC3-I levels were unchanged and cleavage of proLC3 is upregulated in AD (Shin et al., 2019), we suggest that autophagy flux in FAD-linked *PSEN1* patients is induced by potentiating proLC3 expression.

Besides hyperphosphorylation, tau truncation exacerbates aggregation and propagation of tau (Matsumoto et al., 2015, Sokolow et al., 2015, Zhao et al., 2016, Zhou et al., 2018a, Gu et al., 2020). PS1 G206D iPSC-derived neurons show higher levels of the ~22 kDa tau (**Figure 30**), a truncated tau form found in AD and FTD brains with elevated aggregation and propagation activities (Matsumoto et al., 2015, Amadoro et al., 2020). On the contrary, the ~40 kDa truncated tau, also found in AD brains, was slightly reduced in iPSC-derived neurons carrying PS1 G206D mutation and in CQ-treated cells [(Tarutani et al., 2022), **Figure 30**]. All these results allow us to speculate that FAD-linked *PSEN1* mutations can contribute to propagation and/or aggregation of truncated tau leading to tau pathogenesis progression in FAD.

Taken together, our findings suggest that FAD-linked *PSEN1* mutations and genetic PS1 loss potentiate autophagy flux while impairing autolysosomes clearance, likely leading to accumulation, aggregation, and propagation of pathological tau (**Figure 34**).

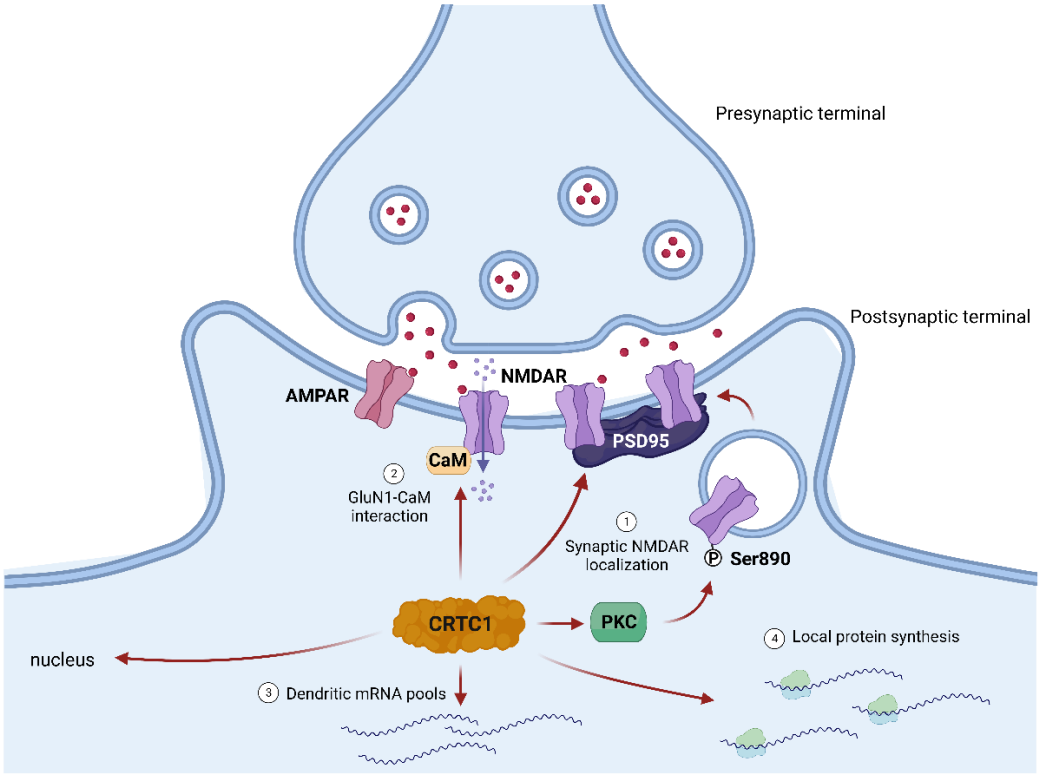

Figure 33. Proposed local roles of CRTC1 at synapses that contribute to synaptic plasticity. Activation of NMDARs and increase intracellular calcium activates synaptic CRTC1 which in turn potentiates PKC-dependent GluN1 phosphorylation at Ser 890 and PSD95 reorganization that contribute to NMDARs delivery and stabilization at the postsynaptic membrane. Thus, positive feedback between NMDAR-mediated neurotransmission and CRTC1 is stablished. Enhancement of calmodulin interaction with GluN1 subunits also strengthen NMDAR-mediated LTP by activating downstream signaling pathways. CRTC1 also contribute to the maintenance of L-LTP by contributing to the localization of dendritic mRNAs that can be locally translated into proteins for the incorporation into postsynaptic sites. Image created with BioRender.

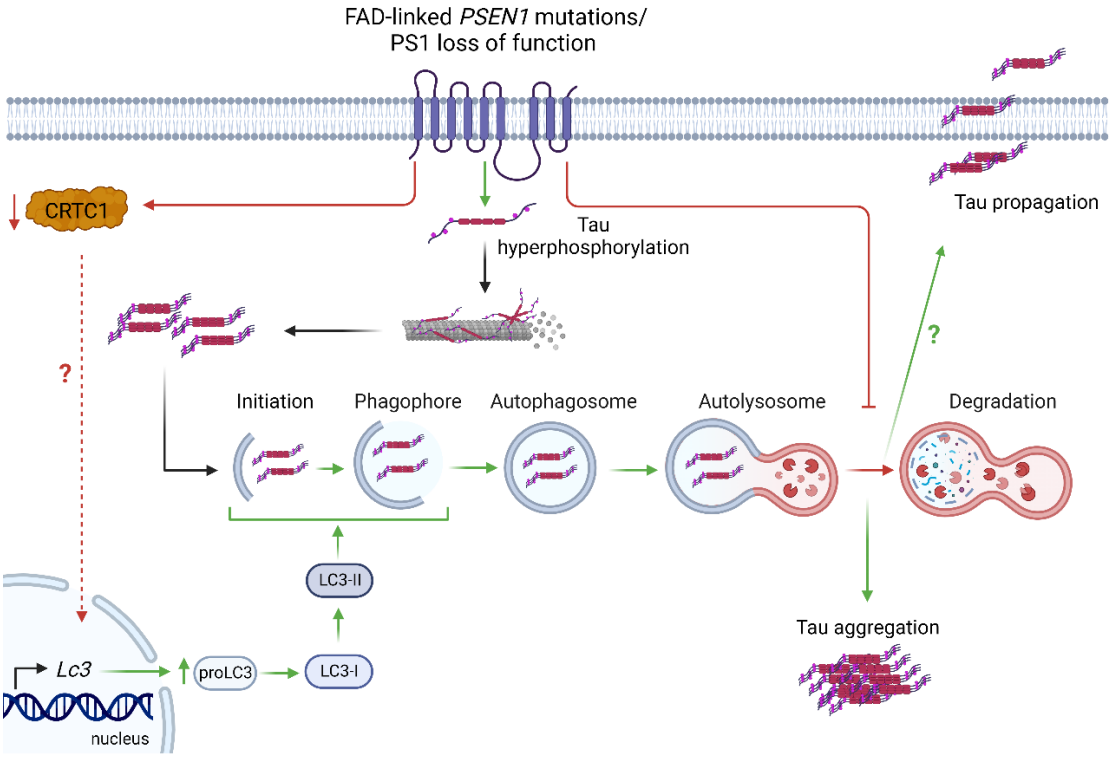

Figure 34. Proposed model of autophagy flux by mutant PS1-linked tauopathies. PS1 loss of function or FAD-linked *PSEN1* mutations potentiate the induction of autophagy flux and impair the clearance of autolysosomes, which may contribute to the aggregation and/or propagation of pathological tau. Genetic inactivation of PS1 leads to tau hyperphosphorylation and disrupted activity-mediated CRTC1 activation (Parra-Damas et al., 2017a, Soto-Faguás et al., 2021). Downregulation of CRTC1 may increase the levels of the autophagy marker LC3, enhancing autophagosomes formation. However, impaired autolysosomes acidification or deficient lysosomal enzymatic activity contributes to the accumulation of dysfunctional autolysosomes and to the aggregation and/or release of hyperphosphorylated tau. Image created with BioRender.

Conclusions

1. CRTC1 is essential for hippocampal-dependent associative memory.

2. CRTC1 modulates NMDAR subunit composition by regulating the levels of GluN1 and GluN2 in the hippocampus.

3. Synaptic CRTC1 contributes to NMDAR-mediated neurotransmission by regulating PKC-dependent GluN1 phosphorylation and localization at postsynapses.

4. CRTC1 enhances GluN1-calmodulin interaction in heterologous cells.

5. CRTC1 positively regulates the localization and translation of dendritic mRNAs.

6. Genetic inactivation of PS1 in PS1 cKO;Tau mice is associated with elevated synaptic phosphorylated tau and autophagy markers, and reduced synaptic CRTC1.

7. FAD-linked *PSEN1* mutations and PS1 loss of function enhance the induction of autophagy flux but impairs autolysosomes clearance likely contributing to tau pathology.

Bibliography

ALBERINI, C. M. 2009. Transcription factors in long-term memory and synaptic plasticity. *Physiol Rev,* 89, 121-45.

ALBERTS, A. S., MONTMINY, M., SHENOLIKAR, S. & FERAMISCO, J. R. 1994. Expression of a peptide inhibitor of protein phosphatase 1 increases phosphorylation and activity of CREB in NIH 3T3 fibroblasts. *Mol Cell Biol,* 14, 4398-407.

ALMEIDA, C. G., TAMPELLINI, D., TAKAHASHI, R. H., GREENGARD, P., LIN, M. T., SNYDER, E. M. & GOURAS, G. K. 2005. Beta-amyloid accumulation in APP mutant neurons reduces PSD-95 and GluR1 in synapses. *Neurobiol Dis,* 20, 187-98.

ALTAREJOS, J. Y., GOEBEL, N., CONKRIGHT, M. D., INOUE, H., XIE, J., ARIAS, C. M., SAWCHENKO, P. E. & MONTMINY, M. 2008. The Creb1 coactivator Crtc1 is required for energy balance and fertility. *Nat Med,* 14, 1112-7.

ALTAREJOS, J. Y. & MONTMINY, M. 2011. CREB and the CRTC co-activators: sensors for hormonal and metabolic signals. *Nat Rev Mol Cell Biol,* 12, 141-51.

AMADORO, G., LATINA, V., CORSETTI, V. & CALISSANO, P. 2020. N-terminal tau truncation in the pathogenesis of Alzheimer's disease (AD): Developing a novel diagnostic and therapeutic approach. *Biochim Biophys Acta Mol Basis Dis,* 1866, 165584.

AMELIO, A. L., CAPUTI, M. & CONKRIGHT, M. D. 2009. Bipartite functions of the CREB co-activators selectively direct alternative splicing or transcriptional activation. *Embo j,* 28, 2733-47.

ANDREOLI, V., DE MARCO, E. V., TRECROCI, F., CITTADELLA, R., DI PALMA, G. & GAMBARDELLA, A. 2014. Potential involvement of GRIN2B encoding the NMDA receptor subunit NR2B in the spectrum of Alzheimer's disease. *J Neural Transm (Vienna),* 121, 533-42.

BABU, J. R., GEETHA, T. & WOOTEN, M. W. 2005. Sequestosome 1/p62 shuttles polyubiquitinated tau for proteasomal degradation. *J Neurochem,* 94, 192-203.

BAGLIETTO-VARGAS, D., PRIETO, G. A., LIMON, A., FORNER, S., RODRIGUEZ-ORTIZ, C. J., IKEMURA, K., AGER, R. R., MEDEIROS, R., TRUJILLO-ESTRADA, L., MARTINI, A. C., KITAZAWA, M., DAVILA, J. C., COTMAN, C. W., GUTIERREZ, A. & LAFERLA, F. M. 2018. Impaired AMPA signaling and cytoskeletal alterations induce early synaptic dysfunction in a mouse model of Alzheimer's disease. *Aging Cell,* 17, e12791.

BAI, L., HOF, P. R., STANDAERT, D. G., XING, Y., NELSON, S. E., YOUNG, A. B. & MAGNUSSON, K. R. 2004. Changes in the expression of the NR2B subunit during aging in macaque monkeys. *Neurobiol Aging,* 25, 201-8.

BAJ, G., LEONE, E., CHAO, M. V. & TONGIORGI, E. 2011. Spatial segregation of BDNF transcripts enables BDNF to differentially shape distinct dendritic compartments. *Proc Natl Acad Sci U S A,* 108, 16813-8.

BARRIA, A., DERKACH, V. & SODERLING, T. 1997. Identification of the Ca2+/calmodulin-dependent protein kinase II regulatory phosphorylation site in the alpha-amino-3-hydroxyl-5-methyl-4-isoxazole-propionate-type glutamate receptor. *J Biol Chem,* 272, 32727-30.

BARRIA, A. & MALINOW, R. 2002. Subunit-specific NMDA receptor trafficking to synapses. *Neuron,* 35, 345-53.

BARROSO-FLORES, J., HERRERA-VALDEZ, M. A., LOPEZ-HUERTA, V. G., GALARRAGA, E. & BARGAS, J. 2015. Diverse short-term dynamics of inhibitory synapses converging on striatal projection neurons: differential changes in a rodent model of Parkinson's disease. *Neural Plast,* 2015, 573543.

BASSELL, G. J., ZHANG, H., BYRD, A. L., FEMINO, A. M., SINGER, R. H., TANEJA, K. L., LIFSHITZ, L. M., HERMAN, I. M. & KOSIK, K. S. 1998. Sorting of beta-actin mRNA and protein to neurites and growth cones in culture. *J Neurosci,* 18, 251-65.

BELLONE, C. & NICOLL, R. A. 2007. Rapid bidirectional switching of synaptic NMDA receptors. *Neuron,* 55, 779-85.

BHATIA, N. K., CARRILLO, E., DURHAM, R. J., BERKA, V. & JAYARAMAN, V. 2020. Allosteric changes in the NMDA receptor associated with calcium-dependent inactivation. *Biophys J,* 119, 2349-2359.

BI, H. & SZE, C. I. 2002. N-methyl-D-aspartate receptor subunit NR2A and NR2B messenger RNA levels are altered in the hippocampus and entorhinal cortex in Alzheimer's disease. *J Neurol Sci,* 200, 11-8.

BIEVER, A., DONLIN-ASP, P. G. & SCHUMAN, E. M. 2019. Local translation in neuronal processes. *Curr Opin Neurobiol,* 57, 141-148.

BILLARD, J. M. & ROUAUD, E. 2007. Deficit of NMDA receptor activation in CA1 hippocampal area of aged rats is rescued by D-cycloserine. *Eur J Neurosci,* 25, 2260-8.

BITTINGER, M. A., MCWHINNIE, E., MELTZER, J., IOURGENKO, V., LATARIO, B., LIU, X., CHEN, C. H., SONG, C., GARZA, D. & LABOW, M. 2004. Activation of cAMP response element-mediated gene expression by regulated nuclear transport of TORC proteins. *Curr Biol,* 14, 2156-61.

BLISS, T. V. & GARDNER-MEDWIN, A. R. 1973. Long-lasting potentiation of synaptic transmission in the dentate area of the unanaestetized rabbit following stimulation of the perforant path. *J Physiol,* 232, 357-74.

BODHINATHAN, K., KUMAR, A. & FOSTER, T. C. 2010. Intracellular redox state alters NMDA receptor response during aging through Ca2+/calmodulin-dependent protein kinase II. *J Neurosci,* 30, 1914-24.

BOLAND, B., KUMAR, A., LEE, S., PLATT, F. M., WEGIEL, J., YU, W. H. & NIXON, R. A. 2008. Autophagy induction and autophagosome clearance in neurons: relationship to autophagic pathology in Alzheimer's disease. *J Neurosci,* 28, 6926-37.

BOLAND, B., YU, W. H., CORTI, O., MOLLEREAU, B., HENRIQUES, A., BEZARD, E., PASTORES, G. M., RUBINSZTEIN, D. C., NIXON, R. A., DUCHEN, M. R., MALLUCCI, G. R., KROEMER, G., LEVINE, B., ESKELINEN, E. L., MOCHEL, F., SPEDDING, M., LOUIS, C., MARTIN, O. R. & MILLAN, M. J. 2018. Promoting the clearance of neurotoxic proteins in neurodegenerative disorders of ageing. *Nat Rev Drug Discov,* 17, 660-688.

BOURTCHULADZE, R., FRENGUELLI, B., BLENDY, J., CIOFFI, D., SCHUTZ, G. & SILVA, A. J. 1994. Deficient long-term memory in mice with a targeted mutation of the cAMP-responsive element-binding protein. *Cell,* 79, 59-68.

BRAAK, H. & BRAAK, E. 1991. Neuropathological stageing of Alzheimer-related changes. *Acta Neuropathol,* 82, 239-59.

BRADSHAW, K. D., EMPTAGE, N. J. & BLISS, T. V. 2003. A role for dendritic protein synthesis in hippocampal late LTP. *Eur J Neurosci,* 18, 3150-2.

BREUILLAUD, L., ROSSETTI, C., MEYLAN, E. M., MÉRINAT, C., HALFON, O., MAGISTRETTI, P. J. & CARDINAUX, J. R. 2012. Deletion of CREB-regulated transcription coactivator 1 induces pathological aggression, depression-related behaviors, and neuroplasticity genes dysregulation in mice. *Biol Psychiatry,* 72, 528-36.

BRIGHTWELL, J. J., GALLAGHER, M. & COLOMBO, P. J. 2004. Hippocampal CREB1 but not CREB2 is decreased in aged rats with spatial memory impairments. *Neurobiol Learn Mem,* 81, 19-26.

BRIM, B. L., HASKELL, R., AWEDIKIAN, R., ELLINWOOD, N. M., JIN, L., KUMAR, A., FOSTER, T. C. & MAGNUSSON, K. R. 2013. Memory in aged mice is rescued by enhanced expression of the GluN2B subunit of the NMDA receptor. *Behav Brain Res,* 238, 211-26.

BRINDLE, P., NAKAJIMA, T. & MONTMINY, M. 1995. Multiple protein kinase A-regulated events are required for transcriptional induction by cAMP. *Proc Natl Acad Sci U S A,* 92, 10521-5.

BURGOYNE, R. D., HELASSA, N., MCCUE, H. V. & HAYNES, L. P. 2019. Calcium sensors in neuronal function and dysfunction. *Cold Spring Harb Perspect Biol,* 11.

BUÉE SCHERRER, V., HOF, P. R., BUÉE, L., LEVEUGLE, B., VERMERSCH, P., PERL, D. P., OLANOW, C. W. & DELACOURTE, A. 1996. Hyperphosphorylated tau proteins differentiate corticobasal degeneration and Pick's disease. *Acta Neuropathol,* 91, 351-9.

CABALLERO, B., BOURDENX, M., LUENGO, E., DIAZ, A., SOHN, P. D., CHEN, X., WANG, C., JUSTE, Y. R., WEGMANN, S., PATEL, B., YOUNG, Z. T., KUO, S. Y., RODRIGUEZ-NAVARRO, J. A., SHAO, H., LOPEZ, M. G., KARCH, C. M., GOATE, A. M., GESTWICKI, J. E., HYMAN, B. T., GAN, L. &

CUERVO, A. M. 2021. Acetylated tau inhibits chaperone-mediated autophagy and promotes tau pathology propagation in mice. *Nat Commun,* 12, 2238.

CAJIGAS, I. J., TUSHEV, G., WILL, T. J., TOM DIECK, S., FUERST, N. & SCHUMAN, E. M. 2012. The local transcriptome in the synaptic neuropil revealed by deep sequencing and high-resolution imaging. *Neuron,* 74, 453-66.

CAO, X., CUI, Z., FENG, R., TANG, Y. P., QIN, Z., MEI, B. & TSIEN, J. Z. 2007. Maintenance of superior learning and memory function in NR2B transgenic mice during ageing. *Eur J Neurosci,* 25, 1815-22.

CARROLL, R. C. & ZUKIN, R. S. 2002. NMDA-receptor trafficking and targeting: implications for synaptic transmission and plasticity. *Trends Neurosci,* 25, 571-7.

CH'NG, T. H., DESALVO, M., LIN, P., VASHISHT, A., WOHLSCHLEGEL, J. A. & MARTIN, K. C. 2015. Cell biological mechanisms of activity-dependent synapse to nucleus translocation of CRTC1 in neurons. *Front Mol Neurosci,* 8, 48.

CH'NG, T. H. & MARTIN, K. C. 2011. Synapse-to-nucleus signaling. *Curr Opin Neurobiol,* 21, 345-52.

CH'NG, T. H., UZGIL, B., LIN, P., AVLIYAKULOV, N. K., O'DELL, T. J. & MARTIN, K. C. 2012. Activity-dependent transport of the transcriptional coactivator CRTC1 from synapse to nucleus. *Cell,* 150, 207-21.

CHATURVEDI, R. K., HENNESSEY, T., JOHRI, A., TIWARI, S. K., MISHRA, D., AGARWAL, S., KIM, Y. S. & BEAL, M. F. 2012. Transducer of regulated CREB-binding proteins (TORCs) transcription and function is impaired in Huntington's disease. *Hum Mol Genet,* 21, 3474-88.

CHEN, L., CHETKOVICH, D. M., PETRALIA, R. S., SWEENEY, N. T., KAWASAKI, Y., WENTHOLD, R. J., BREDT, D. S. & NICOLL, R. A. 2000. Stargazin regulates synaptic targeting of AMPA receptors by two distinct mechanisms. *Nature,* 408, 936-43.

CHEN, Q., ZHOU, Z., ZHANG, L., WANG, Y., ZHANG, Y. W., ZHONG, M., XU, S. C., CHEN, C. H., LI, L. & YU, Z. P. 2012. Tau protein is involved in morphological plasticity in hippocampal neurons in response to BDNF. *Neurochem Int,* 60, 233-42.

CHENG, W., SIEDLECKI-WULLICH, D., CATALÀ-SOLSONA, J., FÁBREGAS, C., FADÓ, R., CASALS, N., SOLÉ, M., UNZETA, M., SAURA, C. A., RODRÍGUEZ-ALVAREZ, J. & MIÑANO-MOLINA, A. J. 2020. Proteasomal-mediated degradation of AKAP150 accompanies AMPAR endocytosis during cLTD. *eNeuro,* 7.

CHOI, S., KIM, W. & CHUNG, J. 2011. Drosophila salt-inducible kinase (SIK) regulates starvation resistance through cAMP-response element-binding protein (CREB)-regulated transcription coactivator (CRTC). *J Biol Chem,* 286, 2658-64.

CHOI, Y. S., LEE, B., CHO, H. Y., REYES, I. B., PU, X. A., SAIDO, T. C., HOYT, K. R. & OBRIETAN, K. 2009. CREB is a key regulator of striatal vulnerability in chemical and genetic models of Huntington's disease. *Neurobiol Dis,* 36, 259-68.

CHONG, C. M., KE, M., TAN, Y., HUANG, Z., ZHANG, K., AI, N., GE, W., QIN, D., LU, J. H. & SU, H. 2018. Presenilin 1 deficiency suppresses autophagy in human neural stem cells through reducing γ-secretase-independent ERK/CREB signaling. *Cell Death Dis,* 9, 879.

CHONG, C. M., TAN, Y., TONG, J., KE, M., ZHANG, K., YAN, L., CEN, X., LU, J. H., CHEN, G., SU, H. & QIN, D. 2022. Presenilin-1 F105C mutation leads to tau accumulation in human neurons via the Akt/mTORC1 signaling pathway. *Cell Biosci,* 12, 131.

CHUNG, D. C., ROEMER, S., PETRUCELLI, L. & DICKSON, D. W. 2021. Cellular and pathological heterogeneity of primary tauopathies. *Mol Neurodegener,* 16, 57.

CHUNG, S., LI, X. & NELSON, S. B. 2002. Short-term depression at thalamocortical synapses contributes to rapid adaptation of cortical sensory responses in vivo. *Neuron,* 34, 437-46.

CIOLLI MATTIOLI, C., ROM, A., FRANKE, V., IMAMI, K., ARREY, G., TERNE, M., WOEHLER, A., AKALIN, A., ULITSKY, I. & CHEKULAEVA, M. 2019. Alternative 3' UTRs direct localization of functionally diverse protein isoforms in neuronal compartments. *Nucleic Acids Res,* 47, 2560-2573.

CITRI, A. & MALENKA, R. C. 2008. Synaptic plasticity: multiple forms, functions, and mechanisms. *Neuropsychopharmacology,* 33, 18-41.

CLAYTON, D. A. & BROWNING, M. D. 2001. Deficits in the expression of the NR2B subunit in the hippocampus of aged Fisher 344 rats. *Neurobiol Aging,* 22, 165-8.

COFFEY, E. E., BECKEL, J. M., LATIES, A. M. & MITCHELL, C. H. 2014. Lysosomal alkalization and dysfunction in human fibroblasts with the Alzheimer's disease-linked presenilin 1 A246E mutation can be reversed with cAMP. *Neuroscience,* 263, 111-24.

COHEN, L. D., ZUCHMAN, R., SOROKINA, O., MÜLLER, A., DIETERICH, D. C., ARMSTRONG, J. D., ZIV, T. & ZIV, N. E. 2013. Metabolic turnover of synaptic proteins: kinetics, interdependencies and implications for synaptic maintenance. *PLoS One,* 8, e63191.

COHEN, S. & GREENBERG, M. E. 2008. Communication between the synapse and the nucleus in neuronal development, plasticity, and disease. *Annu Rev Cell Dev Biol,* 24, 183-209.

COLLEDGE, M., SNYDER, E. M., CROZIER, R. A., SODERLING, J. A., JIN, Y., LANGEBERG, L. K., LU, H., BEAR, M. F. & SCOTT, J. D. 2003. Ubiquitination regulates PSD-95 degradation and AMPA receptor surface expression. *Neuron,* 40, 595-607.

COMERFORD, K. M., LEONARD, M. O., KARHAUSEN, J., CAREY, R., COLGAN, S. P. & TAYLOR, C. T. 2003. Small ubiquitin-related modifier-1 modification mediates resolution of CREB-dependent responses to hypoxia. *Proc Natl Acad Sci U S A,* 100, 986-91.

CONKRIGHT, M. D., CANETTIERI, G., SCREATON, R., GUZMAN, E., MIRAGLIA, L., HOGENESCH, J. B. & MONTMINY, M. 2003. TORCs: transducers of regulated CREB activity. *Mol Cell,* 12, 413-23.

DAVID, D. C., LAYFIELD, R., SERPELL, L., NARAIN, Y., GOEDERT, M. & SPILLANTINI, M. G. 2002. Proteasomal degradation of tau protein. *J Neurochem,* 83, 176-85.

DE STROOPER, B., IWATSUBO, T. & WOLFE, M. S. 2012. Presenilins and γ-secretase: structure, function, and role in Alzheimer Disease. *Cold Spring Harb Perspect Med,* 2, a006304.

DE WILDE, M. C., OVERK, C. R., SIJBEN, J. W. & MASLIAH, E. 2016. Meta-analysis of synaptic pathology in Alzheimer's disease reveals selective molecular vesicular machinery vulnerability. *Alzheimers Dement,* 12, 633-44.

DEJANOVIC, B., HUNTLEY, M. A., DE MAZIÈRE, A., MEILANDT, W. J., WU, T., SRINIVASAN, K., JIANG, Z., GANDHAM, V., FRIEDMAN, B. A., NGU, H., FOREMAN, O., CARANO, R. A. D., CHIH, B., KLUMPERMAN, J., BAKALARSKI, C., HANSON, J. E. & SHENG, M. 2018. Changes in the synaptic proteome in tauopathy and rescue of tau-induced synapse loss by C1q antibodies. *Neuron,* 100, 1322-1336.e7.

DELACOURTE, A., ROBITAILLE, Y., SERGEANT, N., BUÉE, L., HOF, P. R., WATTEZ, A., LAROCHE-CHOLETTE, A., MATHIEU, J., CHAGNON, P. & GAUVREAU, D. 1996. Specific pathological Tau protein variants characterize Pick's disease. *J Neuropathol Exp Neurol,* 55, 159-68.

DELGADO, J. Y., NALL, D. & SELVIN, P. R. 2020. Pin1 binding to phosphorylated PSD-95 regulates the number of functional excitatory synapses. *Front Mol Neurosci,* 13, 10.

DERKACH, V. A., OH, M. C., GUIRE, E. S. & SODERLING, T. R. 2007. Regulatory mechanisms of AMPA receptors in synaptic plasticity. *Nat Rev Neurosci,* 8, 101-13.

DÍAZ-GUERRA, E., ORIA-MURIEL, M. A., MORENO-JIMÉNEZ, E. P., DE ROJASB, I., RODRÍGUEZ, C., RODRÍGUEZ-TRAVER, E., ORERA, M., HERNÁNDEZB, I., RUIZB, A. & VICARIO, C. 2019. Generation of an integration-free iPSC line, ICCSICi006-A, derived from a male Alzheimer's disease patient carrying the PSEN1-G206D mutation. *Stem Cell Res,* 40, 101574.

DIERING, G. H., HEO, S., HUSSAIN, N. K., LIU, B. & HUGANIR, R. L. 2016. Extensive phosphorylation of AMPA receptors in neurons. *Proc Natl Acad Sci U S A,* 113, E4920-7.

DIERING, G. H. & HUGANIR, R. L. 2018. The AMPA receptor code of synaptic plasticity. *Neuron,* 100, 314-329.

DIKIC, I. 2017. Proteasomal and autophagic degradation systems. *Annu Rev Biochem,* 86, 193-224.

EGAN, D., KIM, J., SHAW, R. J. & GUAN, K. L. 2011. The autophagy initiating kinase ULK1 is regulated via opposing phosphorylation by AMPK and mTOR. *Autophagy,* 7, 643-4.

EHLERS, M. D. 2000. Reinsertion or degradation of AMPA receptors determined by activity-dependent endocytic sorting. *Neuron,* 28, 511-25.

EL-FALOUGY, H. & BENUSKA, J. 2006. History, anatomical nomenclature, comparative anatomy and functions of the hippocampal formation. *Bratisl Lek Listy,* 107, 103-6.

EOM, T., ANTAR, L. N., SINGER, R. H. & BASSELL, G. J. 2003. Localization of a beta-actin messenger ribonucleoprotein complex with zipcode-binding protein modulates the density of dendritic filopodia and filopodial synapses. *J Neurosci,* 23, 10433-44.

ESPAÑA, J., VALERO, J., MIÑANO-MOLINA, A. J., MASGRAU, R., MARTÍN, E., GUARDIA-LAGUARTA, C., LLEÓ, A., GIMÉNEZ-LLORT, L., RODRÍGUEZ-ALVAREZ, J. & SAURA, C. A. 2010. beta-Amyloid disrupts activity-dependent gene transcription required for memory through the CREB coactivator CRTC1. *J Neurosci,* 30, 9402-10.

FALCON, B., ZHANG, W., MURZIN, A. G., MURSHUDOV, G., GARRINGER, H. J., VIDAL, R., CROWTHER, R. A., GHETTI, B., SCHERES, S. H. W. & GOEDERT, M. 2018. Structures of filaments from Pick's disease reveal a novel tau protein fold. *Nature,* 561, 137-140.

FARFEL-BECKER, T., RONEY, J. C., CHENG, X. T., LI, S., CUDDY, S. R. & SHENG, Z. H. 2019. Neuronal soma-derived degradative lysosomes are continuously delivered to distal axons to maintain local degradation capacity. *Cell Rep,* 28, 51-64.e4.

FERNANDOPULLE, M. S., LIPPINCOTT-SCHWARTZ, J. & WARD, M. E. 2021. RNA transport and local translation in neurodevelopmental and neurodegenerative disease. *Nat Neurosci,* 24, 622-632.

FERREIRA, I. L., BAJOUCO, L. M., MOTA, S. I., AUBERSON, Y. P., OLIVEIRA, C. R. & REGO, A. C. 2012. Amyloid beta peptide 1-42 disturbs intracellular calcium homeostasis through activation of GluN2B-containing N-methyl-d-aspartate receptors in cortical cultures. *Cell Calcium,* 51, 95-106.

FERRER, I., LÓPEZ-GONZÁLEZ, I., CARMONA, M., ARREGUI, L., DALFÓ, E., TORREJÓN-ESCRIBANO, B., DIEHL, R. & KOVACS, G. G. 2014. Glial and neuronal tau pathology in tauopathies: characterization of disease-specific phenotypes and tau pathology progression. *J Neuropathol Exp Neurol,* 73, 81-97.

FINSTERWALD, C., FIUMELLI, H., CARDINAUX, J. R. & MARTIN, J. L. 2010. Regulation of dendritic development by BDNF requires activation of CRTC1 by glutamate. *J Biol Chem,* 285, 28587-95.

FRANCO, R., AGUINAGA, D., REYES, I., CANELA, E. I., LILLO, J., TARUTANI, A., HASEGAWA, M., DEL SER-BADIA, A., DEL RIO, J. A., KREUTZ, M. R., SAURA, C. A. & NAVARRO, G. 2018. N-Methyl-D-Aspartate receptor link to the MAP kinase pathway in cortical and hippocampal neurons and microglia is dependent on calcium sensors and is blocked by alpha-synuclein, tau, and phospho-tau in non-transgenic and transgenic APPSw,Ind mice. *Front Mol Neurosci,* 11, 273.

FRANDEMICHE, M. L., DE SERANNO, S., RUSH, T., BOREL, E., ELIE, A., ARNAL, I., LANTÉ, F. & BUISSON, A. 2014. Activity-dependent tau protein translocation to excitatory synapse is disrupted by exposure to amyloid-beta oligomers. *J Neurosci,* 34, 6084-97.

FRISONI, G. B., SABATTOLI, F., LEE, A. D., DUTTON, R. A., TOGA, A. W. & THOMPSON, P. M. 2006. In vivo neuropathology of the hippocampal formation in AD: a radial mapping MR-based study. *Neuroimage,* 32, 104-10.

GARDONI, F. & DI LUCA, M. 2021. Protein-protein interactions at the NMDA receptor complex: From synaptic retention to synaptonuclear protein messengers. *Neuropharmacology,* 190, 108551.

GELENS, L. & SAURIN, A. T. 2018. Exploring the function of dynamic phosphorylation-dephosphorylation cycles. *Dev Cell,* 44, 659-663.

GIANDOMENICO, S. L., ALVAREZ-CASTELAO, B. & SCHUMAN, E. M. 2022. Proteostatic regulation in neuronal compartments. *Trends Neurosci,* 45, 41-52.

GINES, S., SEONG, I. S., FOSSALE, E., IVANOVA, E., TRETTEL, F., GUSELLA, J. F., WHEELER, V. C., PERSICHETTI, F. & MACDONALD, M. E. 2003. Specific progressive cAMP reduction implicates energy deficit in presymptomatic Huntington's disease knock-in mice. *Hum Mol Genet,* 12, 497-508.

GIRALT, A., PUIGDELLÍVOL, M., CARRETÓN, O., PAOLETTI, P., VALERO, J., PARRA-DAMAS, A., SAURA, C. A., ALBERCH, J. & GINÉS, S. 2012. Long-term memory deficits in Huntington's disease are associated with reduced CBP histone acetylase activity. *Hum Mol Genet,* 21, 1203-16.

GONG, B., VITOLO, O. V., TRINCHESE, F., LIU, S., SHELANSKI, M. & ARANCIO, O. 2004. Persistent improvement in synaptic and cognitive functions in an Alzheimer mouse model after rolipram treatment. *J Clin Invest,* 114, 1624-34.

GOO, M. S., SANCHO, L., SLEPAK, N., BOASSA, D., DEERINCK, T. J., ELLISMAN, M. H., BLOODGOOD, B. L. & PATRICK, G. N. 2017. Activity-dependent trafficking of lysosomes in dendrites and dendritic spines. *J Cell Biol,* 216, 2499-2513.

GOODMAN, R. H. & SMOLIK, S. 2000. CBP/p300 in cell growth, transformation, and development. *Genes Dev,* 14, 1553-77.

GOTO, Y., NIIDOME, T., AKAIKE, A., KIHARA, T. & SUGIMOTO, H. 2006. Amyloid beta-peptide preconditioning reduces glutamate-induced neurotoxicity by promoting endocytosis of NMDA receptor. *Biochem Biophys Res Commun,* 351, 259-65.

GÖTZ, J., HALLIDAY, G. & NISBET, R. M. 2019. Molecular pathogenesis of the tauopathies. *Annu Rev Pathol,* 14, 239-261.

GRAY, J. A., SHI, Y., USUI, H., DURING, M. J., SAKIMURA, K. & NICOLL, R. A. 2011a. Distinct modes of AMPA receptor suppression at developing synapses by GluN2A and GluN2B: single-cell NMDA receptor subunit deletion in vivo. *Neuron,* 71, 1085-101.

GRAY, S. J., FOTI, S. B., SCHWARTZ, J. W., BACHABOINA, L., TAYLOR-BLAKE, B., COLEMAN, J., EHLERS, M. D., ZYLKA, M. J., MCCOWN, T. J. & SAMULSKI, R. J. 2011b. Optimizing promoters for recombinant adeno-associated virus-mediated gene expression in the peripheral and central nervous system using self-complementary vectors. *Hum Gene Ther,* 22, 1143-53.

GREENBERG, S. G. & DAVIES, P. 1990. A preparation of Alzheimer paired helical filaments that displays distinct tau proteins by polyacrylamide gel electrophoresis. *Proc Natl Acad Sci U S A,* 87, 5827-31.

GREER, P. L. & GREENBERG, M. E. 2008. From synapse to nucleus: calcium-dependent gene transcription in the control of synapse development and function. *Neuron,* 59, 846-60.

GROC, L., HEINE, M., COUSINS, S. L., STEPHENSON, F. A., LOUNIS, B., COGNET, L. & CHOQUET, D. 2006. NMDA receptor surface mobility depends on NR2A-2B subunits. *Proc Natl Acad Sci U S A,* 103, 18769-74.

GROSSHANS, D. R., CLAYTON, D. A., COULTRAP, S. J. & BROWNING, M. D. 2002. LTP leads to rapid surface expression of NMDA but not AMPA receptors in adult rat CA1. *Nat Neurosci,* 5, 27-33.

GU, J., XU, W., JIN, N., LI, L., ZHOU, Y., CHU, D., GONG, C. X., IQBAL, K. & LIU, F. 2020. Truncation of Tau selectively facilitates its pathological activities. *J Biol Chem,* 295, 13812-13828.

GU, Z., LIU, W. & YAN, Z. 2009. β-Amyloid impairs AMPA receptor trafficking and function by reducing Ca2+/calmodulin-dependent protein kinase II synaptic distribution. *J Biol Chem,* 284, 10639-49.

GUNTUPALLI, S., JANG, S. E., ZHU, T., HUGANIR, R. L., WIDAGDO, J. & ANGGONO, V. 2017. GluA1 subunit ubiquitination mediates amyloid-β-induced loss of surface α-amino-3-hydroxy-5-methyl-4-isoxazolepropionic acid (AMPA) receptors. *J Biol Chem,* 292, 8186-8194.

HAN, J., LI, E., CHEN, L., ZHANG, Y., WEI, F., LIU, J., DENG, H. & WANG, Y. 2015. The CREB coactivator CRTC2 controls hepatic lipid metabolism by regulating SREBP1. *Nature,* 524, 243-6.

HANAKI, R., ABE, N., FUJII, T., UENO, A., NISHIO, Y., HIRAOKA, K., SHIMOMURA, T., IIZUKA, O., SHINOHARA, M., HIRAYAMA, K. & MORI, E. 2011. The effects of aging and Alzheimer's disease on associative recognition memory. *Neurol Sci,* 32, 1115-22.

HANSEN, M., RUBINSZTEIN, D. C. & WALKER, D. W. 2018. Autophagy as a promoter of longevity: insights from model organisms. *Nat Rev Mol Cell Biol,* 19, 579-593.

HARA, T., NAKAMURA, K., MATSUI, M., YAMAMOTO, A., NAKAHARA, Y., SUZUKI-MIGISHIMA, R., YOKOYAMA, M., MISHIMA, K., SAITO, I., OKANO, H. & MIZUSHIMA, N. 2006. Suppression of basal autophagy in neural cells causes neurodegenerative disease in mice. *Nature,* 441, 885-9.

HARDINGHAM, G. E. 2006. Pro-survival signalling from the NMDA receptor. *Biochem Soc Trans,* 34, 936-8.

HARDINGHAM, G. E., FUKUNAGA, Y. & BADING, H. 2002. Extrasynaptic NMDARs oppose synaptic NMDARs by triggering CREB shut-off and cell death pathways. *Nat Neurosci,* 5, 405-14.

HARNEY, S. C., JANE, D. E. & ANWYL, R. 2008. Extrasynaptic NR2D-containing NMDARs are recruited to the synapse during LTP of NMDAR-EPSCs. *J Neurosci,* 28, 11685-94.

HAYASHI, Y., SHI, S. H., ESTEBAN, J. A., PICCINI, A., PONCER, J. C. & MALINOW, R. 2000. Driving AMPA receptors into synapses by LTP and CaMKII: requirement for GluR1 and PDZ domain interaction. *Science,* 287, 2262-7.

HEBB, D. 1949. *The organization of behavior: a neuropsychological theory.* New York, Wiley.

HENLEY, J. M. & WILKINSON, K. A. 2013. AMPA receptor trafficking and the mechanisms underlying synaptic plasticity and cognitive aging. *Dialogues Clin Neurosci,* 15, 11-27.

HIPP, M. S., KASTURI, P. & HARTL, F. U. 2019. The proteostasis network and its decline in ageing. *Nat Rev Mol Cell Biol,* 20, 421-435.

HIRANO, Y., MASUDA, T., NAGANOS, S., MATSUNO, M., UENO, K., MIYASHITA, T., HORIUCHI, J. & SAITOE, M. 2013. Fasting launches CRTC to facilitate long-term memory formation in Drosophila. *Science,* 339, 443-6.

HOLLENBECK, P. J. 1993. Products of endocytosis and autophagy are retrieved from axons by regulated retrograde organelle transport. *J Cell Biol,* 121, 305-15.

HOLT, C. E., MARTIN, K. C. & SCHUMAN, E. M. 2019. Local translation in neurons: visualization and function. *Nat Struct Mol Biol,* 26, 557-566.

HOOVER, B. R., REED, M. N., SU, J., PENROD, R. D., KOTILINEK, L. A., GRANT, M. K., PITSTICK, R., CARLSON, G. A., LANIER, L. M., YUAN, L. L., ASHE, K. H. & LIAO, D. 2010. Tau mislocalization to dendritic spines mediates synaptic dysfunction independently of neurodegeneration. *Neuron,* 68, 1067-81.

HORAK, M. & WENTHOLD, R. J. 2009. Different roles of C-terminal cassettes in the trafficking of full-length NR1 subunits to the cell surface. *J Biol Chem,* 284, 9683-91.

HSIEH, H., BOEHM, J., SATO, C., IWATSUBO, T., TOMITA, T., SISODIA, S. & MALINOW, R. 2006. AMPAR removal underlies Abeta-induced synaptic depression and dendritic spine loss. *Neuron,* 52, 831-43.

HUBER, K. M., KAYSER, M. S. & BEAR, M. F. 2000. Role for rapid dendritic protein synthesis in hippocampal mGluR-dependent long-term depression. *Science,* 288, 1254-7.

HUNG, C. O. Y. & LIVESEY, F. J. 2018. Altered γ-secretase processing of APP disrupts lysosome and autophagosome function in monogenic Alzheimer's disease. *Cell Rep,* 25, 3647-3660.e2.

HYMAN, B. T., PHELPS, C. H., BEACH, T. G., BIGIO, E. H., CAIRNS, N. J., CARRILLO, M. C., DICKSON, D. W., DUYCKAERTS, C., FROSCH, M. P., MASLIAH, E., MIRRA, S. S., NELSON, P. T., SCHNEIDER, J. A., THAL, D. R., THIES, B., TROJANOWSKI, J. Q., VINTERS, H. V. & MONTINE, T. J. 2012. National Institute on Aging-Alzheimer's Association guidelines for the neuropathologic assessment of Alzheimer's disease. *Alzheimers Dement,* 8, 1-13.

HYMAN, B. T., VAN HOESEN, G. W., DAMASIO, A. R. & BARNES, C. L. 1984. Alzheimer's disease: cell-specific pathology isolates the hippocampal formation. *Science,* 225, 1168-70.

HYND, M. R., SCOTT, H. L. & DODD, P. R. 2001. Glutamate(NMDA) receptor NR1 subunit mRNA expression in Alzheimer's disease. *J Neurochem,* 78, 175-82.

IACOBUCCI, G. J. & POPESCU, G. K. 2019. Spatial coupling tunes NMDA receptor responses via Ca^{2+} diffusion. *J Neurosci,* 39, 8831-8844.

IMPEY, S., MCCORKLE, S. R., CHA-MOLSTAD, H., DWYER, J. M., YOCHUM, G. S., BOSS, J. M., MCWEENEY, S., DUNN, J. J., MANDEL, G. & GOODMAN, R. H. 2004. Defining the CREB regulon: a genome-wide analysis of transcription factor regulatory regions. *Cell,* 119, 1041-54.

JACKSON, J. S., WITTON, J., JOHNSON, J. D., AHMED, Z., WARD, M., RANDALL, A. D., HUTTON, M. L., ISAAC, J. T., O'NEILL, M. J. & ASHBY, M. C. 2017. Altered synapse stability in the early stages of tauopathy. *Cell Rep,* 18, 3063-3068.

JAGANNATH, A., BUTLER, R., GODINHO, S. I. H., COUCH, Y., BROWN, L. A., VASUDEVAN, S. R., FLANAGAN, K. C., ANTHONY, D., CHURCHILL, G. C., WOOD, M. J. A., STEINER, G., EBELING, M., HOSSBACH, M., WETTSTEIN, J. G., DUFFIELD, G. E., GATTI, S., HANKINS, M. W., FOSTER, R. G. & PEIRSON, S. N. 2013. The CRTC1-SIK1 pathway regulates entrainment of the circadian clock. *Cell,* 154, 1100-1111.

JEONG, H., COHEN, D. E., CUI, L., SUPINSKI, A., SAVAS, J. N., MAZZULLI, J. R., YATES, J. R., BORDONE, L., GUARENTE, L. & KRAINC, D. 2011. Sirt1 mediates neuroprotection from mutant huntingtin by activation of the TORC1 and CREB transcriptional pathway. *Nat Med,* 18, 159-65.

JI, C., TANG, M., ZEIDLER, C., HÖHFELD, J. & JOHNSON, G. V. 2019. BAG3 and SYNPO (synaptopodin) facilitate phospho-MAPT/Tau degradation via autophagy in neuronal processes. *Autophagy,* 15, 1199-1213.

JIANG, M. & CHEN, G. 2006. High Ca2+-phosphate transfection efficiency in low-density neuronal cultures. *Nat Protoc,* 1, 695-700.

JORDAN, B. A. & KREUTZ, M. R. 2009. Nucleocytoplasmic protein shuttling: the direct route in synapse-to-nucleus signaling. *Trends Neurosci,* 32, 392-401.

JOSSELYN, S. A., SHI, C., CARLEZON, W. A., NEVE, R. L., NESTLER, E. J. & DAVIS, M. 2001. Long-term memory is facilitated by cAMP response element-binding protein overexpression in the amygdala. *J Neurosci,* 21, 2404-12.

KALLERGI, E., DASKALAKI, A. D., KOLAXI, A., CAMUS, C., IOANNOU, E., MERCALDO, V., HABERKANT, P., STEIN, F., SIDIROPOULOU, K., DALEZIOS, Y., SAVITSKI, M. M., BAGNI, C., CHOQUET, D., HOSY, E. & NIKOLETOPOULOU, V. 2022. Dendritic autophagy degrades postsynaptic proteins and is required for long-term synaptic depression in mice. *Nat Commun,* 13, 680.

KANDEL, E. R. 2001. The molecular biology of memory storage: a dialog between genes and synapses. *Biosci Rep,* 21, 565-611.

KANNO, H., HANDA, K., MURAKAMI, T., AIZAWA, T. & OZAWA, H. 2022. Chaperone-Mediated Autophagy in neurodegenerative diseases and acute neurological insults in the central nervous system. *Cells,* 11. 1205.

KATSUMATA, K., NISHIYAMA, J., INOUE, T., MIZUSHIMA, N., TAKEDA, J. & YUZAKI, M. 2010. Dynein- and activity-dependent retrograde transport of autophagosomes in neuronal axons. *Autophagy,* 6, 378-85.

KAUSHIK, R., GROCHOWSKA, K. M., BUTNARU, I. & KREUTZ, M. R. 2014. Protein trafficking from synapse to nucleus in control of activity-dependent gene expression. *Neuroscience,* 280, 340-50.

KECK, S., NITSCH, R., GRUNE, T. & ULLRICH, O. 2003. Proteasome inhibition by paired helical filament-tau in brains of patients with Alzheimer's disease. *J Neurochem,* 85, 115-22.

KEE, B. L., ARIAS, J. & MONTMINY, M. R. 1996. Adaptor-mediated recruitment of RNA polymerase II to a signal-dependent activator. *J Biol Chem,* 271, 2373-5.

KELLER, J. N., HANNI, K. B. & MARKESBERY, W. R. 2000. Impaired proteasome function in Alzheimer's disease. *J Neurochem,* 75, 436-9.

KIDA, S., JOSSELYN, S. A., PEÑA DE ORTIZ, S., KOGAN, J. H., CHEVERE, I., MASUSHIGE, S. & SILVA, A. J. 2002. CREB required for the stability of new and reactivated fear memories. *Nat Neurosci,* 5, 348-55.

KIM, E. C., LEE, M. J., SHIN, S. Y., SEOL, G. H., HAN, S. H., YEE, J., KIM, C. & MIN, S. S. 2013. Phorbol 12-Myristate 13-Acetate enhances long-term potentiation in the hippocampus through activation of protein kinase Cδ and ε. *Korean J Physiol Pharmacol,* 17, 51-6.

KIM, M., LEE, H., HUR, J. H., CHOE, J. & LIM, C. 2016. CRTC Potentiates light-independent timeless transcription to sustain circadian rhythms in Drosophila. *Sci Rep,* 6, 32113.

KIM, M. J., FUTAI, K., JO, J., HAYASHI, Y., CHO, K. & SHENG, M. 2007. Synaptic accumulation of PSD-95 and synaptic function regulated by phosphorylation of serine-295 of PSD-95. *Neuron,* 56, 488-502.

KIMURA, S., NODA, T. & YOSHIMORI, T. 2008. Dynein-dependent movement of autophagosomes mediates efficient encounters with lysosomes. *Cell Struct Funct,* 33, 109-22.

KOCH, G., DI LORENZO, F., DEL OLMO, M. F., BONNÍ, S., PONZO, V., CALTAGIRONE, C., BOZZALI, M. & MARTORANA, A. 2016. Reversal of LTP-like cortical plasticity in Alzheimer's disease patients with tau-related faster clinical progression. *J Alzheimers Dis,* 50, 605-16.

KOMATSU, M., WAGURI, S., CHIBA, T., MURATA, S., IWATA, J., TANIDA, I., UENO, T., KOIKE, M., UCHIYAMA, Y., KOMINAMI, E. & TANAKA, K. 2006. Loss of autophagy in the central nervous system causes neurodegeneration in mice. *Nature,* 441, 880-4.

KOURI, N., WHITWELL, J. L., JOSEPHS, K. A., RADEMAKERS, R. & DICKSON, D. W. 2011. Corticobasal degeneration: a pathologically distinct 4R tauopathy. *Nat Rev Neurol,* 7, 263-72.

KOVACS, K. A., STEULLET, P., STEINMANN, M., DO, K. Q., MAGISTRETTI, P. J., HALFON, O. & CARDINAUX, J. R. 2007. TORC1 is a calcium- and cAMP-sensitive coincidence detector involved in hippocampal long-term synaptic plasticity. *Proc Natl Acad Sci U S A,* 104, 4700-5.

KRISTENSEN, A. S., JENKINS, M. A., BANKE, T. G., SCHOUSBOE, A., MAKINO, Y., JOHNSON, R. C., HUGANIR, R. & TRAYNELIS, S. F. 2011. Mechanism of Ca2+/calmodulin-dependent kinase II regulation of AMPA receptor gating. *Nat Neurosci,* 14, 727-35.

KSIEZAK-REDING, H., MORGAN, K., MATTIACE, L. A., DAVIES, P., LIU, W. K., YEN, S. H., WEIDENHEIM, K. & DICKSON, D. W. 1994. Ultrastructure and biochemical composition of paired helical filaments in corticobasal degeneration. *Am J Pathol,* 145, 1496-508.

KUDO, K., WATI, H., QIAO, C., ARITA, J. & KANBA, S. 2005. Age-related disturbance of memory and CREB phosphorylation in CA1 area of hippocampus of rats. *Brain Res,* 1054, 30-7.

KULKARNI, V. V., ANAND, A., HERR, J. B., MIRANDA, C., VOGEL, M. C. & MADAY, S. 2021. Synaptic activity controls autophagic vacuole motility and function in dendrites. *J Cell Biol,* 220, 6.

KWON, H. B. & CASTILLO, P. E. 2008. Long-term potentiation selectively expressed by NMDA receptors at hippocampal mossy fiber synapses. *Neuron,* 57, 108-20.

LAN, J. Y., SKEBERDIS, V. A., JOVER, T., GROOMS, S. Y., LIN, Y., ARANEDA, R. C., ZHENG, X., BENNETT, M. V. & ZUKIN, R. S. 2001. Protein kinase C modulates NMDA receptor trafficking and gating. *Nat Neurosci,* 4, 382-90.

LASAGNA-REEVES, C. A., CASTILLO-CARRANZA, D. L., GUERRERO-MUOZ, M. J., JACKSON, G. R. & KAYED, R. 2010. Preparation and characterization of neurotoxic tau oligomers. *Biochemistry,* 49, 10039-41.

LAURIE, D. J. & SEEBURG, P. H. 1994. Regional and developmental heterogeneity in splicing of the rat brain NMDAR1 mRNA. *J Neurosci,* 14, 3180-94.

LAVEZZARI, G., MCCALLUM, J., DEWEY, C. M. & ROCHE, K. W. 2004. Subunit-specific regulation of NMDA receptor endocytosis. *J Neurosci,* 24, 6383-91.

LAZAROV, O. & HOLLANDS, C. 2016. Hippocampal neurogenesis: Learning to remember. *Prog Neurobiol,* 138-140, 1-18.

LEE, H. K. 2006. AMPA receptor phosphorylation in synaptic plasticity: insights from knockin mice. *In:* KITTLER, J. T. & MOSS, S. J. (eds.). *The dynamic synapse: molecular methods in ionotropic receptor biology.* Boca Raton (FL): CRC Press/Taylor & Francis. Taylor & Francis Group, LLC, 14.

LEE, J. A., BEIGNEUX, A., AHMAD, S. T., YOUNG, S. G. & GAO, F. B. 2007. ESCRT-III dysfunction causes autophagosome accumulation and neurodegeneration. *Curr Biol,* 17, 1561-7.

LEE, J. H., YU, W. H., KUMAR, A., LEE, S., MOHAN, P. S., PETERHOFF, C. M., WOLFE, D. M., MARTINEZ-VICENTE, M., MASSEY, A. C., SOVAK, G., UCHIYAMA, Y., WESTAWAY, D., CUERVO, A. M. & NIXON, R. A. 2010. Lysosomal proteolysis and autophagy require presenilin 1 and are disrupted by Alzheimer-related PS1 mutations. *Cell,* 141, 1146-58.

LEE, S., SATO, Y. & NIXON, R. A. 2011. Lysosomal proteolysis inhibition selectively disrupts axonal transport of degradative organelles and causes an Alzheimer's-like axonal dystrophy. *J Neurosci,* 31, 7817-30.

LEE, V. M., BALIN, B. J., OTVOS, L. & TROJANOWSKI, J. Q. 1991. A68: a major subunit of paired helical filaments and derivatized forms of normal Tau. *Science,* 251, 675-8.

LEE, V. M., GOEDERT, M. & TROJANOWSKI, J. Q. 2001. Neurodegenerative tauopathies. *Annu Rev Neurosci,* 24, 1121-59.

LEVINE, B. & KROEMER, G. 2008. Autophagy in the pathogenesis of disease. *Cell,* 132, 27-42.

LI, L., KIM, H. J., ROH, J. H., KIM, M., KOH, W., KIM, Y., HEO, H., CHUNG, J., NAKANISHI, M., YOON, T., HONG, C. P., SEO, S. W., NA, D. L. & SONG, J. 2020. Pathological manifestation of the induced pluripotent stem cell-derived cortical neurons from an early-onset Alzheimer's disease patient carrying a presenilin-1 mutation (S170F). *Cell Prolif,* 53, e12798.

LI, S., JIN, M., KOEGLSPERGER, T., SHEPARDSON, N. E., SHANKAR, G. M. & SELKOE, D. J. 2011a. Soluble Aβ oligomers inhibit long-term potentiation through a mechanism involving excessive activation of extrasynaptic NR2B-containing NMDA receptors. *J Neurosci,* 31, 6627-38.

LI, S., ZHANG, C., TAKEMORI, H., ZHOU, Y. & XIONG, Z. Q. 2009. TORC1 regulates activity-dependent CREB-target gene transcription and dendritic growth of developing cortical neurons. *J Neurosci,* 29, 2334-43.

LI, X., COYLE, D., MAGUIRE, L., WATSON, D. R. & MCGINNITY, T. M. 2011b. Gray matter concentration and effective connectivity changes in Alzheimer's disease: a longitudinal structural MRI study. *Neuroradiology,* 53, 733-48.

LI, X. G., HONG, X. Y., WANG, Y. L., ZHANG, S. J., ZHANG, J. F., LI, X. C., LIU, Y. C., SUN, D. S., FENG, Q., YE, J. W., GAO, Y., KE, D., WANG, Q., LI, H. L., YE, K., LIU, G. P. & WANG, J. Z. 2019. Tau accumulation triggers STAT1-dependent memory deficits by suppressing NMDA receptor expression. *EMBO Rep,* 20.

LIANG, Y., LIU, Y., HOU, B., ZHANG, W., LIU, M., SUN, Y. E., MA, Z. & GU, X. 2016. CREB-regulated transcription coactivator 1 enhances CREB-dependent gene expression in spinal cord to maintain the bone cancer pain in mice. *Mol Pain,* 12.

LIANG, Z., LIU, F., GRUNDKE-IQBAL, I., IQBAL, K. & GONG, C. X. 2007. Down-regulation of cAMP-dependent protein kinase by over-activated calpain in Alzheimer disease brain. *J Neurochem,* 103, 2462-70.

LIE, P. P. Y., YANG, D. S., STAVRIDES, P., GOULBOURNE, C. N., ZHENG, P., MOHAN, P. S., CATALDO, A. M. & NIXON, R. A. 2021. Post-Golgi carriers, not lysosomes, confer lysosomal properties to pre-degradative organelles in normal and dystrophic axons. *Cell Rep,* 35, 109034.

LIE, P. P. Y., YOO, L., GOULBOURNE, C. N., BERG, M. J., STAVRIDES, P., HUO, C., LEE, J. H. & NIXON, R. A. 2022. Axonal transport of late endosomes and amphisomes is selectively modulated by local Ca^{2+} efflux and disrupted by PSEN1 loss of function. *Sci Adv,* 8, eabj5716.

LIN, Y., JOVER-MENGUAL, T., WONG, J., BENNETT, M. V. & ZUKIN, R. S. 2006. PSD-95 and PKC converge in regulating NMDA receptor trafficking and gating. *Proc Natl Acad Sci U S A,* 103, 19902-7.

LIN, Y., SKEBERDIS, V. A., FRANCESCONI, A., BENNETT, M. V. & ZUKIN, R. S. 2004. Postsynaptic density protein-95 regulates NMDA channel gating and surface expression. *J Neurosci,* 24, 10138-48.

LIU, H. P., LIN, W. Y., LIU, S. H., WANG, W. F., TSAI, C. H., WU, B. T., WANG, C. K. & TSAI, F. J. 2009. Genetic variation in N-methyl-D-aspartate receptor subunit NR3A but not NR3B influences susceptibility to Alzheimer's disease. *Dement Geriatr Cogn Disord,* 28, 521-7.

LOERCH, P. M., LU, T., DAKIN, K. A., VANN, J. M., ISAACS, A., GEULA, C., WANG, J., PAN, Y., GABUZDA, D. H., LI, C., PROLLA, T. A. & YANKNER, B. A. 2008. Evolution of the aging brain transcriptome and synaptic regulation. *PLoS One,* 3, e3329.

LU, Q., HUTCHINS, A. E., DOYLE, C. M., LUNDBLAD, J. R. & KWOK, R. P. 2003. Acetylation of cAMP-responsive element-binding protein (CREB) by CREB-binding protein enhances CREB-dependent transcription. *J Biol Chem,* 278, 15727-34.

LU, W., SHI, Y., JACKSON, A. C., BJORGAN, K., DURING, M. J., SPRENGEL, R., SEEBURG, P. H. & NICOLL, R. A. 2009. Subunit composition of synaptic AMPA receptors revealed by a single-cell genetic approach. *Neuron,* 62, 254-68.

LYNCH, M. A. 2004. Long-term potentiation and memory. *Physiol Rev,* 84, 87-136.

MA, Q. L., HARRIS-WHITE, M. E., UBEDA, O. J., SIMMONS, M., BEECH, W., LIM, G. P., TETER, B., FRAUTSCHY, S. A. & COLE, G. M. 2007. Evidence of Abeta- and transgene-dependent defects in ERK-CREB signaling in Alzheimer's models. *J Neurochem,* 103, 1594-607.

MADAY, S. & HOLZBAUR, E. L. 2016. Compartment-specific regulation of autophagy in primary neurons. *J Neurosci,* 36, 5933-45.

MAGNUSSON, K. R. 2000. Declines in mRNA expression of different subunits may account for differential effects of aging on agonist and antagonist binding to the NMDA receptor. *J Neurosci,* 20, 1666-74.

MAGNUSSON, K. R., BRIM, B. L. & DAS, S. R. 2010. Selective vulnerabilities of N-methyl-D-aspartate (NMDA) receptors during brain aging. *Front Aging Neurosci,* 2, 11.

MAGNUSSON, K. R., NELSON, S. E. & YOUNG, A. B. 2002. Age-related changes in the protein expression of subunits of the NMDA receptor. *Brain Res Mol Brain Res,* 99, 40-5.

MALENKA, R. C. & BEAR, M. F. 2004. LTP and LTD: an embarrassment of riches. *Neuron,* 44, 5-21.

MALENKA, R. C. & NICOLL, R. A. 1999. Long-term potentiation--a decade of progress? *Science,* 285, 1870-4.

MAMMEN, A. L., KAMEYAMA, K., ROCHE, K. W. & HUGANIR, R. L. 1997. Phosphorylation of the alpha-amino-3-hydroxy-5-methylisoxazole4-propionic acid receptor GluR1 subunit by calcium/calmodulin-dependent kinase II. *J Biol Chem,* 272, 32528-33.

MARKRAM, H., HELM, P. J. & SAKMANN, B. 1995. Dendritic calcium transients evoked by single back-propagating action potentials in rat neocortical pyramidal neurons. *J Physiol,* 485 (Pt 1), 1-20.

MARTIN, S. J., DE HOZ, L. & MORRIS, R. G. 2005. Retrograde amnesia: neither partial nor complete hippocampal lesions in rats result in preferential sparing of remote spatial memory, even after reminding. *Neuropsychologia,* 43, 609-24.

MATOS, M. R., VISSER, E., KRAMVIS, I., VAN DER LOO, R. J., GEBUIS, T., ZALM, R., RAO-RUIZ, P., MANSVELDER, H. D., SMIT, A. B. & VAN DEN OEVER, M. C. 2019. Memory strength gates the involvement of a CREB-dependent cortical fear engram in remote memory. *Nat Commun,* 10, 2315.

MATSUMOTO, S. E., MOTOI, Y., ISHIGURO, K., TABIRA, T., KAMETANI, F., HASEGAWA, M. & HATTORI, N. 2015. The twenty-four KDa C-terminal tau fragment increases with aging in tauopathy mice: implications of prion-like properties. *Hum Mol Genet,* 24, 6403-16.

MATSUMURA, S., ISHIKAWA, F., SASAKI, T., TERKELSEN, M. K., RAVNSKJAER, K., JINNO, T., TANAKA, J., GOTO, T. & INOUE, K. 2021. Loss of CREB coactivator CRTC1 in SF1 cells leads to hyperphagia and obesity by high-fat diet but not normal chow diet. *Endocrinology,* 162, 9

MATSUO, N., REIJMERS, L. & MAYFORD, M. 2008. Spine-type-specific recruitment of newly synthesized AMPA receptors with learning. *Science,* 319, 1104-7.

MAUTHE, M., ORHON, I., ROCCHI, C., ZHOU, X., LUHR, M., HIJLKEMA, K. J., COPPES, R. P., ENGEDAL, N., MARI, M. & REGGIORI, F. 2018. Chloroquine inhibits autophagic flux by decreasing autophagosome-lysosome fusion. *Autophagy,* 14, 1435-1455.

MCILHINNEY, R. A., LE BOURDELLÈS, B., MOLNÁR, E., TRICAUD, N., STREIT, P. & WHITING, P. J. 1998. Assembly intracellular targeting and cell surface expression of the human N-methyl-D-aspartate receptor subunits NR1a and NR2A in transfected cells. *Neuropharmacology,* 37, 1355-67.

MEER, E. J., WANG, D. O., KIM, S., BARR, I., GUO, F. & MARTIN, K. C. 2012. Identification of a cis-acting element that localizes mRNA to synapses. *Proc Natl Acad Sci U S A,* 109, 4639-44.

MEIER, S., BELL, M., LYONS, D. N., RODRIGUEZ-RIVERA, J., INGRAM, A., FONTAINE, S. N., MECHAS, E., CHEN, J., WOLOZIN, B., LEVINE, H., ZHU, H. & ABISAMBRA, J. F. 2016. Pathological tau promotes neuronal damage by impairing ribosomal function and decreasing protein synthesis. *J Neurosci,* 36, 1001-7.

MEJÍA-GUERRA, M. K. & LAREO, L. R. 2005. In silico identification of regulatory elements of GRIN1 genes. *OMICS,* 9, 106-15.

MENDIOROZ, M., CELARAIN, N., ALTUNA, M., SÁNCHEZ-RUIZ DE GORDOA, J., ZELAYA, M. V., ROLDÁN, M., RUBIO, I., LARUMBE, R., ERRO, M. E., MÉNDEZ, I. & ECHÁVARRI, C. 2016. CRTC1 gene is differentially methylated in the human hippocampus in Alzheimer's disease. *Alzheimers Res Ther,* 8, 15.

MERKURJEV, D., HONG, W. T., IIDA, K., OOMOTO, I., GOLDIE, B. J., YAMAGUTI, H., OHARA, T., KAWAGUCHI, S. Y., HIRANO, T., MARTIN, K. C., PELLEGRINI, M. & WANG, D. O. 2018. Synaptic N(6)-methyladenosine (m(6)A) epitranscriptome reveals functional partitioning of localized transcripts. *Nat Neurosci,* 21, 1004-1014.

MILLER, S., YASUDA, M., COATS, J. K., JONES, Y., MARTONE, M. E. & MAYFORD, M. 2002. Disruption of dendritic translation of CaMKIIalpha impairs stabilization of synaptic plasticity and memory consolidation. *Neuron,* 36, 507-19.

MIÑANO-MOLINA, A. J., ESPAÑA, J., MARTÍN, E., BARNEDA-ZAHONERO, B., FADÓ, R., SOLÉ, M., TRULLÁS, R., SAURA, C. A. & RODRÍGUEZ-ALVAREZ, J. 2011. Soluble oligomers of amyloid-β peptide disrupt membrane trafficking of α-amino-3-hydroxy-5-methylisoxazole-4-propionic acid receptor contributing to early synapse dysfunction. *J Biol Chem,* 286, 27311-21.

MIZUSHIMA, N., YOSHIMORI, T. & LEVINE, B. 2010. Methods in mammalian autophagy research. *Cell,* 140, 313-26.

MONYER, H., BURNASHEV, N., LAURIE, D. J., SAKMANN, B. & SEEBURG, P. H. 1994. Developmental and regional expression in the rat brain and functional properties of four NMDA receptors. *Neuron,* 12, 529-40.

MORABITO, M. A., SHENG, M. & TSAI, L. H. 2004. Cyclin-dependent kinase 5 phosphorylates the N-terminal domain of the postsynaptic density protein PSD-95 in neurons. *J Neurosci,* 24, 865-76.

MORRIS, R. G. M., ANDERSON, E., LYNCH, G. S. & BAUDRY, M. 1986. Selective impairment of learning and blockade of long-term potentiation by an N-methyl-D-aspartate receptor antagonist, AP5. *Nature,* 319, 774-776.

MUKHERJEE, S. & MANAHAN-VAUGHAN, D. 2013. Role of metabotropic glutamate receptors in persistent forms of hippocampal plasticity and learning. *Neuropharmacology,* 66, 65-81.

MURAYAMA, S., MORI, H., IHARA, Y. & TOMONAGA, M. 1990. Immunocytochemical and ultrastructural studies of Pick's disease. *Ann Neurol,* 27, 394-405.

MURPHY, T. H., WORLEY, P. F. & BARABAN, J. M. 1991. L-type voltage-sensitive calcium channels mediate synaptic activation of immediate early genes. *Neuron,* 7, 625-35.

MURRAY, M. E., KOURI, N., LIN, W. L., JACK, C. R., DICKSON, D. W. & VEMURI, P. 2014. Clinicopathologic assessment and imaging of tauopathies in neurodegenerative dementias. *Alzheimers Res Ther,* 6, 1.

NA, Y., PARK, S., LEE, C., KIM, D. K., PARK, J. M., SOCKANATHAN, S., HUGANIR, R. L. & WORLEY, P. F. 2016. Real-time imaging reveals properties of glutamate-induced Arc/Arg 3.1 translation in neuronal dendrites. *Neuron,* 91, 561-73.

NEELY, K. M., GREEN, K. N. & LAFERLA, F. M. 2011. Presenilin is necessary for efficient proteolysis through the autophagy-lysosome system in a γ-secretase-independent manner. *J Neurosci,* 31, 2781-91.

NELSON, C. D., KIM, M. J., HSIN, H., CHEN, Y. & SHENG, M. 2013. Phosphorylation of threonine-19 of PSD-95 by GSK-3β is required for PSD-95 mobilization and long-term depression. *J Neurosci,* 33, 12122-35.

NEVES, G., COOKE, S. F. & BLISS, T. V. 2008. Synaptic plasticity, memory and the hippocampus: a neural network approach to causality. *Nat Rev Neurosci,* 9, 65-75.

NI, S., HUANG, H., HE, D., CHEN, H., WANG, C., ZHAO, X., CHEN, X., CUI, W., ZHOU, W. & ZHANG, J. 2019. Adeno-associated virus-mediated over-expression of CREB-regulated transcription coactivator 1 in the hippocampal dentate gyrus ameliorates lipopolysaccharide-induced depression-like behaviour in mice. *J Neurochem,* 149, 111-125.

NICOLL, R. A., KAUER, J. A. & MALENKA, R. C. 1988. The current excitement in long-term potentiation. *Neuron,* 1, 97-103.

NIKOLETOPOULOU, V., SIDIROPOULOU, K., KALLERGI, E., DALEZIOS, Y. & TAVERNARAKIS, N. 2017. Modulation of autophagy by BDNF underlies synaptic plasticity. *Cell Metab,* 26, 230-242.e5.

NIXON, R. A., WEGIEL, J., KUMAR, A., YU, W. H., PETERHOFF, C., CATALDO, A. & CUERVO, A. M. 2005. Extensive involvement of autophagy in Alzheimer disease: an immuno-electron microscopy study. *J Neuropathol Exp Neurol,* 64, 113-22.

NONAKA, M., KIM, R., FUKUSHIMA, H., SASAKI, K., SUZUKI, K., OKAMURA, M., ISHII, Y., KAWASHIMA, T., KAMIJO, S., TAKEMOTO-KIMURA, S., OKUNO, H., KIDA, S. & BITO, H. 2014. Region-specific activation of CRTC1-CREB signaling mediates long-term fear memory. *Neuron,* 84, 92-106.

NOWAK, L., BREGESTOVSKI, P., ASCHER, P., HERBET, A. & PROCHIANTZ, A. 1984. Magnesium gates glutamate-activated channels in mouse central neurones. *Nature,* 307, 462-5.

OEDEKOVEN, C. S., JANSEN, A., KEIDEL, J. L., KIRCHER, T. & LEUBE, D. 2015. The influence of age and mild cognitive impairment on associative memory performance and underlying brain networks. *Brain Imaging Behav,* 9, 776-89.

OGRYZKO, V. V., SCHILTZ, R. L., RUSSANOVA, V., HOWARD, B. H. & NAKATANI, Y. 1996. The transcriptional coactivators p300 and CBP are histone acetyltransferases. *Cell,* 87, 953-9.

ONTL, T., XING, Y., BAI, L., KENNEDY, E., NELSON, S., WAKEMAN, M. & MAGNUSSON, K. 2004. Development and aging of N-methyl-D-aspartate receptor expression in the prefrontal/frontal cortex of mice. *Neuroscience,* 123, 467-79.

OSTROFF, L. E., FIALA, J. C., ALLWARDT, B. & HARRIS, K. M. 2002. Polyribosomes redistribute from dendritic shafts into spines with enlarged synapses during LTP in developing rat hippocampal slices. *Neuron,* 35, 535-45.

OSTROFF, L. E., WATSON, D. J., CAO, G., PARKER, P. H., SMITH, H. & HARRIS, K. M. 2018. Shifting patterns of polyribosome accumulation at synapses over the course of hippocampal long-term potentiation. *Hippocampus,* 28, 416-430.

PACHERNEGG, S., STRUTZ-SEEBOHM, N. & HOLLMANN, M. 2012. GluN3 subunit-containing NMDA receptors: not just one-trick ponies. *Trends Neurosci,* 35, 240-9.

PAN, Y., HE, X., LI, C., LI, Y., LI, W., ZHANG, H., WANG, Y., ZHOU, G., YANG, J., LI, J., QU, J., WANG, H., GAO, Z., SHEN, Y., LI, T., HU, H. & MA, H. 2021. Neuronal activity recruits the CRTC1/CREB axis to drive transcription-dependent autophagy for maintaining late-phase LTD. *Cell Rep,* 36, 109398.

PANG, Z. P. & SÜDHOF, T. C. 2010. Cell biology of Ca2+-triggered exocytosis. *Curr Opin Cell Biol,* 22, 496-505.

PAOLETTI, P. 2011. Molecular basis of NMDA receptor functional diversity. *Eur J Neurosci,* 33, 1351-65.

PAOLETTI, P., BELLONE, C. & ZHOU, Q. 2013. NMDA receptor subunit diversity: impact on receptor properties, synaptic plasticity and disease. *Nat Rev Neurosci,* 14, 383-400.

PARRA-DAMAS, A., CHEN, M., ENRIQUEZ-BARRETO, L., ORTEGA, L., ACOSTA, S., PERNA, J. C., FULLANA, M. N., AGUILERA, J., RODRIGUEZ-ALVAREZ, J. & SAURA, C. A. 2017a. CRTC1 function during memory encoding is disrupted in neurodegeneration. *Biol Psychiatry*, 81, 111-123.

PARRA-DAMAS, A., RUBIÓ-FERRARONS, L., SHEN, J. & SAURA, C. A. 2017b. CRTC1 mediates preferential transcription at neuronal activity-regulated CRE/TATA promoters. *Sci Rep,* 7, 18004.

PARRA-DAMAS, A. & SAURA, C. A. 2019. Synapse-to-nucleus signaling in neurodegenerative and neuropsychiatric disorders. *Biol Psychiatry,* 86, 87-96.

PARRA-DAMAS, A., VALERO, J., CHEN, M., ESPANA, J., MARTIN, E., FERRER, I., RODRIGUEZ-ALVAREZ, J. & SAURA, C. A. 2014. Crtc1 activates a transcriptional program deregulated at early Alzheimer's disease-related stages. *J Neurosci,* 34, 5776-87.

PATTERSON, K. R., REMMERS, C., FU, Y., BROOKER, S., KANAAN, N. M., VANA, L., WARD, S., REYES, J. F., PHILIBERT, K., GLUCKSMAN, M. J. & BINDER, L. I. 2011. Characterization of prefibrillar Tau oligomers in vitro and in Alzheimer disease. *J Biol Chem,* 286, 23063-76.

PENNANEN, C., KIVIPELTO, M., TUOMAINEN, S., HARTIKAINEN, P., HÄNNINEN, T., LAAKSO, M. P., HALLIKAINEN, M., VANHANEN, M., NISSINEN, A., HELKALA, E. L., VAINIO, P., VANNINEN, R., PARTANEN, K. & SOININEN, H. 2004. Hippocampus and entorhinal cortex in mild cognitive impairment and early AD. *Neurobiol Aging,* 25, 303-10.

PORTE, Y., BUHOT, M. C. & MONS, N. 2008. Alteration of CREB phosphorylation and spatial memory deficits in aged 129T2/Sv mice. *Neurobiol Aging,* 29, 1533-46.

PRICE, J. L. & DREVETS, W. C. 2010. Neurocircuitry of mood disorders. *Neuropsychopharmacology,* 35, 192-216.

PROBST, A., TOLNAY, M., LANGUI, D., GOEDERT, M. & SPILLANTINI, M. G. 1996. Pick's disease: hyperphosphorylated tau protein segregates to the somatoaxonal compartment. *Acta Neuropathol,* 92, 588-96.

PRYBYLOWSKI, K., CHANG, K., SANS, N., KAN, L., VICINI, S. & WENTHOLD, R. J. 2005. The synaptic localization of NR2B-containing NMDA receptors is controlled by interactions with PDZ proteins and AP-2. *Neuron,* 47, 845-57.

RAMÓN Y CAJAL, S. 1894. Consideraciones generales sobre la morfología de la célula nerviosa. Madrid, Moya.

REINER, A. & LEVITZ, J. 2018. Glutamatergic signaling in the central nervous system: ionotropic and metabotropic receptors in concert. *Neuron,* 98, 1080-1098.

REXACH, J. E., CLARK, P. M., MASON, D. E., NEVE, R. L., PETERS, E. C. & HSIEH-WILSON, L. C. 2012. Dynamic O-GlcNAc modification regulates CREB-mediated gene expression and memory formation. *Nat Chem Biol,* 8, 253-61.

ROCHE, K. W., O'BRIEN, R. J., MAMMEN, A. L., BERNHARDT, J. & HUGANIR, R. L. 1996. Characterization of multiple phosphorylation sites on the AMPA receptor GluR1 subunit. *Neuron,* 16, 1179-88.

ROCHE, K. W., STANDLEY, S., MCCALLUM, J., DUNE LY, C., EHLERS, M. D. & WENTHOLD, R. J. 2001. Molecular determinants of NMDA receptor internalization. *Nat Neurosci,* 4, 794-802.

RÖNICKE, R., MIKHAYLOVA, M., RÖNICKE, S., MEINHARDT, J., SCHRÖDER, U. H., FÄNDRICH, M., REISER, G., KREUTZ, M. R. & REYMANN, K. G. 2011. Early neuronal dysfunction by amyloid β oligomers depends on activation of NR2B-containing NMDA receptors. *Neurobiol Aging,* 32, 2219-28.

ROSSETTI, C., SCIARRA, D., PETIT, J. M., EAP, C. B., HALFON, O., MAGISTRETTI, P. J., BOUTREL, B. & CARDINAUX, J. R. 2017. Gender-specific alteration of energy balance and circadian

locomotor activity in the Crtc1 knockout mouse model of depression. *Transl Psychiatry,* 7, 1269.

SAKAMOTO, K., NORONA, F. E., ALZATE-CORREA, D., SCARBERRY, D., HOYT, K. R. & OBRIETAN, K. 2013. Clock and light regulation of the CREB coactivator CRTC1 in the suprachiasmatic circadian clock. *J Neurosci,* 33, 9021-7.

SALTER, M. W., DONG, Y., KALIA, L. V., LIU, X. J. & PITCHER, G. 2009. Regulation of NMDA Receptors by Kinases and Phosphatases. *In:* VAN DONGEN, A. M. (ed.). *Biology of the NMDA Receptor.* Boca Raton (FL): CRC Press/Taylor & Francis, 7.

SÁNCHEZ-PÉREZ, A. M. & FELIPO, V. 2005. Serines 890 and 896 of the NMDA receptor subunit NR1 are differentially phosphorylated by protein kinase C isoforms. *Neurochem Int,* 47, 84-91.

SÁNCHEZ-VALLE, R., LLADÓ, A., EZQUERRA, M., REY, M. J., RAMI, L. & MOLINUEVO, J. L. 2007. A novel mutation in the PSEN1 gene (L286P) associated with familial early-onset dementia of Alzheimer type and lobar haematomas. *Eur J Neurol,* 14, 1409-12.

SANTPERE, G., PUIG, B. & FERRER, I. 2006. Low molecular weight species of tau in Alzheimer's disease are dependent on tau phosphorylation sites but not on delayed post-mortem delay in tissue processing. *Neurosci Lett,* 399, 106-10.

SAURA, C. A. & CARDINAUX, J. R. 2017. Emerging roles of CREB-regulated transcription coactivators in brain physiology and pathology. *Trends Neurosci,* 40, 720-733.

SAURA, C. A. & VALERO, J. 2011. The role of CREB signaling in Alzheimer's disease and other cognitive disorders. *Rev Neurosci,* 22, 153-69.

SCANNEVIN, R. H. & HUGANIR, R. L. 2000. Postsynaptic organization and regulation of excitatory synapses. *Nat Rev Neurosci,* 1, 133-41.

SCHEEFHALS, N. & MACGILLAVRY, H. D. 2018. Functional organization of postsynaptic glutamate receptors. *Mol Cell Neurosci,* 91, 82-94.

SCHEFF, S. W., PRICE, D. A., SCHMITT, F. A. & MUFSON, E. J. 2006. Hippocampal synaptic loss in early Alzheimer's disease and mild cognitive impairment. *Neurobiol Aging,* 27, 1372-84.

SCHUCK, S. 2020. Microautophagy - distinct molecular mechanisms handle cargoes of many sizes. *J Cell Sci,* 133.

SCHWENK, J., BAEHRENS, D., HAUPT, A., BILDL, W., BOUDKKAZI, S., ROEPER, J., FAKLER, B. & SCHULTE, U. 2014. Regional diversity and developmental dynamics of the AMPA-receptor proteome in the mammalian brain. *Neuron,* 84, 41-54.

SCOTT, D. B., BLANPIED, T. A. & EHLERS, M. D. 2003. Coordinated PKA and PKC phosphorylation suppresses RXR-mediated ER retention and regulates the surface delivery of NMDA receptors. *Neuropharmacology,* 45, 755-67.

SCOVILLE, W. B. & MILNER, B. 1957. Loss of recent memory after bilateral hippocampal lesions. *J Neurol Neurosurg Psychiatry,* 20, 11-21.

SEKERES, M. J., MERCALDO, V., RICHARDS, B., SARGIN, D., MAHADEVAN, V., WOODIN, M. A., FRANKLAND, P. W. & JOSSELYN, S. A. 2012. Increasing CRTC1 function in the dentate gyrus during memory formation or reactivation increases memory strength without compromising memory quality. *J Neurosci,* 32, 17857-68.

SELKOE, D. J. 2002. Alzheimer's disease is a synaptic failure. *Science,* 298, 789-91.

SEN, A., HONGPAISAN, J., WANG, D., NELSON, T. J. & ALKON, D. L. 2016. Protein kinase Cϵ (PKCϵ) promotes synaptogenesis through membrane accumulation of the postsynaptic density protein PSD-95. *J Biol Chem,* 291, 16462-76.

SEOK, S., FU, T., CHOI, S. E., LI, Y., ZHU, R., KUMAR, S., SUN, X., YOON, G., KANG, Y., ZHONG, W., MA, J., KEMPER, B. & KEMPER, J. K. 2014. Transcriptional regulation of autophagy by an FXR-CREB axis. *Nature,* 516, 108-11.

SHEHATA, M., MATSUMURA, H., OKUBO-SUZUKI, R., OHKAWA, N. & INOKUCHI, K. 2012. Neuronal stimulation induces autophagy in hippocampal neurons that is involved in AMPA receptor degradation after chemical long-term depression. *J Neurosci,* 32, 10413-22.

SHEN, R., WANG, B., GIRIBALDI, M. G., AYRES, J., THOMAS, J. B. & MONTMINY, M. 2016. Neuronal energy-sensing pathway promotes energy balance by modulating disease tolerance. *Proc Natl Acad Sci U S A,* 113, E3307-14.

SHENG, M., CUMMINGS, J., ROLDAN, L. A., JAN, Y. N. & JAN, L. Y. 1994. Changing subunit composition of heteromeric NMDA receptors during development of rat cortex. *Nature,* 368, 144-7.

SHI, S., HAYASHI, Y., ESTEBAN, J. A. & MALINOW, R. 2001. Subunit-specific rules governing AMPA receptor trafficking to synapses in hippocampal pyramidal neurons. *Cell,* 105, 331-43.

SHIN, J. H., PARK, S. J., JO, D. S., PARK, N. Y., KIM, J. B., BAE, J. E., JO, Y. K., HWANG, J. J., LEE, J. A., JO, D. G., KIM, J. C., JUNG, Y. K., KOH, J. Y. & CHO, D. H. 2019. Down-regulated TMED10 in Alzheimer disease induces autophagy via ATG4B activation. *Autophagy,* 15, 1495-1505.

SI, Y., XUE, X., LIU, S., FENG, C., ZHANG, H., ZHANG, S., REN, Y., MA, H., DONG, Y., LI, H., XIE, L. & ZHU, Z. 2021. CRTC1 signaling involvement in depression-like behavior of prenatally stressed offspring rat. *Behav Brain Res,* 399, 113000.

SMALL, S. A., SCHOBEL, S. A., BUXTON, R. B., WITTER, M. P. & BARNES, C. A. 2011. A pathophysiological framework of hippocampal dysfunction in ageing and disease. *Nat Rev Neurosci,* 12, 585-601.

SNYDER, E. M., NONG, Y., ALMEIDA, C. G., PAUL, S., MORAN, T., CHOI, E. Y., NAIRN, A. C., SALTER, M. W., LOMBROSO, P. J., GOURAS, G. K. & GREENGARD, P. 2005. Regulation of NMDA receptor trafficking by amyloid-beta. *Nat Neurosci,* 8, 1051-8.

SOKOLOW, S., HENKINS, K. M., BILOUSOVA, T., GONZALEZ, B., VINTERS, H. V., MILLER, C. A., CORNWELL, L., POON, W. W. & GYLYS, K. H. 2015. Pre-synaptic C-terminal truncated tau is released from cortical synapses in Alzheimer's disease. *J Neurochem,* 133, 368-79.

SOTO-FAGUÁS, C. M., SANCHEZ-MOLINA, P. & SAURA, C. A. 2021. Loss of presenilin function enhances tau phosphorylation and aggregation in mice. *Acta Neuropathol Commun,* 9, 162.

STEIN, J. L., HUA, X., MORRA, J. H., LEE, S., HIBAR, D. P., HO, A. J., LEOW, A. D., TOGA, A. W., SUL, J. H., KANG, H. M., ESKIN, E., SAYKIN, A. J., SHEN, L., FOROUD, T., PANKRATZ, N., HUENTELMAN, M. J., CRAIG, D. W., GERBER, J. D., ALLEN, A. N., CORNEVEAUX, J. J., STEPHAN, D. A., WEBSTER, J., DECHAIRO, B. M., POTKIN, S. G., JACK, C. R., WEINER, M. W., THOMPSON, P. M. & INITIATIVE, A. S. D. N. 2010. Genome-wide analysis reveals novel genes influencing temporal lobe structure with relevance to neurodegeneration in Alzheimer's disease. *Neuroimage,* 51, 542-54.

STEINBERG, J. P., TAKAMIYA, K., SHEN, Y., XIA, J., RUBIO, M. E., YU, S., JIN, W., THOMAS, G. M., LINDEN, D. J. & HUGANIR, R. L. 2006. Targeted in vivo mutations of the AMPA receptor subunit GluR2 and its interacting protein PICK1 eliminate cerebellar long-term depression. *Neuron,* 49, 845-60.

STEINER, P., HIGLEY, M. J., XU, W., CZERVIONKE, B. L., MALENKA, R. C. & SABATINI, B. L. 2008. Destabilization of the postsynaptic density by PSD-95 serine 73 phosphorylation inhibits spine growth and synaptic plasticity. *Neuron,* 60, 788-802.

STEWARD, O. & LEVY, W. B. 1982. Preferential localization of polyribosomes under the base of dendritic spines in granule cells of the dentate gyrus. *J Neurosci,* 2, 284-91.

SUH, Y. H., CHANG, K. & ROCHE, K. W. 2018. Metabotropic glutamate receptor trafficking. *Mol Cell Neurosci,* 91, 10-24.

SUMMERS, K. C., BOGARD, A. S. & TAVALIN, S. J. 2019. Preferential generation of Ca(2+)-permeable AMPA receptors by AKAP79-anchored protein kinase C proceeds via GluA1 subunit phosphorylation at Ser-831. *J Biol Chem,* 294, 5521-5535.

SZE, C., BI, H., KLEINSCHMIDT-DEMASTERS, B. K., FILLEY, C. M. & MARTIN, L. J. 2001. N-Methyl-D-aspartate receptor subunit proteins and their phosphorylation status are altered selectively in Alzheimer's disease. *J Neurol Sci,* 182, 151-9.

TAKEMOTO, K., IWANARI, H., TADA, H., SUYAMA, K., SANO, A., NAGAI, T., HAMAKUBO, T. & TAKAHASHI, T. 2017. Optical inactivation of synaptic AMPA receptors erases fear memory. *Nat Biotechnol,* 35, 38-47.

TARUTANI, A., ADACHI, T., AKATSU, H., HASHIZUME, Y., HASEGAWA, K., SAITO, Y., ROBINSON, A. C., MANN, D. M. A., YOSHIDA, M., MURAYAMA, S. & HASEGAWA, M. 2022. Ultrastructural and biochemical classification of pathogenic tau, α-synuclein and TDP-43. *Acta Neuropathol,* 143, 613-640.

TOM DIECK, S., KOCHEN, L., HANUS, C., HEUMÜLLER, M., BARTNIK, I., NASSIM-ASSIR, B., MERK, K., MOSLER, T., GARG, S., BUNSE, S., TIRRELL, D. A. & SCHUMAN, E. M. 2015. Direct visualization of newly synthesized target proteins in situ. *Nat Methods,* 12, 411-4.

TONEGAWA, S., LIU, X., RAMIREZ, S. & REDONDO, R. 2015. Memory engram cells have come of age. *Neuron,* 87, 918-31.

TONG, L., THORNTON, P. L., BALAZS, R. & COTMAN, C. W. 2001. Beta -amyloid-(1-42) impairs activity-dependent cAMP-response element-binding protein signaling in neurons at concentrations in which cell survival Is not compromised. *J Biol Chem,* 276, 17301-6.

TRAYNELIS, S. F., WOLLMUTH, L. P., MCBAIN, C. J., MENNITI, F. S., VANCE, K. M., OGDEN, K. K., HANSEN, K. B., YUAN, H., MYERS, S. J. & DINGLEDINE, R. 2010. Glutamate receptor ion channels: structure, regulation, and function. *Pharmacol Rev,* 62, 405-96.

TUSHEV, G., GLOCK, C., HEUMÜLLER, M., BIEVER, A., JOVANOVIC, M. & SCHUMAN, E. M. 2018. Alternative 3' UTRs modify the localization, regulatory potential, stability, and plasticity of mRNAs in neuronal compartments. *Neuron,* 98, 495-511.e6.

UCAR, A., GUPTA, S. K., FIEDLER, J., ERIKCI, E., KARDASINSKI, M., BATKAI, S., DANGWAL, S., KUMARSWAMY, R., BANG, C., HOLZMANN, A., REMKE, J., CAPRIO, M., JENTZSCH, C., ENGELHARDT, S., GEISENDORF, S., GLAS, C., HOFMANN, T. G., NESSLING, M., RICHTER, K., SCHIFFER, M., CARRIER, L., NAPP, L. C., BAUERSACHS, J., CHOWDHURY, K. & THUM, T. 2012. The miRNA-212/132 family regulates both cardiac hypertrophy and cardiomyocyte autophagy. *Nat Commun,* 3, 1078.

UCHIDA, S., TEUBNER, B. J., HEVI, C., HARA, K., KOBAYASHI, A., DAVE, R. M., SHINTAKU, T., JAIKHAN, P., YAMAGATA, H., SUZUKI, T., WATANABE, Y., ZAKHARENKO, S. S. & SHUMYATSKY, G. P. 2017. CRTC1 nuclear translocation following learning modulates memory strength via exchange of chromatin remodeling complexes on the Fgf1 gene. *Cell Rep,* 18, 352-366.

VICKERS, C. A., DICKSON, K. S. & WYLLIE, D. J. 2005. Induction and maintenance of late-phase long-term potentiation in isolated dendrites of rat hippocampal CA1 pyramidal neurones. *J Physiol,* 568, 803-13.

VISSEL, B., KRUPP, J. J., HEINEMANN, S. F. & WESTBROOK, G. L. 2001. A use-dependent tyrosine dephosphorylation of NMDA receptors is independent of ion flux. *Nat Neurosci,* 4, 587-96.

VITOLO, O. V., SANT'ANGELO, A., COSTANZO, V., BATTAGLIA, F., ARANCIO, O. & SHELANSKI, M. 2002. Amyloid beta -peptide inhibition of the PKA/CREB pathway and long-term potentiation: reversibility by drugs that enhance cAMP signaling. *Proc Natl Acad Sci U S A,* 99, 13217-21.

WADZINSKI, B. E., WHEAT, W. H., JASPERS, S., PERUSKI, L. F., JR., LICKTEIG, R. L., JOHNSON, G. L. & KLEMM, D. J. 1993. Nuclear protein phosphatase 2A dephosphorylates protein kinase A-phosphorylated CREB and regulates CREB transcriptional stimulation. *Mol Cell Biol,* 13, 2822-34.

WANG, Y., MARTINEZ-VICENTE, M., KRÜGER, U., KAUSHIK, S., WONG, E., MANDELKOW, E. M., CUERVO, A. M. & MANDELKOW, E. 2009. Tau fragmentation, aggregation and clearance: the dual role of lysosomal processing. *Hum Mol Genet,* 18, 4153-70.

WATANABE, S., HONG, M., LASSER-ROSS, N. & ROSS, W. N. 2006. Modulation of calcium wave propagation in the dendrites and to the soma of rat hippocampal pyramidal neurons. *J Physiol,* 575, 455-68.

WENTHOLD, R. J., PETRALIA, R. S., BLAHOS, J. II., & NIEDZIELSKI, A. S. 1996. Evidence for multiple AMPA receptor complexes in hippocampal CA1/CA2 neurons. *J Neurosci,* 16, 1982-9.

WEST, A. E., CHEN, W. G., DALVA, M. B., DOLMETSCH, R. E., KORNHAUSER, J. M., SHAYWITZ, A. J., TAKASU, M. A., TAO, X. & GREENBERG, M. E. 2001. Calcium regulation of neuronal gene expression. *Proc Natl Acad Sci U S A,* 98, 11024-31.

WHITCOMB, D. J., HOGG, E. L., REGAN, P., PIERS, T., NARAYAN, P., WHITEHEAD, G., WINTERS, B. L., KIM, D. H., KIM, E., ST GEORGE-HYSLOP, P., KLENERMAN, D., COLLINGRIDGE, G. L., JO, J. & CHO, K. 2015. Intracellular oligomeric amyloid-beta rapidly regulates GluA1 subunit of AMPA receptor in the hippocampus. *Sci Rep,* 5, 10934.

WHITLOCK, J. R., HEYNEN, A. J., SHULER, M. G. & BEAR, M. F. 2006. Learning induces long-term potentiation in the hippocampus. *Science,* 313, 1093-7.

WILSON, E. N., ABELA, A. R., DO CARMO, S., ALLARD, S., MARKS, A. R., WELIKOVITCH, L. A., DUCATENZEILER, A., CHUDASAMA, Y. & CUELLO, A. C. 2017. Intraneuronal amyloid beta accumulation disrupts hippocampal CRTC1-dependent gene expression and cognitive function in a rat model of Alzheimer disease. *Cereb Cortex,* 27, 1501-1511.

WINKLER, A., MAHAL, B., ZIEGLGÄNSBERGER, W. & SPANAGEL, R. 1999. Accurate quantification of the mRNA of NMDAR1 splice variants measured by competitive RT-PCR. *Brain Res Brain Res Protoc,* 4, 69-81.

WON, S. Y., PARK, M. H., YOU, S. T., CHOI, S. W., KIM, H. K., MCLEAN, C., BAE, S. C., KIM, S. R., JIN, B. K., LEE, K. H., SHIN, E. Y. & KIM, E. G. 2016. Nigral dopaminergic PAK4 prevents neurodegeneration in rat models of Parkinson's disease. *Sci Transl Med,* 8, 367ra170.

WONG, E. & CUERVO, A. M. 2010. Autophagy gone awry in neurodegenerative diseases. *Nat Neurosci,* 13, 805-11.

WU, Y. Y., CHENG, I. H., LEE, C. C., CHIU, M. J., LEE, M. J., CHEN, T. F. & HSU, J. L. 2011. Clinical phenotype of G206D mutation in the presenilin 1 gene in pathologically confirmed familial Alzheimer's disease. *J Alzheimers Dis,* 25, 145-50.

WYTTENBACH, A., SWARTZ, J., KITA, H., THYKJAER, T., CARMICHAEL, J., BRADLEY, J., BROWN, R., MAXWELL, M., SCHAPIRA, A., ORNTOFT, T. F., KATO, K. & RUBINSZTEIN, D. C. 2001. Polyglutamine expansions cause decreased CRE-mediated transcription and early gene expression changes prior to cell death in an inducible cell model of Huntington's disease. *Hum Mol Genet,* 10, 1829-45.

XIA, Z. & STORM, D. R. 2005. The role of calmodulin as a signal integrator for synaptic plasticity. *Nat Rev Neurosci,* 6, 267-76.

YAMAMOTO-SASAKI, M., OZAWA, H., SAITO, T., RÖSLER, M. & RIEDERER, P. 1999. Impaired phosphorylation of cyclic AMP response element binding protein in the hippocampus of dementia of the Alzheimer type. *Brain Res,* 824, 300-3.

YAN, P., XUE, Z., LI, D., NI, S., WANG, C., JIN, X., ZHOU, D., LI, X., ZHAO, X., CHEN, X., CUI, W., XU, D., ZHOU, W. & ZHANG, J. 2021. Dysregulated CRTC1-BDNF signaling pathway in the hippocampus contributes to Aβ oligomer-induced long-term synaptic plasticity and memory impairment. *Exp Neurol,* 345, 113812.

YAP, C. C., DIGILIO, L., MCMAHON, L. P., WANG, T. & WINCKLER, B. 2022. Dynein is required for Rab7-dependent endosome maturation, retrograde dendritic transport, and degradation. *J Neurosci*.

YASHIRO, K. & PHILPOT, B. D. 2008. Regulation of NMDA receptor subunit expression and its implications for LTD, LTP, and metaplasticity. *Neuropharmacology,* 55, 1081-94.

YIN, J. C., WALLACH, J. S., DEL VECCHIO, M., WILDER, E. L., ZHOU, H., QUINN, W. G. & TULLY, T. 1994. Induction of a dominant negative CREB transgene specifically blocks long-term memory in Drosophila. *Cell,* 79, 49-58.

YOON, Y. J., WU, B., BUXBAUM, A. R., DAS, S., TSAI, A., ENGLISH, B. P., GRIMM, J. B., LAVIS, L. D. & SINGER, R. H. 2016. Glutamate-induced RNA localization and translation in neurons. *Proc Natl Acad Sci U S A,* 113, E6877-e6886.

YOSHIYAMA, Y., HIGUCHI, M., ZHANG, B., HUANG, S. M., IWATA, N., SAIDO, T. C., MAEDA, J., SUHARA, T., TROJANOWSKI, J. Q. & LEE, V. M. 2007. Synapse loss and microglial activation precede tangles in a P301S tauopathy mouse model. *Neuron,* 53, 337-51.

YOUNTS, T. J., MONDAY, H. R., DUDOK, B., KLEIN, M. E., JORDAN, B. A., KATONA, I. & CASTILLO, P. E. 2016. Presynaptic protein synthesis is required for long-term plasticity of GABA release. *Neuron,* 92, 479-492.

YU, H., SAURA, C. A., CHOI, S. Y., SUN, L. D., YANG, X., HANDLER, M., KAWARABAYASHI, T., YOUNKIN, L., FEDELES, B., WILSON, M. A., YOUNKIN, S., KANDEL, E. R., KIRKWOOD, A. & SHEN, J. 2001. APP processing and synaptic plasticity in presenilin-1 conditional knockout mice. *Neuron,* 31, 713-26.

ZHANG, W., TARUTANI, A., NEWELL, K. L., MURZIN, A. G., MATSUBARA, T., FALCON, B., VIDAL, R., GARRINGER, H. J., SHI, Y., IKEUCHI, T., MURAYAMA, S., GHETTI, B., HASEGAWA, M., GOEDERT, M. & SCHERES, S. H. W. 2020. Novel tau filament fold in corticobasal degeneration. *Nature,* 580, 283-287.

ZHANG, Y., GUO, O., HUO, Y., WANG, G. & MAN, H. Y. 2018. Amyloid-β induces AMPA receptor ubiquitination and degradation in primary neurons and human brains of Alzheimer's disease. *J Alzheimers Dis,* 62, 1789-1801.

ZHAO, W. Q., SANTINI, F., BREESE, R., ROSS, D., ZHANG, X. D., STONE, D. J., FERRER, M., TOWNSEND, M., WOLFE, A. L., SEAGER, M. A., KINNEY, G. G., SHUGHRUE, P. J. & RAY, W. J. 2010. Inhibition of calcineurin-mediated endocytosis and alpha-amino-3-hydroxy-5-methyl-4-isoxazolepropionic acid (AMPA) receptors prevents amyloid beta oligomer-induced synaptic disruption. *J Biol Chem,* 285, 7619-32.

ZHAO, X., KOTILINEK, L. A., SMITH, B., HLYNIALUK, C., ZAHS, K., RAMSDEN, M., CLEARY, J. & ASHE, K. H. 2016. Caspase-2 cleavage of tau reversibly impairs memory. *Nat Med,* 22, 1268-1276.

ZHAO, X., ROSENKE, R., KRONEMANN, D., BRIM, B., DAS, S. R., DUNAH, A. W. & MAGNUSSON, K. R. 2009. The effects of aging on N-methyl-D-aspartate receptor subunits in the synaptic membrane and relationships to long-term spatial memory. *Neuroscience,* 162, 933-45.

ZHOU, L. & DUAN, J. 2018. The C-terminus of NMDAR GluN1-1a subunit translocates to nucleus and regulates synaptic function. *Front Cell Neurosci,* 12, 334.

ZHOU, L. & DUAN, J. 2021. The NMDAR GluN1-1a C-terminus binds to CaM and regulates synaptic function. *Biochem Biophys Res Commun,* 534, 323-329.

ZHOU, Y., SHI, J., CHU, D., HU, W., GUAN, Z., GONG, C. X., IQBAL, K. & LIU, F. 2018a. Relevance of phosphorylation and truncation of tau to the etiopathogenesis of Alzheimer's disease. *Front Aging Neurosci,* 10, 27.

ZHOU, Y., WON, J., KARLSSON, M. G., ZHOU, M., ROGERSON, T., BALAJI, J., NEVE, R., POIRAZI, P. & SILVA, A. J. 2009. CREB regulates excitability and the allocation of memory to subsets of neurons in the amygdala. *Nat Neurosci,* 12, 1438-43.

ZHOU, Y., WU, H., LI, S., CHEN, Q., CHENG, X. W., ZHENG, J., TAKEMORI, H. & XIONG, Z. Q. 2006. Requirement of TORC1 for late-phase long-term potentiation in the hippocampus. *PLoS One,* 1, e16.

ZHOU, Z., LIU, A., XIA, S., LEUNG, C., QI, J., MENG, Y., XIE, W., PARK, P., COLLINGRIDGE, G. L. & JIA, Z. 2018b. The C-terminal tails of endogenous GluA1 and GluA2 differentially contribute to hippocampal synaptic plasticity and learning. *Nat Neurosci,* 21, 50-62.

ZHU, J. J., ESTEBAN, J. A., HAYASHI, Y. & MALINOW, R. 2000. Postnatal synaptic potentiation: delivery of GluR4-containing AMPA receptors by spontaneous activity. *Nat Neurosci,* 3, 1098-106.

ZOU, X., LIN, Q. & WILLIS, W. D. 2002. Role of protein kinase A in phosphorylation of NMDA receptor 1 subunits in dorsal horn and spinothalamic tract neurons after intradermal injection of capsaicin in rats. *Neuroscience,* 115, 775-86.

ZUCKER, R. S. & REGEHR, W. G. 2002. Short-term synaptic plasticity. *Annu Rev Physiol,* 64, 355-405.

Acknowledgements

El primer agradecimiento debe ser para mi director de tesis, el Dr. Carles Saura, por abrirme las puertas del Laboratorio hará ya seis años para que pudiera realizar las prácticas de máster. Pero, sobre todo, por animarme y confiar en mí para realizar la tesis doctoral. Te estaré siempre agradecida por la oportunidad que me diste al hacer la estancia, que me ha hecho crecer no solamente a nivel científico sino también a nivel personal. Acabo esta etapa habiendo adquirido habilidades científicas y de pensamiento crítico por las cuales te estoy completamente agradecida. Gracias por dejar adentrarme en este fascinante mundo de la neurociencia de la mano de todas las personas que forman y han formado parte de este maravilloso grupo que es Saura Lab.

Agradezco, también, al Dr. Bryen Jordan por permitirme realizar la estancia en su Laboratorio, una de las etapas más enriquecedora de la tesis, y por la confianza al involucrarme en otros proyectos más allá de los que teníamos planteados inicialmente, siempre intentado que sacara el máximo provecho de la estancia.

Igualmente, me gustaría dar las gracias a la Dra. Gemma Navarro y al Dr. Rafael Franco, mis supervisores durante las prácticas de final de grado, y con los que he tenido la suerte de volver a coincidir durante esta etapa. Gracias por dejarme volver al laboratorio donde todo empezó.

Un agradecimiento especial a mis padres y mi hermano. Mamá y Papá, gracias por estar siempre cerca, aunque estuvierais en la distancia, y, sobre todo, por estar más cerca que nunca en los momentos más duros. Gracias por los valores que me habéis transmitido, siempre habéis sido y seréis mis referentes. Pero, sobre todo, gracias por vuestro cariño, confianza y apoyo incondicional. Dani, el mejor hermano mayor que cualquier hermana pudiera imaginar. La persona que más de cerca ha aguantado mis enfados y mal genio cuando algo no salía bien, pero que siempre ha sabido hacerme reír en los peores momentos. Gracias por tus consejos y tus mimitos cuando más los necesitaba. Esta tesis también es en gran parte mérito vuestro.

Quiero acordarme también de mi tieta Elvi, que siempre se interesó por cómo iban progresando mis experimentos y que, creo, habría disfrutado leyendo esta tesis. De mi tío Teo, que en sus visitas a Barcelona siempre reserva una noche para hablar largamente de ciencia con sus sobrinos. Y, también, de mi tiet Enric, el artista de la familia, por hacerme esta portada de tesis tan maravillosa.

Quiero mostrar mi agradecimiento a todas y cada una de las personas que han pasado por el Laboratorio durante estos años; espero no olvidarme de nadie. A Lilian, que me guio en mis primeros pasos en el laboratorio y que siempre recordaré con cariño. A Arnaldo, por todos los momentos vividos tanto dentro como fuera del laboratorio. A Míriam, por acogerme con los brazos abiertos desde el primer día, por esa felicidad que transmitía y por confiar en mí para ayudarte en

la recta final de tu tesis. También por las cervezas después del laboratorio, cenas y fiestas de Mataró. A Laura, mi compañera de despacho durante mucho tiempo. Por las risas tontas de última hora de la tarde, y por los ánimos con la generación de lentivirus y las luciferasas, o las "Lucis" como nos gustaba llamarlas a nosotras. Porque todo queda simplemente en subir a cultivos y hacer "pim, pim, pim". A Carlos, por todas las horas compartidas delante del ordenador, en la poyata, en cultivos, en el ferro, pero sobre todo fuera del laboratorio. Por transmitirme esa tranquilidad tan típica tuya cuando me ahogaba hasta en un vaso de agua. Pero, sobre todo, por culturizarme enseñándome lo mejor del andaluz. Vaya *jartá* de reír que nos hemos *pegao* estos años con todas las anécdotas y con los memes, vídeos y tweets que le enseñabas a una ignorante de las redes como soy yo. A Lola, Loli, Lolilla, Lolailo o Mary Pains Little Church, mejor mote que nadie te pudiera haber puesto (gracias, Òscar). Creo que eres consciente de lo importante que ha sido tenerte no solo como compañera de laboratorio sino también como amiga. Al entrar prácticamente de la mano en esta etapa, hemos creado un tándem que nos ha permitido apoyarnos la una en la otra en todo momento. Porque los éxitos y fracasos de cada una los hemos vivido como si fueran propios. Celebro nuestra amistad ahora y siempre. A Ángel, porque a pesar de que de todos nosotros es la persona menos habladora, transmite una tranquilidad indispensable para que funcionemos como equipo. Gracias por ser tan buen compañero, siempre dispuesto a ayudar. A Mar, gracias simplemente por aparecer en el camino. Por llegar como un soplo de aire fresco, llena de energía, vitalidad y motivación. Por preocuparte, aconsejarme y animarme a que sacara siempre lo mejor de mí. Te admiro y te deseo todos los éxitos en esta nueva etapa que has comenzado y que estoy segura, llegarán. A Alejandra, por ayudarme en la estresante recta final de la tesis y por enseñarme que todo problema se soluciona con unas buenas patatas bravas. A Xavi, por los ánimos a base de chocolatinas, por tu energía y por estar siempre dispuesto a escuchar. Te deseo todo lo mejor en tu doctorado.

Gracias también a todos los técnicos que han pasado por el Laboratorio, que sin su buen hacer y ayuda esto tampoco habría sido posible: Naroa, Marc, Edgar, Irene, Navera, Gemma, Evelyn, Mercé, Syra y Erika. Pero especialmente a Òscar. Gracias por llenar el laboratorio de buen rollo y música a todo volumen. Quiero agradecer también el apoyo de todos los estudiantes de máster. A Paula, con la que coincidí haciendo las prácticas, y a todos los que vinieron después: Luis, Noelia, Laura, Rafa e Iria.

Quiero acordarme de toda la gente *old school*, con los que compartir ese momento de desconexión y relax que era la hora de comer: era todo un placer. También por todos los grandes momentos vividos en los bares, terrazas y cenas de Navidad. Gracias Abel, Arantxa, Dolo y Raquel. Porque

sigamos manteniéndonos en contacto durante muchos años más. No quiero olvidarme de Paula, esa sevillana que llegó a ser casi una infiltrada en Saura Lab. Gracias de corazón por todo, especialmente por conseguir con tu simpatía y alegría que siempre hubiera buen rollo, manteniendo así al grupo unido, y recibir siempre con los brazos abiertos a las personas que han ido llegando.

Agradecer el buen compañerismo a todas mis compañeras de Unidad, que más de una vez me han salvado un experimento en el último momento. Gracias Nora, Sergio, Eli, Guille, las Lauras, Elena, Paola, Meri, Neus, Paula, Francina, Sally, Mireia, Raquel, las Montses y Anna. Pero especialmente a Irene, la última en llegar, pero que se ha convertido en poco tiempo en una gran amiga. Gracias por el apoyo tanto emocional como material. Sabes que sin tus préstamos no habría podido acabar los Westerns de esta tesis. Te deseo todo lo mejor.

Quiero agradecer también la ayuda y profesionalidad de las técnicos, Cris, Susana y Núria, siempre dispuestas a solucionar cualquier problema o duda que me pudiera surgir.

Quiero acordarme también de mis compañeros de laboratorio durante la estancia: Jaafar, Hoon, Ilana y Abigail. Gracias Jafaar por dedicarme parte de tu tiempo a enseñarme el mundo CRISPR-Cas. Recuerdo con cariño las interesantes charlas que teníamos sobre lo divino y lo humano. Espero volverme a encontrar con todos vosotros.

Agradezco haber estado acompañada durante todo este periodo por un grupo de personas a las cuales no cambiaría por nada en el mundo. Sara, Raquel y Laia, cada una de nuestro padre y nuestra madre, pero la amistad que hemos creado es algo indescriptible. Solo quiero que esto perdure, sea donde sea que acabemos cada una de nosotras, porque aún nos quedan muchas islas en el mundo por visitar. Salva, Álex y David, gracias por todo el cariño y por la alegría que desprendéis. A los que fueron compañeros de piso, Bruno, Diego y Adrián, porque sigamos celebrando fiestas allá dónde viváis. Rebeca, gracias a ti también por todo.

Darles las gracias a las de siempre, Blanca, Lucía, Carla, María y Ana, que me han visto crecer y de quienes siempre he tenido el cariño y apoyo necesario para finalizar esta tesis. Blanca, gracias por escucharme cuando lo necesitaba y recordarme la necesidad de tener una actitud zen. A Lucía y a Carla, las que mejor han comprendido mis frustraciones y que me han intentado ayudar en todo lo que han podido. A María, porque el simple hecho de que me enviaras un video me recordaba que te tenía ahí para lo que fuera. A Ana, la verdadera escritora del grupo, gracias por todos los años de amistad.

Agradecer a Anna, por todas las meteduras de pata en las prácticas de laboratorio de la carrera, de las cuales no sé si aprendimos algo, pero que recuerdo con cariño. Por todas las risas en la biblio, en la *gespeta* y en *Pensión Lolita*. Gracias por todo tu apoyo desde la distancia durante estos años. También quiero agradecer todo el cariño y ánimo de mis compañeras de voluntariado, especialmente a Cris, Noelia y Joana.

Quiero acordarme de la familia que formé estando de estancia y que hicieron que cada instante mereciera la pena: Paola, Coralie, Claudia, Luisa, Claudia Morganti, Michela, Roberto, Antonio, Sam, François y baby Franci. También de todas aquellas personas con las que tuve el placer de coincidir en las *beer hours*. Gracias Claudia, porque por casualidades de la vida nos encontramos y gracias a ti conocí a toda esta gente maravillosa. Paola, fue una suerte que coincidiéramos las dos estando de estancia, y que a pesar de la distancia y los confinamientos continuáramos nuestra amistad cuando regresamos. Gracias Coralie, por todo y más, fuiste y seguirás siendo como una hermana mayor. A todos los demás, mil veces gracias porque *Friends are family we choose*.

Gracias tesis, porque a pesar de las dificultades, has permitido que me cruce en el camino con gente extraordinaria a la cual espero mantener siempre cerca.